

V. T. NGUYEN ISSN 0343-8090

Improving the Representation of Hydrological Connectivity  
in Conceptual Models

---

# Improving the Representation of Hydrological Connectivity in Conceptual Models

---

Von der Fakultät für Bauingenieurwesen und  
Geodäsie der Gottfried Wilhelm Leibniz Universität Hannover

zur Erlangung des akademischen Grades  
Doktor-Ingenieur  
- Dr.-Ing. -

genehmigte Dissertation

von

Van Tam Nguyen, M.Sc.  
geboren am 11.08.1985 in Bac Ninh

2020

Referent: PD. Dr.-Ing. Jörg Dietrich

Korreferent: Prof. Dr. rer. nat. habil. Martin Volk

Tag der Promotion: 03.03.2020

# Acknowledgements

First of all, I would like to thank Prof. Dr.-Ing. Uwe Haberlandt and PD. Dr.-Ing. Jörg Dietrich for giving me a chance to do this PhD at the Institute of Hydrology and Water Resources Management. I would like to thank my PhD supervisor, PD. Dr.-Ing. Jörg Dietrich, for his scientific guidance and support during my PhD. His guidance and knowledge have helped me to have a scientifically sound approach to new problems and to become a SWAT developer. I am also very thankful for his support in my personal life during my research.

Special thanks go to Dr.-Ing. Ana Callau for offering me the HIWI position during my Master's study at WAWI. The working experience that I had during this time has helped me in learning FORTRAN, R, statistics, which were very useful for my PhD research.

I want to thank all of my colleagues at the Institute of Hydrology and Water Resources Management for the fruitful discussion during the "Klausurtagungen". To Bhumiika Uniyal, I would like to thank for her help in proof-reading all of my manuscripts and also for her contribution to my research. Special thanks go to all of the anonymous reviewers of my papers, whose comments significantly improved the quality of the papers.

I would also like to thank Stefan and Prajna for sharing the office with me. I want to thank Ana, Mathias, Anne, Prajna, Bruno, Bora, Luisa, Bhumika, Quynh, Stefan, and Hannes for sharing their fun time with me during the last four years.

Last but not least, I would like to thank my parents for their sacrifice for my education, to my wife and my son for supporting me spiritually throughout the PhD research.



# Declaration

I, Van Tam Nguyen, hereby declare that:

1. I know the regulations for doctoral candidates and have met all the requirements. I agree with an examination under the provisions of the doctoral regulations.
2. I have completed the thesis independently; used materials by others shall be listed in the references
3. I did not pay any monetary benefits for regards to content.
4. This work contains no material which has been accepted for the award of any other degree or diploma at any other university or tertiary institution.
5. The same or partly similar work has not been submitted at any other university or academic institution.
6. I agree that my thesis can be used for verifying the compliance with scientific standards, in particular using electronic data processing programs.

The relevant permission that might be needed from the journals to reproduce the published works are granted from the copyright holders.

Leipzig, March 5, 2020

Van Tam Nguyen

# Abstract

Understanding hydrological connectivity is one of the main objectives in hydrological research. Hydrological models have been proved to be an efficient tool for a better understanding of hydrological connectivity. Conceptual models have shown certain advantages compared to physically-based distributed models in terms of data requirement and computational time. However, the hydrological connectivity in conceptual models is usually not well represented. In this study, the Soil and Water Assessment Tool (SWAT) was selected for further improvements to have a better representation and simulation of hydrological connectivity.

SWAT is a semi-distributed hydrological model used to simulate the effect of land use management practices on water, sediment, and nutrient yields at a basin scale. SWAT has been tested and applied worldwide. However, the non-spatial characteristic of the hydrologic response unit (HRU) concept used in SWAT has been identified as one of the main disadvantages for modeling hydrological connectivity. In this study, the hydrologic routing subroutine of SWAT was examined and the groundwater subroutine was modified to account for hydrological connectivity in porous and karst-dominated aquifers.

Results show that the current hydrologic routing subroutines of SWAT are not able to simulate hydrological connectivity between river segments in the river network. The Muskingum routing method in SWAT could (1) cause unphysical oscillations in the simulated streamflow and (2) overestimate the evapotranspiration loss in the river and results in a hydrologic disconnectivity during low flow periods. For improving the representation of hydrological connectivity in the subsurface porous aquifer, the multicell aquifer model was proposed and incorporated into SWAT. The modified model, the so-called SWAT-MCA model, was validated in two basins located in Niedersachsen, Germany. The results show that the SWAT-MCA model could well simulate the regional groundwater flow and return flow from aquifer to stream. For improving the representation of hydrological connectivity in the karst-dominated aquifer due to interbasin groundwater flow (IGF) was added to SWAT, the SWAT\_IGF was developed. The developed model was applied in

a karst area located in the Southwest Harz Mountains, Germany. The model was validated with the observed streamflow and spring flow. Results show that the SWAT\_IGF could well represent the hydrological connection due to interbasin groundwater flow in karst areas. The modified models, SWAT-MCA and SWAT\_IGF could be applied for other regions to regional groundwater flow in porous aquifer and IGF in karst-dominated aquifers.

Keywords: SWAT, hydrological connectivity, flood routing, karst, groundwater flow

# Kurzfassung

Das Verständnis der hydrologischen Konnektivität ist eine der Hauptaufgaben in der hydrologischen Forschung. Hydrologische Modelle haben sich als effizientes Werkzeug für ein besseres Verständnis der hydrologischen Konnektivität erwiesen. Konzeptmodelle haben im Vergleich zu physisch basierten verteilten Modellen hinsichtlich Datenbedarf und Rechenzeit gewisse Vorteile gezeigt. Die hydrologische Konnektivität in in konzeptuellen Modellen ist jedoch nicht gut dargestellt. In dieser Studie wurde das Soil and Water Assessment Tool (SWAT) für weitere Verbesserungen ausgewählt, um die hydrologische Konnektivität besser darstellen und simulieren zu können.

SWAT ist ein semi-verteilttes hydrologisches Modell, das verwendet wird, um die Auswirkungen von Landmanagementpraktiken auf den Wasser-, Sediment- und Nährstoffhaushalt in Flussgebieten zu simulieren. SWAT wurde weltweit getestet und angewendet. Die nichträumlichen Eigenschaften des in SWAT verwendeten HRU-Konzepts (Hydrologic Response Unit) wurden jedoch als einer der Hauptnachteile für die Modellierung der hydrologischen Konnektivität identifiziert. In dieser Studie wurde das Unterprogramm für hydrologisches Routing von SWAT weiter getestet und das Grundwasser-Unterprogramm wurde modifiziert, um die hydrologische Konnektivität in porösen und karstdominierten Aquiferen zu berücksichtigen.

Die Ergebnisse zeigen, dass die aktuellen Unterprogramme für hydrologisches Routing von SWAT keine hydrologischen Verbindungen im Flussnetz simulieren können. Das Muskingum-Routing-Verfahren in SWAT könnte (1) unphysikalische Oszillationen im simulierten Stromfluss verursachen und (2) den Evapotranspirationsverlust im Fluss überschätzen und zu einer hydrologischen Diskonnektivität bei niedrigen Abflüssen. Zur Verbesserung der Darstellung der hydrologischen Konnektivität im unterirdischen porösen Aquifer wurde das Multicell-Aquifer Modell in SWAT integriert. Das modifizierte Modell, das sogenannte SWAT-MCA Modell, wurde in zwei Flussgebieten in Niedersachsen validiert. Die Ergebnisse zeigen, dass das SWAT-MCA Modell den regionalen Grundwasserfluss gut simulieren kann. Um die Darstellung der hydrologischen Konnektivität im

karstdominierten Grundwasserleiter durch Interbasin Groundwater Flow (IGF) in SWAT zu verbessern, wurde der SWAT\_IGF entwickelt. Der SWAT\_IGF wurde in einem Karstgebiet im Südwesten des Harzes in Deutschland angewendet. Das Modell wurde mit dem beobachteten Abfluss des Flusses und der Karstquelle validiert. Die Ergebnisse zeigen, dass der SWAT\_IGF die hydrologische Verbindung aufgrund des Grundwasserflusses zwischen den Becken in Karstgebieten gut darstellen könnte. Die modifizierten Modelle SWAT-MCA und SWAT-IGF könnten für andere Regionen eingesetzt werden, um IGF in porösen und karstdominierten Aquiferen zu simulieren.

**Schlüsselwörter:** SWAT, hydrologische Konnektivität, Hochwasserführung, Karst, Grundwasserfluss



# Abbreviations

a.m.s.l	above mean sea level
BGR	Bundesanstalt für Geowissenschaften und Rohstoffe
DEM	Digital Elevation Model
DWD	Deutscher Wetterdienst
ET <sub>a</sub>	Actual Evapotranspiration
HRU	Hydrologic Response Unit
IGF	Interbasin Groundwater Flow
LU	Landscape Unit
MCA	Multicell Aquifer Model
NLWKN	Niedersächsische Landesbetrieb für Wasserwirtschaft, Küsten- & Naturschutz
NSE	Nash–Sutcliffe Efficiency
PBIAS	Percentage BIAS
SWAT	Soil and Water Assessment Tool

# Contents

<b>1</b>	<b>Introduction</b>	<b>1</b>
1.1	Research Problem and Motivation . . . . .	1
1.2	Literature Review . . . . .	4
1.2.1	SWAT . . . . .	4
1.2.2	Current approaches and challenges for simulating hydrological connectivity with SWAT . . . . .	8
1.3	Research Objectives and Methodology . . . . .	14
1.4	Thesis Structure and Author Contribution . . . . .	15
<b>2</b>	<b>Verification and Correction of the Hydrologic Routing in the SWAT</b>	<b>22</b>
2.1	Introduction . . . . .	23
2.2	Theoretical Background . . . . .	24
2.2.1	Variable Storage Method . . . . .	24
2.2.2	Muskingum Method . . . . .	25
2.3	Hydrologic Routing with SWAT . . . . .	26
2.3.1	Variable Storage Routing Subroutine . . . . .	26
2.3.2	Muskingum Routing Subroutine . . . . .	27
2.4	Verification Examples . . . . .	28
2.4.1	Study Area and Data . . . . .	28
2.4.2	Simulation Scenarios . . . . .	28
2.4.3	Results and Discussions . . . . .	30
2.5	Conclusions and Recommendations . . . . .	33

2.6	Funding . . . . .	34
2.7	Acknowledgments . . . . .	34
2.8	Conflicts of Interest . . . . .	34
<b>3</b>	<b>Modification of the SWAT Model to Simulate Regional Groundwater Flow Using A Multi-Cell Aquifer</b>	<b>37</b>
3.1	Introduction . . . . .	38
3.2	Methodology . . . . .	41
3.2.1	The original groundwater module of SWAT . . . . .	41
3.2.2	The modified groundwater module . . . . .	42
3.2.3	Input data preparation . . . . .	46
3.2.4	Model integration framework . . . . .	46
3.3	Case Study . . . . .	47
3.3.1	Study areas and data . . . . .	47
3.3.2	Spatial discretization . . . . .	50
3.3.3	Calibration and validation strategy . . . . .	52
3.4	Results and Discussion . . . . .	54
3.4.1	Calibrated parameter values . . . . .	54
3.4.2	Overall water balance . . . . .	54
3.4.3	Stream discharge . . . . .	55
3.4.4	Groundwater levels . . . . .	57
3.5	Conclusion and Recommendations . . . . .	63
<b>4</b>	<b>Modeling Interbasin Groundwater Flow in Karst Areas: Model Development, Application, and Calibration Strategy</b>	<b>71</b>
4.1	Introduction . . . . .	72
4.2	Methodology . . . . .	75
4.2.1	The original SWAT model . . . . .	75
4.2.2	The modified SWAT model for IGF . . . . .	76

4.3	Case Study . . . . .	80
4.3.1	Study area and data . . . . .	80
4.3.2	Geology . . . . .	83
4.3.3	Hydrogeology . . . . .	83
4.4	Model setup, calibration and validation . . . . .	86
4.4.1	Model setup . . . . .	86
4.4.2	Calibration and validation strategy . . . . .	86
4.5	Results and discussion . . . . .	89
4.5.1	Sensitivity analysis and best calibrated parameter set . . . . .	89
4.5.2	The role of using MOD16 ETa and multi-site streamflow data and for model calibration . . . . .	90
4.5.3	Simulated streamflow . . . . .	93
4.5.4	Simulated karst groundwater storage variation . . . . .	96
4.6	Conclusions and recommendations . . . . .	97
<b>5</b>	<b>Conclusion and Future Outlooks</b>	<b>107</b>
5.1	Conclusions . . . . .	107
5.1.1	Hydrological connectivity in the river network . . . . .	108
5.1.2	Subsurface hydrological connectivity in porous aquifer . . . . .	108
5.1.3	Subsurface hydrological connectivity in karst-dominated aquifer . . . . .	109
5.2	Future Outlooks . . . . .	110
5.2.1	General . . . . .	110
5.2.2	Original SWAT model . . . . .	110
5.2.3	SWAT-MCA model . . . . .	111
5.2.4	SWAT-IGF model . . . . .	112

# List of Tables

2.1	List of the hydrologic routing subroutines used for this study. . . . .	30
2.2	Model performance statistics for flood event 1 (17 January 1990 to 17 April 1990, Figures 2.2a,b) and flood event 2 (18 December 1990 to 1 February 1991, Figures 2.2c,d). . . . .	32
3.1	The overlapping area matrix between HRUs and cells . . . . .	46
3.2	Characteristics of the study areas . . . . .	48
3.3	Best calibrated parameter values of the original SWAT and SWAT-MCA models . . . . .	53
3.4	Performance of the calibrated SWAT and SWAT-MCA model (in terms of streamflow at the Oetzmühle and Süttoorf gauging stations) . . . . .	60
4.1	Selected parameter for sensitivity analysis and sensitivity ranking . . . . .	87
4.2	List of calibration scenarios and the corresponding weights in the objective function . . . . .	88
4.3	Selected parameters for calibration and the best parameter values . . . . .	89
4.4	Model performance statistics and characteristics of the 95PPU band. Numbers outside parentheses indicate values of the calibration period while numbers inside parentheses indicate values of the validation period. . . . .	92



# List of Figures

1.1	The water cycle and global distribution of water resources (Oki and Kanae, 2006). . . . .	2
1.2	Land phase processes in SWAT (modified from Neitsch et al., 2011) . . . . .	5
1.3	Stream processes in SWAT (modified from Neitsch et al., 2011) . . . . .	6
1.4	Discretization of the basin using a) the catena and b)grid approaches in SWAT (Arnold et al., 2010). . . . .	10
1.5	Hydrological connectivity between different landscape units in the grid-based SWAT model (Arnold et al., 2010). . . . .	10
1.6	The schematic description of the SWAT-MODFLOW model (Kim et al., 2008). . . . .	11
1.7	Hydrological connectivity between different spatial objects in SWAT+ (Bieger et al, 2017). SUR is surface runoff, LAT is lateral flow, RHG is groundwater recharge, TOT is total flow. . . . .	12
1.8	Representation of hydrological connectivity between upland area, floodplain, and river in SWAT+ (Bieger et al, 2019). . . . .	13
2.1	Location of the Weser River segment and its tributary rivers. . . . .	29
2.2	Simulated outflow at the Vlotho gauging station for two flood events using (a,c) V2009 and V2012 and (b,d) M2012 and M2012*. . . . .	31
2.3	Flow duration curves of the simulated streamflow (logarithmic scale) at the (a) Welsede, (b) Afferde, and (c) Uchtdorf gauging stations during 1990–2000 with M2012 and M2012*. . . . .	33

3.1	Schematic representation of the vertical structure of the modified groundwater module in SWAT. $Q_{surf}$ , $Q_{lat}$ , $Q_{r,local}$ , $Q_{r,regional}$ , and $Q_{regional}$ are the surface run-off, lateral flow, return flow from local aquifer, return flow from regional aquifer, and regional groundwater flow, respectively. The numbers indicate the average annual water balance components in millimeters per year in the Wipperaue (numbers outside parentheses) and the Neetze (numbers inside parentheses) basins . . . . .	43
3.2	Schematic representation of the multicell aquifer model . . . . .	45
3.3	Integration framework of the soil and water assessment tool–multicell aquifer model . . . . .	47
3.4	Location and digital elevation model (DEM) of the Neetze and Wipperaue basins . . . . .	49
3.5	Delineation of the subbasin and the regional groundwater aquifer of (a) the Neetze basin and (b) the Wipperaue basin . . . . .	51
3.6	Observed and simulated streamflows from (a, c) the original SWAT models and (b, d) the SWAT-MCA model at the Oetzmühle (Wipperaue basin) and Süttoorf (Neetze basin) gauging stations during 1980–2007. A portion of the semi-log plot was shown in normal plot (a) to show that it is difficult to see the quality of the simulated low flow with normal plot. SWAT = soil and water assessment tool; MCA = multicell aquifer . . . . .	56
3.7	Flow duration curves of the observed and simulated streamflows at the Oetzmühle gauging station from the SWAT and SWAT-MCA models during 1980–2007. SWAT = soil and water assessment tool; MCA = multicell aquifer . . . . .	57
3.8	Time series plots of the observed and simulated groundwater levels during 1980–2007 and statistical indices (Nash–Sutcliffe efficiency [NSE], percent bias [PBIAS], and ratio of the root mean square error to the standard deviation of measured data [RSR]): (a) good match between observed and simulated groundwater levels, (b) mismatch between the time of occurrences of the high and low groundwater levels between observed and simulated groundwater levels, and (c) well reproduced of short- and long-term groundwater fluctuations. Boxplots of the absolute differences between simulated and observed groundwater levels are attached to the right of the time series plots . . . . .	58

3.9	Time series plots of the observed and simulated groundwater levels during 1980–2007 in cells that are strongly affected by the cones of depression of the extraction wells located nearby . . . . .	62
4.1	Conceptual models of the SWAT_IGF model. (A) the conceptual model for the non-karst area (the original conceptual model of SWAT), (B) the conceptual model for the karst area (modified from SWAT). $Q_{surf}$ is the surface runoff, $Q_{lat}$ is the lateral flow, $w_{revap}$ is the groundwater revap, $w_{rshallow}$ and $w_{rdeep}$ are the shallow and deep groundwater recharge, respectively, other variables were described in text. . . . .	77
4.2	The study area with the Digital Elevation Model. . . . .	81
4.3	Distribution of (A) land use/land cover, (B) soil, and (C) slope with sub-basin numbers in the study area. . . . .	82
4.4	Geological map of the study area (BGR). Location of the faults and different types of streams were identified according to Thürschau (1913) and Grimmelmann (1992). More information about the geological cross-section could be found in Grimmelmann (1992). . . . .	84
4.5	Time series plot of MOD16 ETa and simulated ETa from the calibration scenario S2. . . . .	91
4.6	Scatter plots of $NSE_{ETa}$ versus $NSE_{Q_{Lindau}}$ , $NSE_{Q_{Scharzfeld}}$ and $NSE_{Q_{Kupferhütte}}$ for behavioral simulations in the calibration scenario S2 (from 2000-2005). The red cross indicates the simulation corresponding to the best parameter set. . . . .	91
4.7	Time series plots of streamflows and flow duration curves (attached to the right of the respective time series plot) of the observed and the simulated streamflow from SWAT_IGF during the calibration period (2000-2005). The simulated streamflow at the Rhume spring (blue line) using the original SWAT was added in (G). For a better visualization, only the 95PPU band for the Rhume spring was shown. . . . .	94
4.8	Time series plots of streamflows and the flow duration curves (attached to the right of the respective time series plot) of the observed and the simulated streamflow from SWAT_IGF during the validation period (2006-2010). The simulated streamflow at the Rhume spring (blue line) using the original SWAT was added in (G). . . . .	95

4.9	Variations of the simulated karst groundwater storage (the matrix and conduit storage reservoirs) and the observed groundwater levels. . . . .	96
-----	--	----

# Chapter 1

## Introduction

### 1.1 Research Problem and Motivation

Water covers most of the earth's surface and it is one of the vital sources of life. The water cycle (Figure 1.1) is one of the governing processes on Earth and it plays an important role in the Earth's climate self-regulation (Allen, 2009; Nordstrom et al., 2005). Water is abundant on Earth, however, only 2.5% of the total water amount is freshwater. In addition, only a small portion of freshwater is accessible (Oki and Kanae, 2006). Freshwater distribution on Earth varies with space and time (Piao et al., 2010). The uneven distribution of water could cause water shortage or flood (Imamura and Van To, 1997; Oki and Kanae, 2006; Shiklomanov, 1991). Water shortage or flood has been identified as one of the controlling factors of social and economic welfare (Gleick, 1993; Lehner et al., 2006).

The natural redistribution of water on the Earth's surface and subsurface occurs in the form of surface and subsurface flows. Different landscape units could be hydrologically connected by surface and/or subsurface flows (Garven, 1995; Tockner et al., 1999). The hydrological connection between different landscape units is called hydrological connectivity. Hydrological connectivity describes the linkage between upstream with downstream, surface with subsurface, hillslope with riparian zone, terrestrial with aquatic (Covino, 2017). These linkages can occur at various spatio-temporal scales (local to regional scales) and different directions (vertical, lateral, longitudinal) (Covino, 2017). These linkages control the transport of water and solute and affect the hydrological cycles.

In a broader sense, hydrological connectivity refers to the transfer of water and its associated components (e.g., nutrients and sediments) between different landscape units



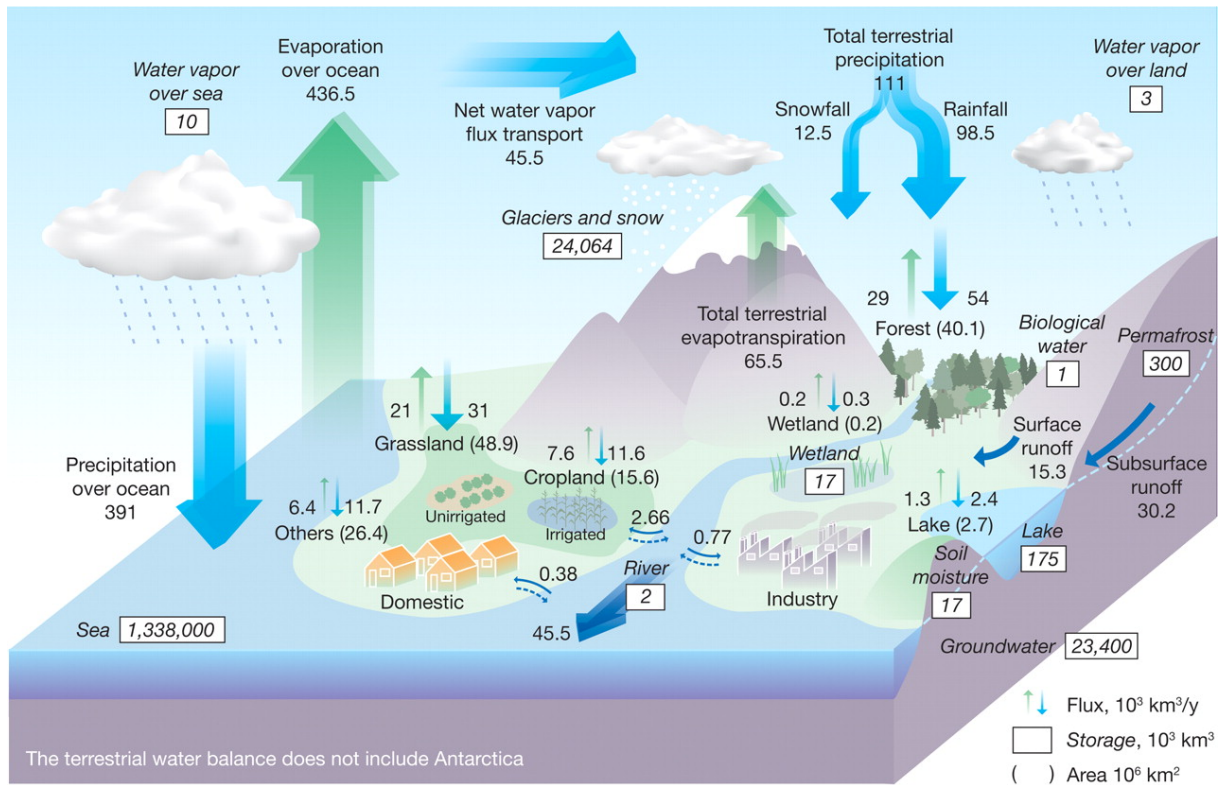


Figure 1.1: The water cycle and global distribution of water resources (Oki and Kanae, 2006).

(e.g., hillslope, floodplain, and river) or between different components of the hydrological cycle (Pringle, 2003). It should be noted that there exist different definitions of hydrological connectivity depending on the geomorphic domain (Bracken et al., 2013). Understanding the hydrological connectivity between different landscape units could help water resource managers in formulating appropriate management strategies, especially in terms of transboundary water resources management (Bracken et al., 2013). For example, identifying the critical source areas which contribute most of the pollutants and their hydrological connection with other landscape units are crucial for developing effective measures. This has been long of interest in the hydrological community (e.g., Covino, 2017; Niraula et al., 2013; Srinivasan and McDowell, 2009). In the region where interbasin groundwater flow is significant, understanding the transport of water and solute fluxes via interbasin groundwater flow (subsurface connectivity) has significant implications for water management.

There have been various studies focused on improving the understanding the hydrological connectivity. Different approaches could be used to understand different types of hydrological connectivity, ranging from experimental studies to numerical study using hydrological models (Bracken et al., 2013). This study focuses on developing modeling

tools to have a better representation and understanding of hydrological connectivity. In this study, the term “hydrological connectivity” is restricted to (1) the lateral surface and subsurface flow between different landscape units and (2) the vertical flow between the soil layers and the aquifer.

Various models have been developed to help in understanding and predicting the hydrological connectivity, ranging from lumped conceptual to distributed physically-based models. Lumped conceptual models consider a whole basin as a single unit. They only consider the vertical hydrological connectivity between different vertical storages (e.g., percolation of water between different soil layers, and groundwater recharge). Some examples of these models are the NAM (Nielsen and Hansen, 1973), PDM (Moore, 2007) and VHM (Willems, 2014) models.

In conceptual (semi-)distributed models, a basin is divided into subbasins and further divided into smaller spatial units. One of the most frequently used methods for basin delineation is the hydrologic response unit (HRU) concept (Leavesley et al., 1983). Within the HRU concept, each HRU has a unique combination of land use, soil type and slope within a subbasin. HRU is considered to be homogeneous in hydrologic response. A single HRU can be scattered over different areas in a subbasin. Some models of this type are the Soil and Water Assessment Tool (SWAT, Arnold et al., 1998), Hydrologiska Byråns Vattenbalansavdelning (HBV, Bergström, 1992), Precipitation-Runoff Modeling System (PRMS, Markstrom et al., 2015), and Hydrological Predictions for the Environment model (HYPE, Lindström et al., 2010). In these models, hydrological connectivity is considered (1) between different soil layers and aquifers within an HRU (vertical hydrological connectivity), and (2) between subbasins via the stream network (longitudinal hydrological connectivity). In general, the subsurface of each HRU in conceptual models is assumed as a system of connected reservoirs. These reservoirs represent the water storage in different soil zones and in the aquifers. Flow between these reservoirs is often simulated using simple routing equations. There is no lateral hydrological connectivity (surface and subsurface flows) between HRUs. Flow from each HRU is assumed to be independent of other HRUs and it does not interact with each other. The summation of all HRUs’ responses within a subbasin is considered as the subbasin’s response.

Other delineation approaches were also used in (semi-)distributed models. For example, the Water Erosion Prediction Project (WEPP, Flanagan and Nearing, 2015) model divides a basin into hillslope, channel, and impoundment. The mesoscale hydrologic model (mHM, Kumar et al., 2013; Samaniego et al., 2010) divides a basin into grid cells. However, both of the aforementioned models do not model the subsurface flow between

different landscape units.

With physically-based distributed models, e.g., the Modular Three-Dimensional Finite-Difference Ground-Water Flow Model (MODFLOW, [Harbaugh and McDonald, 1996](#)), HydroGeoSphere ([Therrien et al., 2009](#)), and OpenGeoSys ([Kolditz et al., 2012](#)), the study area is divided into grid cells and surface and subsurface flow between grid cells is simulated by using physical equations (e.g, Darcy’s law and Richards’ equation). However, the disadvantages of physically-based distributed models are the extensive requirement of data and computational capacity.

Compared to physically-based distributed models, conceptual (semi-)distributed models often require less simulation time while preserving the spatial heterogeneity in land use and soil type. The main disadvantage of the conceptual distributed models is the lack of lateral hydrological connectivity between HRUs or subbasins (e.g., SWAT, HBV, HYPE). Some studies have compared the performance between physically distributed models and conceptual distributed models (e.g., [Devia et al., 2015](#); [Liu et al., 2016](#)). Results show that more complex models do not always guarantee a better result than simpler models.

SWAT is a conceptual distributed model for assessing the impact of land use management practices on water, sediment, and chemical yields at a basin-scale ([Arnold et al., 1998](#)). SWAT has been widely used and tested worldwide ([Arnold and Fohrer, 2005](#)). SWAT has been proved to be a unique model which could incorporate various natural and anthropogenic processes (e.g., dynamic land use change, sediment, and nutrients flow in karst) ([Arnold and Fohrer, 2005](#); [Pai and Saraswat, 2011](#); [Nerantzaki et al., 2015](#)). Therefore, improving SWAT for simulation of hydrological connectivity will bring a significant benefit to the SWAT community.

## 1.2 Literature Review

### 1.2.1 SWAT

In SWAT, a basin is divided into subbasins which are further divided into HRUs according to different land use, soil type, and slope classes ([Arnold et al., 1998](#); [Neitsch et al., 2011](#)). One HRU could be scattered across different places within a subbasin. SWAT simulates two phases of the hydrological cycle, the land phase (HRU-related processes, [Figure 1.2](#)) and the routing phase (stream-related process, [Figure 1.3](#)). The HRU-related processes are evapotranspiration, surface runoff, lateral flow, infiltration, percolation, groundwater

recharge, return flow, etc. (Figure 1.2). The stream processes are flow and transport in the stream network (Figure 1.3).

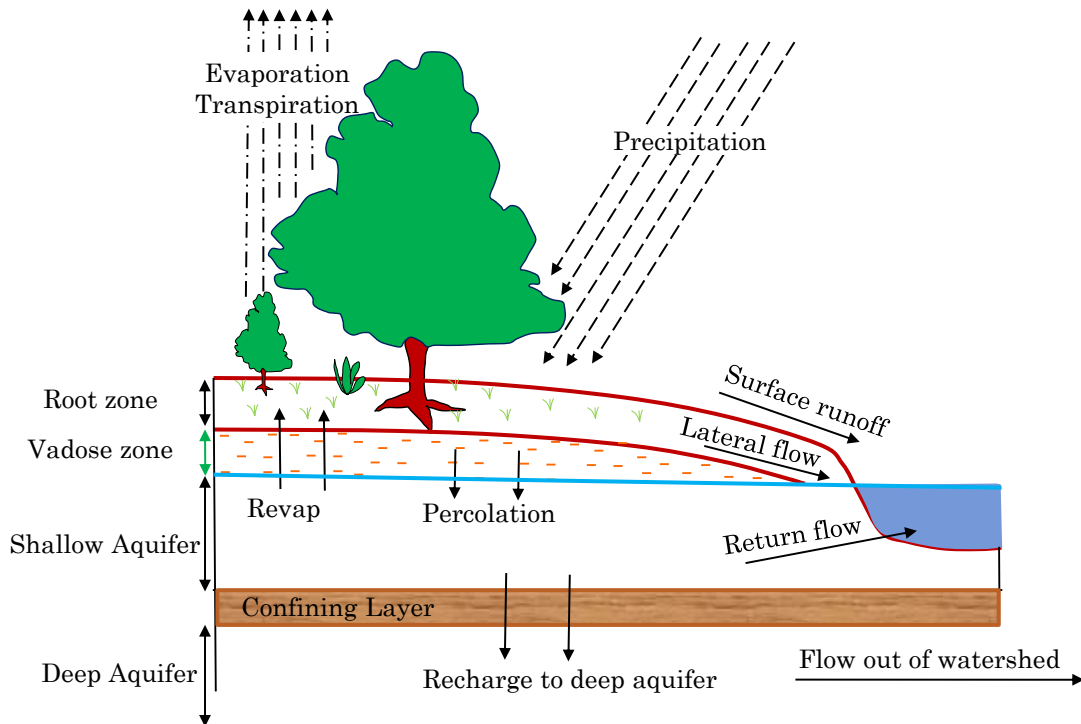


Figure 1.2: Land phase processes in SWAT (modified from Neitsch et al., 2011)

The land phase considers hydrological connectivity in the vertical direction between different soil layers and between the soil zone and the aquifers. The soil layers and aquifers are represented as a system of connected reservoirs. Infiltrated rainfall first fills up the uppermost soil layer. If the water content in the soil layer exceeds its field capacity, the excess water will be routed to the next soil layer. The infiltrated water that exits the bottom of the soil profile is considered as groundwater recharge. Groundwater recharge is split into shallow groundwater and deep groundwater recharge. Recharge to the deep aquifer is considered as a loss from the system (Figure 1.2).

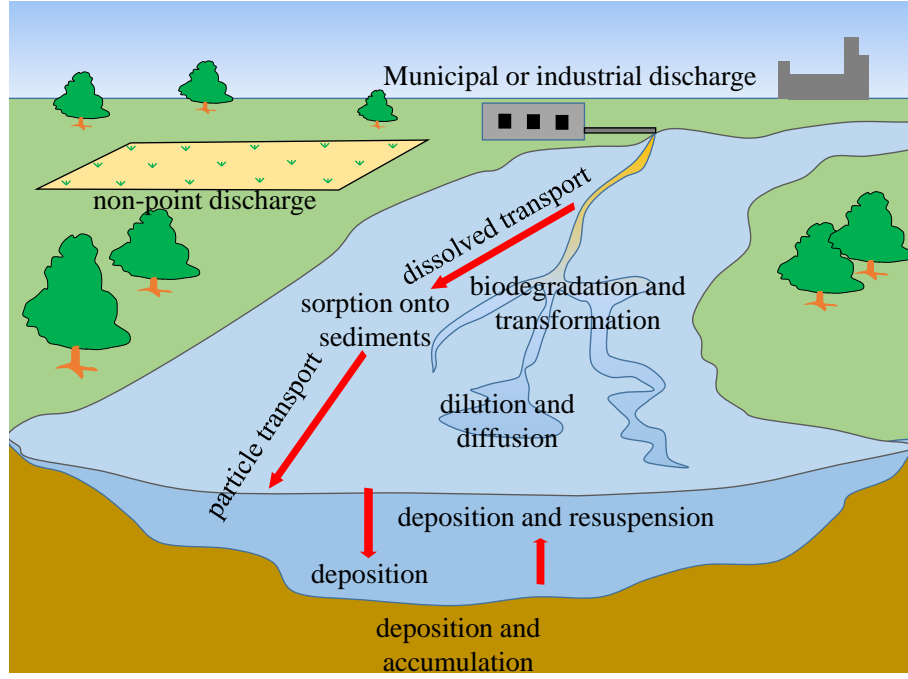


Figure 1.3: Stream processes in SWAT (modified from Neitsch et al., 2011)

The daily water balance for the soil zone (all soil layers) for an HRU (Figure 1.2) is calculated as follows (Arnold et al., 1998; Neitsch et al., 2011):

$$SW_i = SW_{i-1} + P_i - Q_{surf} - ET_a - w_{seep} - Q_{lat} \quad (1.1)$$

where  $SW_i$  and  $SW_{i-1}$  (mm H<sub>2</sub>O) are the total soil water content in the soil on day  $i$  and  $i - 1$ , respectively,  $P_i$  (mm H<sub>2</sub>O) is the amount of precipitation on day  $i$ ,  $Q_{surf}$ ,  $ET_a$ ,  $w_{seep}$ , and  $Q_{lat}$  (mm H<sub>2</sub>O) are the amount of surface runoff, actual evapotranspiration, percolated water out of the soil profile, and the total amount of lateral flow from all soil layers on day  $i$ .

In each HRU, infiltrated water is routed from the topsoil layer to the aquifer using the routing technique described below. Water percolates from the upper soil layer to the lower soil layer if the water content in the upper soil layer exceeds the field capacity. In this case, the amount of drainable water volume  $SW_{ly,excess}$  (mm H<sub>2</sub>O) from the upper soil layer is calculated as follows:

$$SW_{ly,excess} = SW_{ly} - FC_{ly} \quad (1.2)$$

where  $SW_{ly}$  and  $FC_{ly}$  (mm H<sub>2</sub>O) are the soil water content and the field capacity of the upper soil layer on day  $i$ , respectively. The actual amount of water percolating to the

lower soil layer,  $w_{per,ly}$  (mm H<sub>2</sub>O), is:

$$w_{per,ly} = SW_{ly,excess} \cdot (1 - e^{-\Delta t/TT_{per}}) \quad (1.3)$$

where  $\Delta t$  (hour) is the number of hours in a day, and  $TT_{per}$  (hour) is the travel time for percolation within the respective soil layer, which is expressed as follows:

$$TT_{per} = \frac{SAT_{ly} - FC_{ly}}{K_{sat}} \quad (1.4)$$

where  $SAT_{ly}$  (mm H<sub>2</sub>O) is the amount of water in the soil when the soil is fully saturated,  $K_{sat}$  (mm/h) is the saturated hydraulic conductivity of the soil layer.

Percolated water out of the lowest soil layer and infiltration losses from secondary channels, ponds and wetlands are considered as groundwater recharge,  $w_{seep}$  (mm H<sub>2</sub>O). The hydraulic connection between the lowest layer, the unsaturated zone, and the shallow aquifer is represented by the groundwater delay time,  $\delta_{gw}$  (days). Therefore, the actual amount of groundwater recharge,  $w_{rchrg,i}$  (mm H<sub>2</sub>O), to both shallow and deep aquifers during day  $i$  is:

$$w_{rchrg,i} = (1 - e^{-1/\delta_{gw}}) \cdot w_{seep} + e^{-1/\delta_{gw}} \cdot w_{rchrg,i-1} \quad (1.5)$$

where  $w_{rchrg,i-1}$  is the total groundwater recharge on previous day. The total groundwater recharge is separated into shallow,  $w_{rchrg,sh}$ , and deep groundwater recharge,  $w_{rchrg,deep}$ , as follows:

$$w_{rchrg,sh} = (1 - \beta_{deep}) \cdot w_{rchrg,i} \quad (1.6)$$

$$w_{rchrg,deep} = \beta_{deep} \cdot w_{rchrg,i} \quad (1.7)$$

where  $\beta_{deep}$  is the portion of recharge to the deep aquifer. The daily water balance for the shallow aquifer is expressed as follows:

$$aq_{sh,i} = aq_{sh,i-1} + w_{rchrg,sh} - Q_{gw} - w_{revap} - w_{pump} \quad (1.8)$$

where  $aq_{sh,i}$  and  $aq_{sh,i-1}$  (mm H<sub>2</sub>O) are the amount of water in the shallow aquifer on day  $i$  and  $i - 1$ ,  $Q_{gw}$ ,  $w_{revap}$ ,  $w_{pump}$  (mm H<sub>2</sub>O) are the return flow from shallow aquifer,

revaporation, and pumping, respectively. Recharge to the deep aquifer is considered as loss from the system.

In SWAT, there is no lateral hydrological connectivity between HRUs due to their non-spatial characteristics. Summation of all HRU responses within a subbasin is considered as a subbasin response. Streamflow generated from upstream subbasin is routed to downstream subbasin using a simple hydrological routing method. Streamflow is considered as the only hydrological connection between subbasins in SWAT.

## 1.2.2 Current approaches and challenges for simulating hydrological connectivity with SWAT

Some studies have been conducted to improve the representation of hydrological connectivity in SWAT. These studies focus on improving (1) the hydrological connectivity between river segments in the river network (e.g., [Kim and Lee, 2010](#); [Nguyen et al., 2018a](#); [Pati et al., 2018](#)), (2) the hydrological connectivity between HRUs within a subbasin (e.g., [Arnold et al., 2010](#); [Rathjens et al., 2015](#)), and (3) hydrological connectivity in the subsurface (e.g., [Bailey et al., 2016](#); [Kim et al., 2008](#)).

[Kim and Lee \(2010\)](#) found that the Muskingum routing method used in SWAT is inappropriate for estimating the shape and magnitude of the flood wave as it moves from the upstream to downstream. The Muskingum method used in SWAT ([Cunge, 1969](#); [USDA, 2004](#)) could cause unphysical oscillations during the recession and an underestimation of the peak flows. The modified Muskingum method proposed by [Kim and Lee \(2010\)](#) was proved to be an error-free and a robust approach for stream routing. [Nguyen et al. \(2018a\)](#) integrated SWAT with the HEC-RAS model (which uses the hydraulic method for flood routing). HEC-RAS model has been widely used to simulate hydrological connectivity in the stream network. Results showed that the coupled model could represent changes of the flood waves better than the original SWAT. [Pati et al. \(2018\)](#) replaced the Muskingum routing method in SWAT with the variable parameter MacCarthy-Muskingum (VPMM). They found that the VPMM could account for the nonlinear behavior of the flood wave in small slope and steep slope channels.

For improving the representation of hydrological connectivity between landscape units in SWAT, different landscape delineation techniques were proposed, e.g., the catena and grid delineation techniques ([Arnold et al., 2010](#); [Rathjens et al., 2015](#)). With these delineation techniques, the spatial location of each landscape unit is identified for flow routing. Therefore, the flow routing between these landscape units is possible. With the catena

approach, the basin is divided into a divide, hillslope, and valley bottom (Figure 1.4). Hydrological connectivity between the divide, hillslope, and valley bottom can be represented by surface runoff, lateral flow, and groundwater flow between these landscape units (Figure ?? Arnold et al., 2010). The catena approach could be used to assess the impact of upslope management on downslope landscape units (Arnold et al., 2010).

In the catena approach, flow is routed according to the surface topographic gradient (from the divide to the hillslope and the valley bottom). In lowland regions, however, the topographic gradient could be small and groundwater flow might not follow the surface topographic gradient. In addition, the catena approach only simulates hydrological connectivity within a basin. Therefore, the catena approach is not applicable for modeling interbasin groundwater flow. Furthermore, there is no general technique for an automatic delineation using the catena approach (Arnold et al., 2010; Gallant and Dowling, 2003).

In the grid base version, the basin is divided into grid cells. Surface and subsurface runoff follow surface topographic gradient. Hydrological connectivity between grid cells was simulated in the same way as the catena approach (Figure 1.5). The application of the grid version of SWAT, however, is not difficult for large river basins (Arnold et al., 2010). This is because of the extensive requirements of input data and computational capacity (Arnold et al., 2010).



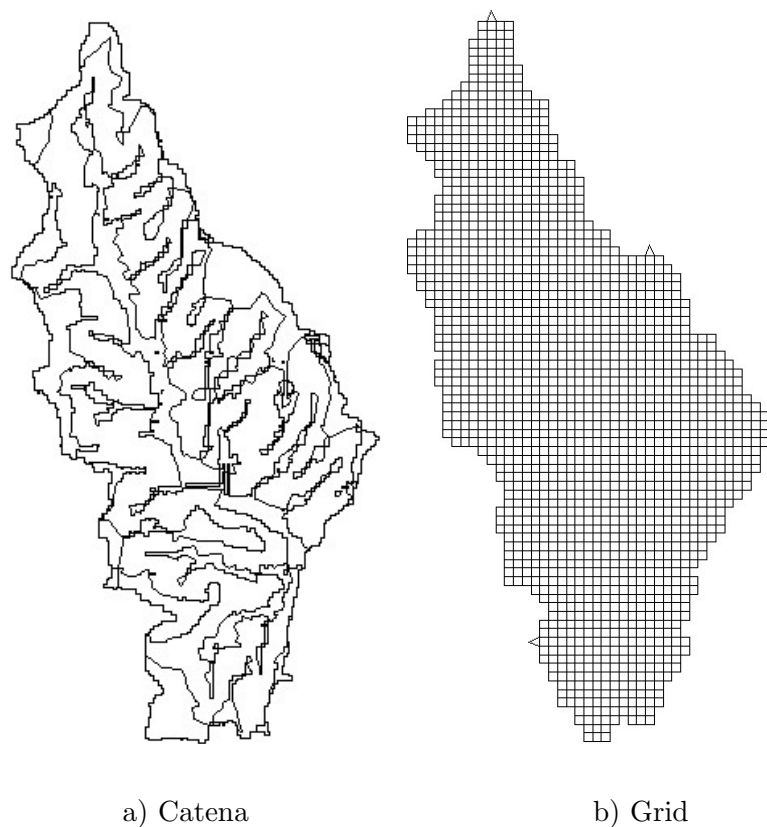


Figure 1.4: Discretization of the basin using a) the catena and b) grid approaches in SWAT (Arnold et al., 2010).

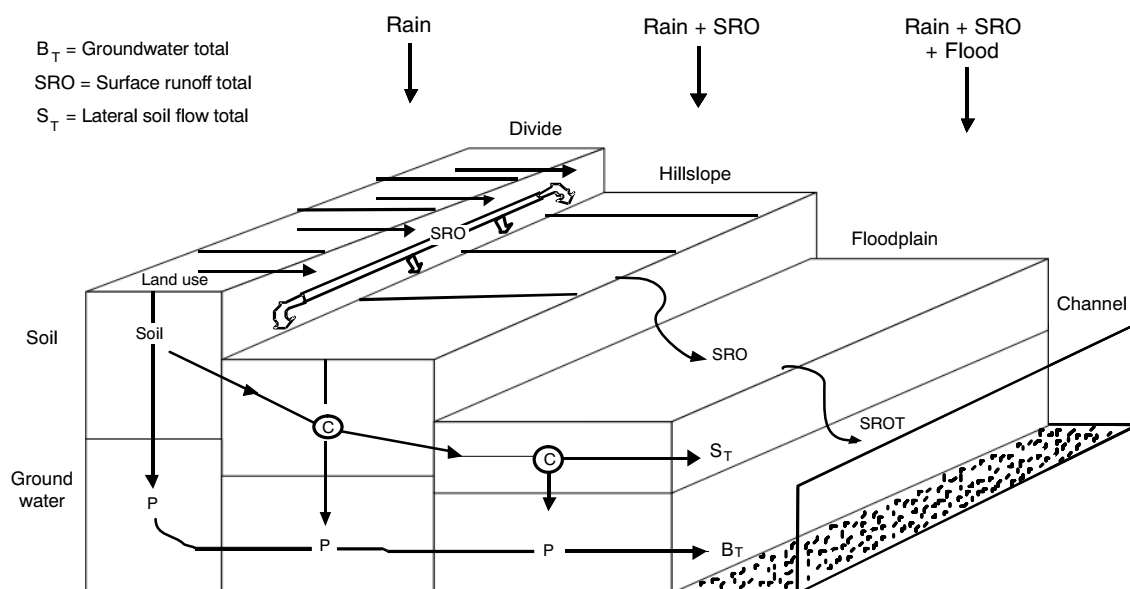


Figure 1.5: Hydrological connectivity between different landscape units in the grid-based SWAT model (Arnold et al., 2010).

Recent studies have integrated SWAT with the Modular Three-Dimensional Finite-Difference Ground-Water Flow Model (MODFLOW, Harbaugh and McDonald, 1996) to improve the subsurface hydrological connectivity (Kim et al., 2008). In this integrated SWAT-MODFLOW model, SWAT is used to simulate land surface processes and soil-water dynamics. The percolated water out of the soil profile from SWAT is considered as input (groundwater recharge) for the MODFLOW model Fig. 1.6. Results show that the couple SWAT-MODFLOW model was able to capture surface, subsurface flow, and river-aquifer interaction better than the original SWAT model (Kim et al., 2008). However, the MODFLOW model is a physically-based distributed groundwater model, which requires extensive input data and computational time. In regions where hydrogeological data are scarce, the applicability and performance of the SWAT-MODFLOW are questionable.

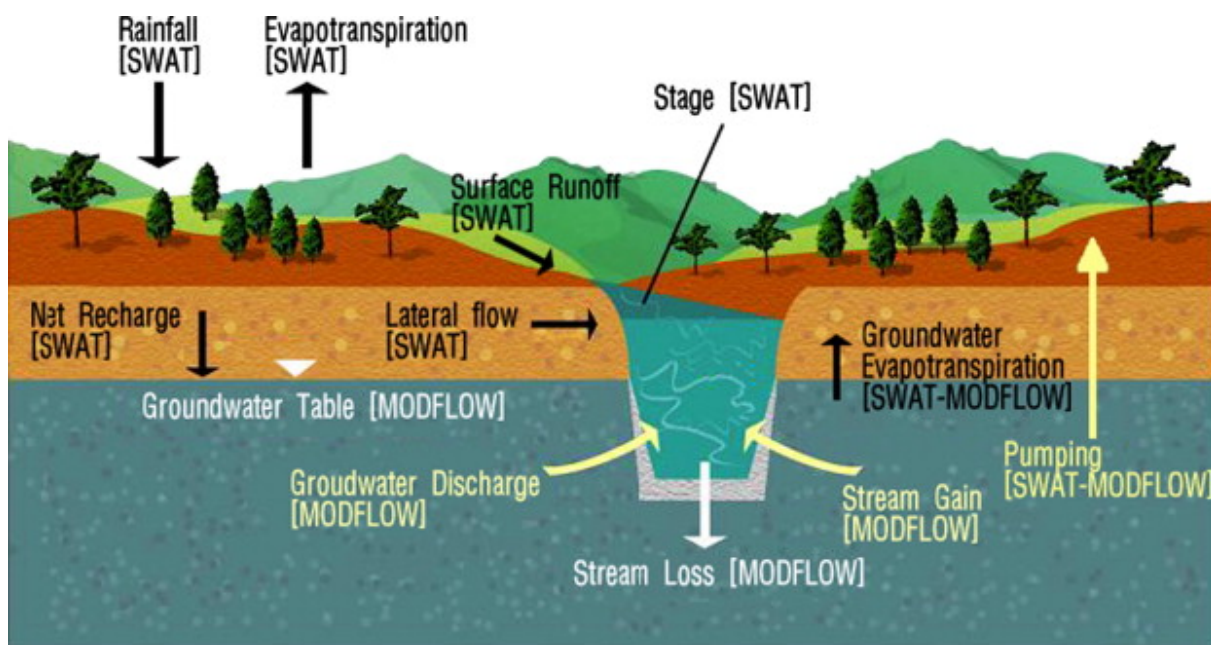


Figure 1.6: The schematic description of the SWAT-MODFLOW model (Kim et al., 2008).

For improving the simulation of hydrological connectivity in karst areas, different versions of the modified SWAT model were introduced, e.g., the KarstSWAT (Palanisamy and Workman, 2014) and KSWAT (Malagó et al., 2016; Nerantzaki et al., 2015) models. The KarstSWAT model was developed mainly to represent the hydrological connection between sinkholes and springs (flow from sinkholes to springs). However, springs could be fed by diffuse recharge sources (areal recharge). The KSWAT model combines the two sub-models, the *adapted SWAT model* (Fig. 3, Malagó et al., 2016) and the *karst-flow model* (Nikolaidis et al., 2013). The KSWAT model assumes that percolated water out of the soil profile is karst groundwater recharge (Fig. 3, Malagó et al., 2016). This assumption might be invalid if the underlying aquifer of a subbasin is not entirely a karst aquifer

(e.g., Palanisamy and Workman, 2014). In this case, part of the infiltrated water could be hydrologically connected with streamflow in form of lateral flow and baseflow. In addition, the *adapted SWAT model* does not differentiate different components of recharge (concentrated recharge and diffuse recharge). The *karst-flow model* uses the two-linear-storage reservoir model to represent the hydrological connection between recharge (which is simulated by the *adapted SWAT model* or from the original SWAT model) and spring. Discharge from the two reservoirs of the *karst-flow model* represents discharge from the conduit system and matrix (Malagó et al., 2016). The KSWAT model does not differentiate between diffuse recharge and concentrated recharge, and between matrix storage and conduit storage.

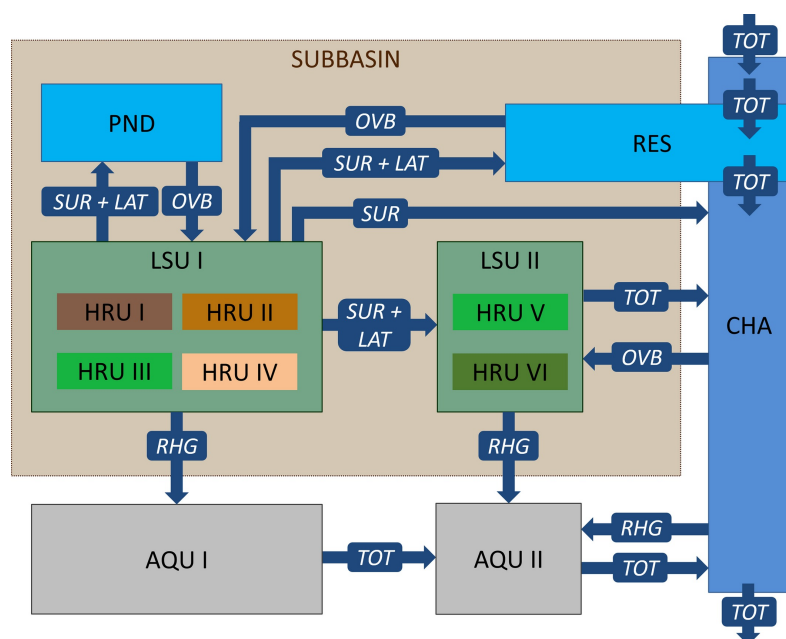


Figure 1.7: Hydrological connectivity between different spatial objects in SWAT+ (Bieger et al, 2017). SUR is surface runoff, LAT is lateral flow, RHG is groundwater recharge, TOT is total flow.

A recent revised version of SWAT, so-called SWAT+, has been developed and could be used to simulate hydrological connectivity in a very flexible way (Bieger et al, 2017). Within SWAT+, landscape units (LUs), HRUs, aquifer (AQU), channel (CHA), reservoir (RES), pond (PND) are considered as different spatial objects. The hydrological connection between these spatial objects is defined by the users (Figure 1.7). The aquifer delineation in SWAT+ is no longer tied to HRU and basin delineation. Due to the flexibility of SWAT+, it could be used to represent various kinds of hydrological connections. For example, SWAT+ was used to represent the hydrological connection between upland areas, flood plain, and river (Bieger et al, 2019). The SWAT+ model could potentially

be used to simulate interbasin groundwater flow by hydrologically connecting different aquifer units. However, the main difficulties with SWAT+ are the identification (or verification) of the hydrological connection and its magnitude between different spatial objects. For a large river basin that has numerous spatial objects, defining these connections could require extensive work.

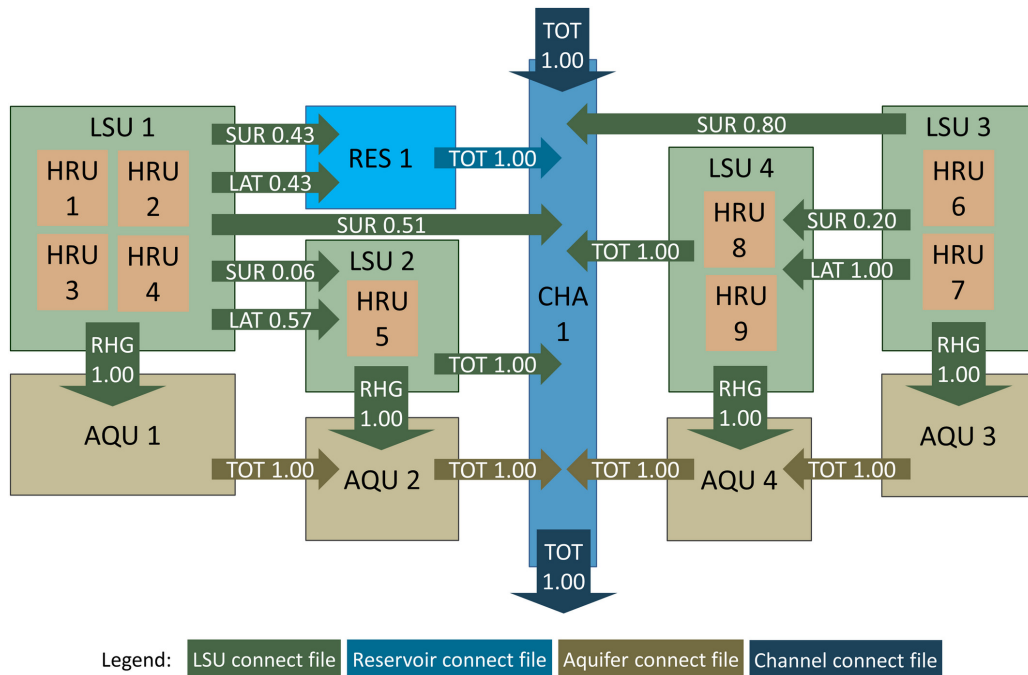


Figure 1.8: Representation of hydrological connectivity between upland area, floodplain, and river in SWAT+ (Bieger et al., 2019).

Compared to the original SWAT model, the SWAT+ model has a higher number of model parameters due to the additional parameters for defining the hydrological connection between different spatial objects. The uncertainty and equifinality of the additional parameters introduced in SWAT+ have not been fully explored. The magnitude of hydrological connection between different spatial objects in SWAT+ is often difficult to validate directly/indirectly with measured/observed data. Therefore, the improvement of the SWAT+ model compared to the SWAT is in question.

Besides the major changes to the SWAT model structure as aforementioned, there have been several minor changes to improve the representation of hydrological connectivity. For example, (Rahman et al., 2016) modified the wetland module of SWAT to improve the representation of hydrological connectivity between riparian depressional wetlands, rivers, and aquifers. Hoang et al (2017) added a routing function to hydrological connect the upland areas with the riparian zones.

### 1.3 Research Objectives and Methodology

The main objective of this research is to improve the representation of hydrological connectivity in a conceptual distributed model, the Soil and Water Assessment Tool (SWAT) model. Specifically, the hydrological connectivity in this research refers to (1) the hydrological connection between river segments in the river network, (2) the regional groundwater flow (interbasin groundwater flow) in porous aquifers, and (3) the regional groundwater flow in karst-dominated aquifers.

To have a better understanding of the hydrological connectivity between river segments in the river network, a detailed review and testing of the flood routing methods (Muskingum and variable storage method) of SWAT were conducted. The advantages and disadvantages of each routing method were discussed. The flood routing subroutines of SWAT were tested and validated separately from other subroutines. Testing the flood routing is one of the prerequisite objectives. This is because the flood routing is one of the main components of the model. It describes the changes of the flood waves along the river network. In other words, it describes the hydrological connection and the transformation of the flood wave as it moves from upstream to downstream sections of a reach.

To represent hydrological connectivity in porous aquifers, a different delineation technique for the subsurface was proposed. The new delineation technique is expected to be simple and can be done automatically. In addition to the new discretization technique, a physically-sound approach for modeling hydrological connectivity between the subsurface units were proposed. For these aforementioned objectives, the Thiessen polygon technique was used for delineating the aquifer and Darcy's law was used to simulate flow between aquifer units. A linear-storage reservoir was used to simulate the hydrological connection (via baseflow) between the aquifer and stream. The proposed model should be able to capture groundwater flow dynamics and surface runoff

For a better representation of hydrological connectivity in karst-dominated aquifers, a new discretization technique was introduced. The proposed discretization is expected to be independent of the surface topographic basin and be able to differentiate between karst and non-karst areas, karst recharge and discharge areas. To achieve these objectives, the discretization technique was based on the geological map and information obtained tracer tests. This is because the information obtained from tracer tests indicates the hydrological between different areas in the karst region. For modeling hydrological connectivity between different areas in karst areas, a two-reservoir model was proposed to represent different types of recharge and discharge in the karst area.

The overall results of this research are expected (1) to have a better simulation of hydrological connectivity between different river segments in the river network, and (2) to offer a compromise solution between physically based and conceptual models for simulating regional groundwater in porous aquifers and (3) to have new approach for simulating interbasin groundwater flow in karst-dominated aquifers. Although the SWAT model was specially selected in this study, the methodology presented here could also be applied for other conceptual distributed models.

## 1.4 Thesis Structure and Author Contribution

The remainder of this study was structured as follows.

1. Chapter 2 presents an approach for improving the simulation of hydrological connectivity between river segments in the river network with SWAT. In this chapter, the two flood routing techniques used in SWAT as well as their implementations in the code were reviewed and discussed. Application and testing of the revised code for flood routing in a reach segment located in the Wesser catchment were presented.

Chapter 2 is the paper *Verification and Correction of the Hydrologic Routing in the Soil and Water Assessment Tool* published in *Water* (Nguyen et al., 2018). In this paper, the author contributed to the formulation of the idea, reviewing and developing the model code, and writing of the paper.

2. Chapter 3 presents a solution for improving the simulation of regional groundwater flow in porous aquifers. In this chapter, different approaches as well as their advantages and disadvantages for simulating hydrological connectivity (regional groundwater flow) in porous aquifers were discussed. It is followed by a description of the modified groundwater module using the Multicell Aquifer Model (MCA). The case study section presents the application of the proposed models in two different sub-basins located in Niedersachsen, Germany. The remainders of chapter 3 represent the model results, discussion, conclusion and recommendations.

Chapter 3 is the paper *Modification of the SWAT Model to Simulate Regional Groundwater Flow Using A Multi-Cell Aquifer* published in *Hydrological Processes* (Nguyen and Dietrich, 2018). In this paper, the author developed the idea, wrote the paper, and set up test cases with the co-author. The model code was written by the author.

3. Chapter 4 introduces a new approach for improving the simulation of subsurface connectivity in karst-dominated aquifers. In this chapter, a detailed review of the karst system and its hydrological characteristics were presented. Different models for simulating hydrological connectivities in the karst aquifer, especially inter-basin groundwater flow between different basins, were discussed. It is followed by the formulation of the modified SWAT model using a two-reservoir model and the case study in southwest Harz Mountains, Niedersachsen, Germany. The result and discussions, conclusion and recommendations were presented in the remainders of chapter 3.

This chapter is the paper *Modeling Interbasin Groundwater Flow in Karst Areas: Model Development, Application, and Calibration Strategy* published in the Environmental Modelling and Software (Nguyen et al., 2020). In this paper, the author formulated the problem, test case study and wrote the paper with the co-authors. The model code was written by the author.

4. Chapter 5 summarizes the main findings from this research. In addition, this chapter also provides some suggestions for further improvements of the original SWAT as well as the modified SWAT model in this study.

## Bibliography

- Allen, P.A., 2009. Earth surface processes. John Wiley & Sons.
- Arnold, J.G., Allen, P.M., Volk, M., Williams, J.R., Bosch, D.D., 2010. Assessment of different representations of spatial variability on SWAT model performance. Transactions of the ASABE, 53(5), 1433-1443.
- Arnold, J.G., Fohrer, N., 2005. SWAT2000: Current capabilities and research opportunities in applied watershed modelling. Hydrological Processes, 19(3), 563-572.
- Arnold, J.G., Srinivasan, R., Muttiah, R.S., Williams, J.R., 1998. Large area hydrologic modeling and assessment. Part I: model development. Journal of the American Water Resources Association, 34(1), 73-89.
- Bailey, R.T., Wible, T.C., Arabi, M., Records, R.M., Ditty, J., 2016. Assessing regional-scale spatio-temporal patterns of groundwater–surface water interactions using a coupled SWAT-MODFLOW model. Hydrological Processes, 30(23), 4420-4433.



- Bergström, S., 1992. The HBV model: Its structure and applications. Report Hydrology No. 4, Swedish Meteorological and Hydrological Institute.
- Bieger, K., Arnold, J. G., Rathjens, H., White, M. J., Bosch, D. D., Allen, P. M., 2019. Representing the Connectivity of Upland Areas to Floodplains and Streams in SWAT+. JAWRA Journal of the American Water Resources Association.
- Bieger, K., Arnold, J. G., Rathjens, H., White, M. J., Bosch, D. D., Allen, P. M., Volk, M., Srinivasan, R., 2017. Introduction to SWAT+, a completely restructured version of the soil and water assessment tool. JAWRA Journal of the American Water Resources Association, 53(1), 115-130.
- Bracken, L.J., Wainwright, J., Ali, G.A., Tetzlaff, D., Smith, M.W., Reaney, S.M., Roy, A.G., 2013. Concepts of hydrological connectivity: research approaches, pathways and future agendas. Earth-Science Reviews, 119, 17-34.
- Covino, T., 2017. Hydrologic connectivity as a framework for understanding biogeochemical flux through watersheds and along fluvial networks. Geomorphology, 277, 133-144.
- Cunge, J.A., 1969. On the subject of a flood propagation computation method (Muskingum method). Journal of Hydraulic Research, 7, 205-230.
- Devia, G.K., Ganasri, B.P., Dwarakish, G.S., 2015. A review on hydrological models. Aquatic Procedia, 4, 1001-1007.
- Flanagan, D.C., Nearing, M. A., 1995. USDA-Water Erosion Prediction Project: Hillslope profile and watershed model documentation (Vol. 10, pp. 1603-1612). NSERL report.
- Gallant, J.C., Dowling, T.I., 2003. A multiresolution index of valley bottom flatness for mapping depositional areas. Water Resources Res. 39(12), 1347.
- Garven, G., 1995. Continental-scale groundwater flow and geologic processes. Annual Review of Earth and Planetary Sciences, 23(1), 89-117.
- Gleick, P. H., 1993. Water in crisis. Pacific Institute for Studies in Dev., Environment & Security. Stockholm Env. Institute, Oxford Univ. Press.
- Harbaugh, A. W., McDonald, M.G., 1996. User's documentation for MODFLOW-96, an update to the US Geological Survey modular finite-difference ground-water flow model. US Geol. Surv., Open-File Rep. 96-485, 56.



- Hoang, L., van Griensven, A., Mynett, A., 2017. Enhancing the SWAT model for simulating denitrification in riparian zones at the river basin scale. *Environmental modelling & software*, 93, 163-179.
- Imamura, F., Van To, D., 1997. Flood and typhoon disasters in Viet Nam in the half century since 1950. *Natural Hazards*, 15 (1), 71-87.
- Kim, N. W., Chung, I. M., Won, Y. S., Arnold, J. G., 2008. Development and application of the integrated SWAT–MODFLOW model. *Journal of Hydrology*, 356(1-2), 1-16.
- Kim, N. W., Lee, J., 2010. Enhancement of the channel routing module in SWAT. *Hydrological Processes*, 24(1), 96-107.
- Kolditz, O., Bauer, S., Bilke, L., Böttcher, N., Delfs, J. O., Fischer, T.,..., Park, C. H., 2012. OpenGeoSys: an open-source initiative for numerical simulation of thermo-hydro-mechanical/chemical (THM/C) processes in porous media. *Environmental Earth Sciences*, 67(2), 589-599.
- Kumar, R., L. Samaniego, S. Attinger. 2013: Implications of distributed hydrologic model parameterization on water fluxes at multiple scales and locations, *Water Resour. Res.*, 49(1), 360-379.
- Leavesley, G.H., Lichty, R.W., Troutman, B., Saindon, L.G., 1983. Precipitation-runoff modelling system. User's manual. USGS Water Resour. Inst., Report 83-4238.
- Lehner, B., Döll, P., Alcamo, J., Henrichs, T., Kaspar, F., 2006. Estimating the impact of global change on flood and drought risks in Europe: a continental, integrated analysis. *Climatic Change*, 75(3), 273-299.
- Lindström, G., Pers, C., Rosberg, J., Strömqvist, J., Arheimer, B., 2010. Development and testing of the HYPE (Hydrological Predictions for the Environment) water quality model for different spatial scales. *Hydrology research*, 41 (3-4), 295-319.
- Liu, J., Liu, T., Bao, A., De Maeyer, P., Feng, X., Miller, S. N., Chen, X., 2016. Assessment of different modelling studies on the spatial hydrological processes in an arid alpine catchment. *Water resources management*, 30(5), 1757-1770.
- Malagó, A., Efstathiou, D., Bouraoui, F., Nikolaidis, N.P., Franchini, M., Bidoglio, G., Kritsotakis, M., 2016. Regional scale hydrologic modeling of a karst-dominant geomorphology: the case study of the Island of Crete. *Journal of Hydrology*, 540, 64-81.

- Markstrom, S.L., Regan, R.S., Hay, L.E., Viger, R.J., Webb, R.M.T., Payn, R.A., and LaFontaine, J.H., 2015. PRMS-IV, the precipitation-runoff modeling system, version 4, U.S. Geological Survey Techniques and Methods.
- Moore, R.J., 2007. The PDM rainfall-runoff model, *Hydrology and Earth System Sciences*, 11, 483-499.
- Neitsch, S.L., Arnold, J.G., Kiniry, J.R., Williams, J.R., 2011. Soil and Water Assessment Tool theoretical documentation version 2009. Grassland, Soil and Water Research Laboratory, Agricultural Research Service and Blackland Research Center, Texas Agricultural Experiment Station, Temple, Texas.
- Nerantzaki, S.D., Giannakis, G.V., Efstathiou, D., Nikolaidis, N.P., Sibetheros, I.A., Karatzas, G.P., Zacharias, I., 2015. Modeling suspended sediment transport and assessing the impacts of climate change in a karstic Mediterranean watershed. *Science of the Total Environment*, 538, 288-297.
- Nikolaidis, N.P., Bouraoui, F., Bidoglio, G., 2013. Hydrologic and geochemical modeling of a karstic Mediterranean watershed. *J. Hydrol.* 477, 129–138.
- Niraula, R., Kalin, L., Srivastava, P., Anderson, C. J. (2013). Identifying critical source areas of nonpoint source pollution with SWAT and GWLF. *Ecological Modelling*, 268, 123-133.
- Nguyen, K.L., Nguyen, D.L., Tu, L. H., Hong, N. T., Truong, C. D., Tram, V. N. Q., ..., Jeong, J., 2018. Automated procedure of real-time flood forecasting in Vu Gia–Thu Bon river basin, Vietnam by integrating SWAT and HEC–RAS models. *Journal of Water and Climate Change*.
- Nguyen, V.T., Dietrich, J., Uniyal, B., Tran, D.A., 2018. Verification and Correction of the Hydrologic Routing in the Soil and Water Assessment Tool. *Water*, 10, 1419.
- Nguyen, V.T., Dietrich, J., 2018. Modification of the SWAT model to simulate regional groundwater flow using a multicell aquifer. *Hydrological Processes*, 32(7), 939-953.
- Nguyen, V. T., Dietrich, J., Uniyal, B., 2020. Modeling Interbasin Groundwater Flow in Karst Areas: Model Development, Application, and Calibration Strategy. *Environmental Modelling & Software*, 124, 104606.
- Nielsen, S.A., Hansen, E., 1973. Numerical simulation of the rainfall runoff process on a daily basis. *Nordic Hydrology*, 4, 171–190

- Nordstrom, K. M., Gupta, V. K., Chase, T. N., 2005. Role of the hydrological cycle in regulating the planetary climate system of a simple nonlinear dynamical model. *Nonlinear Processes in Geophysics*, 12(5), 741-753.
- Oki, T., Kanae, S., 2006. Global hydrological cycles and world water resources. *Science*, 313 (5790), 1068-1072.
- Pai, N., Saraswat, D., 2011. SWAT2009.LUC: A tool to activate the land use change module in SWAT 2009. *Transactions of the ASABE*, 54(5), 1649-1658.
- Palanisamy, B., Workman, S.R., 2014. Hydrologic modeling of flow through sinkholes located in streambeds of Cane Run stream, Kentucky. *Journal of Hydrologic Engineering*, 20(5), 04014066.
- Pati, A., Sen, S., Perumal, M. (2018). Modified channel-routing scheme for SWAT model. *Journal of Hydrologic Engineering*, 23(6), 04018019.
- Piao, S., Ciais, P., Huang, Y., Shen, Z., Peng, S., Li, J.,..., Friedlingstein, P., 2010. The impacts of climate change on water resources and agriculture in China. *Nature*, 467, 43-51.
- Pringle, C., 2003. What is hydrologic connectivity and why is it ecologically important?. *Hydrological Processes*, 17(13), 2685-2689.
- Rahman, M. M., Thompson, J. R., Flower, R. J., 2016. An enhanced SWAT wetland module to quantify hydraulic interactions between riparian depressional wetlands, rivers and aquifers. *Environmental Modelling & Software*, 84, 263-289.
- Rathjens, H., Oppelt, N., Bosch, D. D., Arnold, J. G., Volk, M., 2015. Development of a grid-based version of the SWAT landscape model. *Hydrological Processes*, 29(6), 900-914.
- Samaniego L., R. Kumar, S. Attinger, 2010. Multiscale parameter regionalization of a grid-based hydrologic model at the mesoscale. *Water Resources Research*, 46, W05523.
- Shiklomanov, I. A., 1998. World water resources: A new appraisal and assessment for the 21st century: A summary of the monograph world water resources. UNESCO.
- Srinivasan, M. S., McDowell, R. W., 2009. Identifying critical source areas for water quality: 1. Mapping and validating transport areas in three headwater catchments in Otago, New Zealand. *Journal of Hydrology*, 379(1-2), 54-67.

Therrien, R., McLaren, R., Sudicky, E., Panday, S., 2009. Hydrogeosphere — A Three-dimensional Numerical Model Describing Fully-integrated Subsurface and Surface Flow and Solute Transport. Univ. of Waterloo, Waterloo.

Tockner, K., Pennetzdorfer, D., Reiner, N., Schiemer, F., Ward, J. V., 1999. Hydrological connectivity, and the exchange of organic matter and nutrients in a dynamic river–floodplain system (Danube, Austria). *Freshwater Biology*, 41(3), 521-535.

Willems, P., 2014. Parsimonious Rainfall-runoff Model Construction Supported by Time Series Processing and Validation of Hydrological Extremes – Part 1: Step-wise Model-Structure Identification and Calibration Approach. *Journal of Hydrology*, 510, 578–590.

United States Department of Agriculture-Natural Resources Conservation Service, 2004. National Engineering Handbook: Part 630-Hydrology, USDA Soil Conservation Service: Washington, DC, USA.

## Chapter 2

# Verification and Correction of the Hydrologic Routing in the SWAT

Nguyen, V. T., Dietrich, J., Uniyal, B., Tran, D. A., 2018. Verification and Correction of the Hydrologic Routing in the Soil and Water Assessment Tool. *Water*, 10, 1419.

### Abstract

The Soil and Water Assessment Tool (SWAT) is one of the most widely used eco-hydrological models. SWAT has been undergoing constant changes since its development. However, compartment review and testing of SWAT, especially the hydrologic routing functions, are comparably limited. In this study, the daily hydrologic routing subroutines of different SWAT versions were reviewed and tested using a well observed segment of the Weser River located in Germany. Results show several problems with the routing subroutines of SWAT. The variable storage subroutine of SWAT (Revision 664) does not transform the stream flow. Unphysical results could be obtained with the variable storage routing of SWAT (Revision 528). The Muskingum subroutine of SWAT (Revisions 664 and 528) overestimates daily channel evaporation (resulting in a bias of up to 6.3% in streamflow in our case studies) and underestimates daily transmission losses. Simulated results show that the timing and shape of flood waves, as well as the volume of low flows, could be improved with a corrected Muskingum subroutine. Based on the results of this study, we suggest that the SWAT user community review their existing SWAT models to see how the aforementioned issues will affect their methods, findings, and conclusions.

*Keywords:* SWAT; hydrologic routing; flood routing; low flow; Muskingum; variable

*storage*

## 2.1 Introduction

Flood routing is predicting the timing and magnitude of a flood wave at a downstream point of a reach from the known data at an upstream point (Chow, 1964). It plays an important role in flood forecasting, reservoir design, and flood control. In semi-distributed hydrologic models, simplified hydrologic routing methods are often applied for flood routing instead of hydraulic methods. Hydrologic routing also serves as a basic function for sediment and nutrient routing (Arnold et al., 1998). The parameters of hydrologic models are often calibrated against observed streamflow, sediment, and/or nutrient yields. Therefore, having a robust and well-tested hydrologic routing function in hydrologic models is important.

The Soil and Water Assessment Tool (SWAT) is a conceptual semi-distributed hydrologic model used to predict the effect of land use management practices on water, sediment, and nutrient yield (Arnold et al., 1998; Neitsch et al., 2011). SWAT has been undergoing constant changes since its development (Krysanova et al., 2008). SWAT has been tested and applied worldwide (Arnold et al., 2005; Krysanova et al., 2008; Gassman et al., 2007). However, compartment verification of SWAT is limited, especially regarding its hydrologic routing functions.

With SWAT, users can select either the variable storage method (Williams, 1969) or the Muskingum method (Cunge, 1969; USDA, 2004) for hydrologic routing (Neitsch et al., 2011). There have been some modifications to the routing functions in SWAT, e.g., (Kim and Lee, 2010; Pati et al., 2018). Kim and Lee (Kim and Lee, 2010) suggested implementing a nonlinear storage equation obtained by coupling continuity and Manning's equations, to avoid underestimation of peak flows and false signals during the recession period with the Muskingum used in SWAT. Pati et al. (Pati et al., 2018) replaced the Muskingum used in SWAT with the variable parameter McCarthy–Muskingum to enhance channel routing. In the official SWAT revisions (<https://swat.tamu.edu/>), however, the model uses the two aforementioned methods (Cunge, 1969; USDA, 2004; Williams, 1969) for hydrologic routing. Despite this, our preliminary studies show that there is a significant difference in terms of simulated streamflow between the two methods and between the same method in different SWAT versions (as shown in Section 2.4).

The main objective of this study is to explain the differences in simulated stream-

flow and motivate users of the model to draw more attention to the hydrologic routing processes. This study provides (1) an overview into the technical aspects of the two hydrologic routing methods used in SWAT, (2) an insight to the code implementation of these concepts in different SWAT revisions, and (3) an improvement of the SWAT hydrologic routing functions. A case study for a well observed segment of the Weser River, Germany, is used as a verification example.

## 2.2 Theoretical Background

### 2.2.1 Variable Storage Method

The variable storage method is based on the continuity equation ([Williams, 1969](#)):

$$I - O = \frac{dS}{dt} \quad (2.1)$$

where  $I$  ( $\text{m}^3/\text{s}$ ) and  $O$  ( $\text{m}^3/\text{s}$ ) are the inflow and outflow rate for a river reach, respectively,  $t$  (s) is the time,  $S$  ( $\text{m}^3$ ) is the storage. In discrete form, Equation 2.1 becomes

$$\Delta t \cdot \frac{I_1 + I_2}{2} - \Delta t \cdot \frac{O_1 + O_2}{2} = S_2 - S_1 \quad (2.2)$$

where the subscripts “1” and “2” refer to the start and end of the routing time interval  $\Delta t$  (s), respectively. Equation 2.2 can be rearranged to have the following form:

$$I_a + \frac{S_1}{\Delta t} - \frac{O_1}{2} = \frac{S_2}{\Delta t} + \frac{O_2}{2} \quad (2.3)$$

where  $I_a = 0.5(I_1 + I_2)$  is the average inflow rate during the time interval. The travel time,  $T$  (s), is calculated as follows:

$$T = \frac{S_1}{O_1} = \frac{S_2}{O_2} \quad (2.4)$$

Equation 2.3 can be rewritten using Equation 2.4 to obtain the relation between the storage coefficient and the travel time:

$$I_a + \frac{S_1}{\frac{\Delta t}{T} \cdot \frac{S_1}{O_1}} - \frac{O_1}{2} = \frac{S_2}{\frac{\Delta t}{T} \cdot \frac{S_2}{O_2}} + \frac{O_2}{2} \quad (2.5)$$

$$O_2 = \frac{2\Delta t}{2T + \Delta t} \cdot I_a - \left(1 - \frac{2\Delta t}{2T + \Delta t}\right) \cdot O_2 \quad (2.6)$$

$$O_2 = C \cdot \left(I_a + \frac{S_1}{\Delta t}\right) \quad (2.7)$$

where  $C$  is the storage coefficient:

$$C = \frac{2\Delta t}{2T + \Delta t}. \quad (2.8)$$

The condition  $C \leq 1$  must be satisfied to avoid unphysical results.

### 2.2.2 Muskingum Method

The Muskingum method is based on the continuity equation (Equation 2.1 and 2.2) and the empirical linear storage equation (Diskin, 1967; USDA, 2004):

$$S = K[X \cdot I + (1 - X) \cdot O] \quad (2.9)$$

where  $S$  ( $\text{m}^3$ ) is the total storage in channel,  $K$  (s) is the storage constant,  $X$  (-) is a weighting factor, ranging from 0 to 0.5, and  $I$  ( $\text{m}^3/\text{s}$ ) and  $O$  ( $\text{m}^3/\text{s}$ ) are inflow and outflow rate. From Equations 2.2 and 2.9, the following relation can be obtained:

$$O_2 = C_1 \cdot I_2 + C_2 \cdot I_1 + C_3 \cdot O_1 \quad (2.10)$$

where

$$C_1 = \frac{\Delta t - 2KX}{2K(1 - X) + \Delta t} \quad (2.11)$$

$$C_2 = \frac{\Delta t + 2KX}{2K(1 - X) + \Delta t} \quad (2.12)$$

$$C_3 = \frac{2K(1 - X) - \Delta t}{2K(1 - X) + \Delta t} \quad (2.13)$$

where  $C_1$ ,  $C_2$ , and  $C_3$  are coefficients. To avoid numerical instability, the following condition must be satisfied:



$$2KX < \Delta t < 2K(1 - X). \quad (2.14)$$

## 2.3 Hydrologic Routing with SWAT

In this section, the daily variable storage and Muskingum method in SWAT2000, SWAT2005, SWAT2009 (Revision 528), and SWAT2012 (Revision 664) are reviewed. The source code of these SWAT versions was downloaded from the official SWAT website (<https://swat.tamu.edu/>). The daily variable storage and Muskingum routing subroutines in these SWAT versions are named “rtday” and “rtmusk,” respectively.

### 2.3.1 Variable Storage Routing Subroutine

The hydrologic routing in SWAT was originally performed only with the variable storage method (Arnold et al., 1995, 1998). Although the four aforementioned SWAT versions were reported to incorporate the variable storage routing method as described in previous sections (Arnold et al., 2012; Neitsch et al., 2005, 2002; Neitsch et al., 2011), our study showed that the rtday subroutine of SWAT2012 did not perform a transformation of the outflow compared to the inflow. In this subroutine, the outflow from a reach was calculated as follows:

$$rtwtr = vc \cdot rcharea \cdot 86400 \quad (2.15)$$

where  $rtwtr$  ( $\text{m}^3$ ) is the outflow volume during a day,  $rcharea$  ( $\text{m}^2$ ) is the cross-sectional area of flow, 86,400 (s) is the number of seconds in a day,  $vc$  (m/s) is the average flow velocity, calculated as using the equation:

$$vc = \frac{sdti}{rcharea} \quad (2.16)$$

where  $sdti$  ( $\text{m}^3/\text{s}$ ) is the average flow rate, calculated as follows:

$$sdti = \frac{vol}{86,400} \quad (2.17)$$

where  $vol$  ( $\text{m}^3$ ) is the volume of water in reach at the beginning of a day and the inflow volume. Combining Equations 2.15, 2.16, and 2.17 yields

$$rtwtr = vol. \quad (2.18)$$

Equation 2.18 shows that the `rtday` subroutine of SWAT2012 does finally not transform the flow hydrograph. The outflow volume is simply assigned as the volume of water in reach at the beginning of a day, i.e., the inflow volume.

In the `rtday` subroutine of other SWAT versions (SWAT2000, SWAT2005, and SWAT2009), routing is performed using Equation 2.7. In these SWAT versions,  $C$  is assigned as 1, if  $C > 1$  to avoid unphysical results. It means that the outflow volume is assigned the total inflow volume and storage volume.

### 2.3.2 Muskingum Routing Subroutine

The Muskingum routing method in SWAT was reported to follow the concept described in the previous section (Arnold et al., 2012; Neitsch et al., 2005, 2002; Neitsch et al., 2011). However, revision of the “`rtmusk`” subroutine in four SWAT versions shows that SWAT2000 and SWAT2005 do not check the numerical stability condition (Equation 2.14). Within SWAT2009 and SWAT2012, if the numerical stability condition is not satisfied, the daily time step is divided into smaller time steps, 12, 6, or 1 h. However, it does not always guarantee the numerical stability condition. In addition, (1) the calculated evaporation in a reach for each sub-daily time step in SWAT2009 and SWAT2012 was taken as daily evaporation and (2) the calculated transmission losses were not summed up during each time step to have the total amount of transmission losses during a day. These result in an overestimation of reach evaporation and underestimation of transmission losses, which, in combination, can affect the SWAT simulated stream flow in different ways depending on the characteristics of the case study area. Due to the calibration of different parameters of the model against streamflow at the outlet, the parameter uncertainty of the model is increased by the reported issues.

In this study, the `rtmusk` routing subroutine of SWAT2012 was modified (1) by changing the calculation of the internal sub-daily time step to ensure that the numerical stability condition (Equation 2.14) is always met and (2) by correcting the summation of daily channel evaporation and transmission losses from internal time steps. The source code of this modified subroutine is available at [https://github.com/tamnva/updated\\_SWAT2012](https://github.com/tamnva/updated_SWAT2012). The storage constant  $K$  in SWAT is a function of the storage time constant of a reach at 0.1 and at 0.9 bankfull (model parameters `MSK_CO1` and `MSK_CO2`). These and the weighting factor  $X$  (parameter `MSK_X`) in the four aforementioned SWAT versions are

user-defined and their usage was not modified in this study.

## 2.4 Verification Examples





### 2.4.1 Study Area and Data


The study area is a segment of the Weser River between Bad Karlshafen and Vlotho located in Lower Saxony and North Rhine-Westphalia, Germany (Figure 2.1). This Weser River segment has a total length of 142 km, an average slope of 0.01%. Daily inflow data at the Karlshafen gauging station and outflow data at the Vlotho gauging station were obtained from the the Wasser und Schifffahrtsdirektion Mitte. Daily streamflow data at three tributary channels were taken from the Niedersächsische Landesbetrieb für Wasserwirtschaft, Küsten- und Naturschutz (NLWKN). The drainage areas corresponding to the Karlshafen and Vlotho gauging stations are 14,790 km<sup>2</sup> and 17,620 km<sup>2</sup>, respectively. The tributary river Emmer was simulated at the gauging station Welsede (509 km<sup>2</sup>). Weather data in this area were taken from the Deutscher Wetterdienst. The Digital Elevation Model (DEM) of 200 m resolution resolution shows that the elevation of the study area varies between 42 and 522 m above mean sea level (a.m.s.l). Land cover and soil maps were obtained from the CORINE Land Cover project and the Bundesanstalt für Geowissenschaften und Rohstoffe (BGR), respectively.

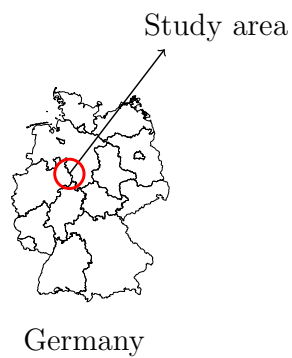
### 2.4.2 Simulation Scenarios

Due to the similarities (1) in the variable storage subroutine between SWAT2000, SWAT2005, and SWAT2009 and (2) in the Muskingum routing subroutine between SWAT2009 and SWAT2012, simulations in this study were only performed with four different routing subroutines (Table 2.1). The numerical instability due to neglecting the condition in Equation 2.14 in the Muskingum routing subroutine of SWAT2000 (or SWAT2005) was discussed in detail by Kim and Lee [Kim and Lee \(2010\)](#). In order to compare the effects of using different hydrologic routing subroutines (Table 2.1) on the simulated streamflow, the runoff generated from the intermediate catchments was simulated using the same subroutines and parameters in all scenarios. This is done to ensure that the simulated runoff entering the Weser River in all simulations is the same. In addition, to minimize the error of simulated flow at the outlet of the study area, (1) observed flow at the Uchtdorf, Afferde, and Welsede gauging stations was used as model inflow condition, and (2) contributing flow from other ungauged tributary channels and intermediate

**Legend**

-  Streamgauge
-  Weser River
-  Tributary channel
-  Subbasin

DEM (a.m.s.l)  
  
522 m  
42 m



0 5 10 20 Kilometers

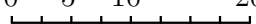


Figure 2.1: Location of the Weser River segment and its tributary rivers.

Table 2.1: List of the hydrologic routing subroutines used for this study.

<b>Flood Routing Subroutine</b>	<b>Description</b>
V2012	Variable Storage routing subroutine of SWAT2012
V2009	Variable Storage routing subroutine of SWAT2009
M2012	Muskingum routing subroutine of SWAT2012
M2012*	corrected Muskingum routing subroutine of SWAT2012

subbasins was simulated by using parameters obtained when calibrating for streamflow at the Welsede gauging station. For hydrologic routing, the best calibrated parameter values of the variable storage and Muskingum in this study are as follows: Manning’s roughness coefficient  $CH\_N(2) = 0.025$ ,  $MSK\_X = 0.25$ ,  $MSK\_CO1 = 0.75$ , and  $MSK\_CO2 = 0.25$ . The channel width (parameter  $CHW2$ ) was overestimated by the ArcSWAT pre-processing and was corrected by evaluating aerial images. The model was simulated for the years 1990–2000. However, in order to demonstrate the hydrologic routing for flood events and for low flow, shorter time periods were evaluated.

### 2.4.3 Results and Discussions

Simulated streamflow at the Vlotho gauging station easily shows by visual evaluation that V2009 and V2012 failed to perform flood routing (Figures 2.2a,c). Nash–Sutcliffe efficiency (NSE, Nash and Sutcliffe, 1970) and percentage bias (PBIAS) show good values due to the high influence of inflow taken from observed values (Table 2.2). For example, (1) the timing of simulated peaks is earlier than the observed and (2) the simulated peaks are higher than the observed. The simulated outflow from V2009 and V2012 is almost identical to inflow. The variable storage method does not show a transformation of the flood wave as it moves downstream. V2012 simply assigns inflow as outflow as previously discussed. The similarities between simulated outflow from V2009 and V2012 are due to the fact that V2009 assigns  $C = 1$  most of the time (to avoid  $C > 1$ ). We found that the unphysical oscillation of simulated flow with V2009 (as shown in the red circles in Figures 2.2a,c) occurs when flow in the channel flood plain occurs (or disappears). This is due to the assumption about the flood plain geometry and the use of the Manning’s equation. The flood plain width in SWAT is assumed five times the top width of the channel. When flow starts to change from non flood-plain flow to flood-plain flow (or from flood-plain flow to non flood-plain flow), there is a sudden increase (or decrease) in the flow velocity, the travel time  $T$ , the storage coefficient  $C$ , and ultimately the simulated outflow. We also

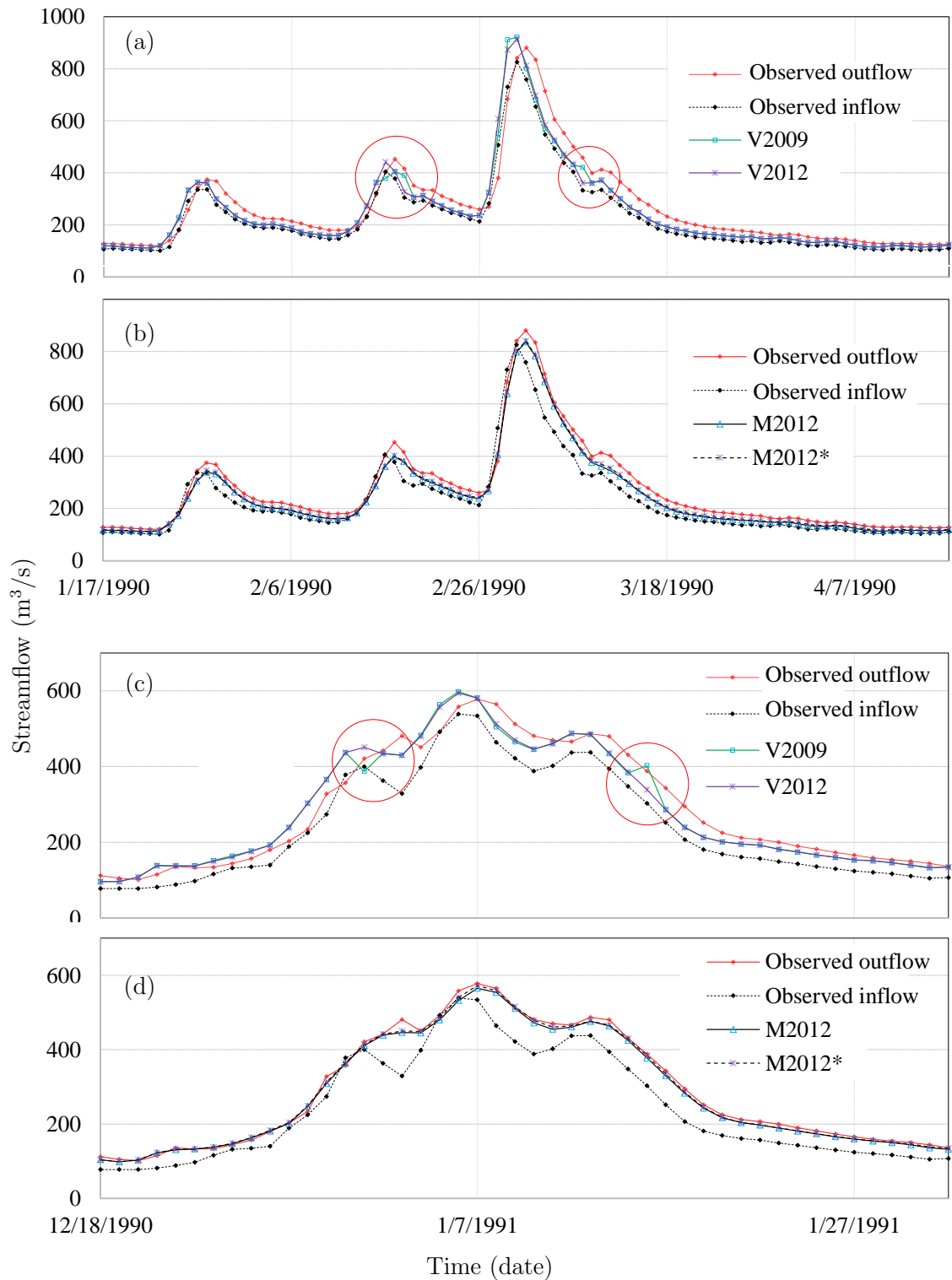


Figure 2.2: Simulated outflow at the Vlotho gauging station for two flood events using (a,c) V2009 and V2012 and (b,d) M2012 and M2012\*.

Table 2.2: Model performance statistics for flood event 1 (17 January 1990 to 17 April 1990, Figures 2.2a,b) and flood event 2 (18 December 1990 to 1 February 1991, Figures 2.2c,d).

Subroutine	Flood Event 1		Flood Event 2	
	NSE	PBIAS	NSE	PBIAS
V2012	0.898	7.24	0.955	1.34
V2009	0.902	7.24	0.953	1.27
M2012	0.975	8.49	0.995	2.35
M2012*	0.981	7.25	0.997	1.49

found that, in the case  $C > 1$ , changing the simulation time step during a simulation in order to have  $C \leq 1$  could also cause the same problem. The simulation time step should be the same for the entire simulation time. A solution to this problem could be selecting a sufficiently small time step (small  $\Delta t$ ) and a sufficiently long river section (high  $T$ ), but this is event-based and reach-specific. Therefore, the V2009 and V2012 are not practical for long-term simulations at basin-scale.

Figures 2.2b,d shows simulated outflow at the Vlotho gauging station using M2012 and M2012\*. It is seen that simulated outflow from M2012 and M2012\* is better than that from V2009 and V2012 (Figures 2.2a,c and Table 2.2). The timing of simulated peaks and the shape of the flood wave matched well with observed outflow. The effect of the overestimation of channel evaporation with M2012 is negligible in this case (Figures 2.2b,d) because the flow rate is high compared to the evaporation rate. The underestimation of flow from M2012 and M2012\* as shown by the PBIAS (Table 2.2) is also due to the underestimation of flow from tributary reach and intermediate subbasins. The effect of overestimating channel evaporation with on simulated streamflow with M2012 during flood events is negligible (Figure 2.2 and Table 2.2).

The effect of overestimation of channel evaporation on simulated streamflow with M2012 is more pronounced when the entire catchment response is evaluated, especially during periods of low flows. Figures 2.3a–c shows the simulated flow duration curves at three gauging stations (Figure 2.1) using M2012 and M2012\* during 1990–2000. It is seen that the effect of overestimating channel evaporation on low flow ( $iQ_{75}$ ) is significant. The simulated streamflow volumes (from 1990 to 2000) with M2012 at the Welsede, Afferde, and Uchtdorf gauging stations are 6.3%, 2.4%, and 4.2%, respectively, less than that with M2012\*. The effect of overestimation of channel evaporation with M2012 is expected to increase with an increase in (1) river density, (2) channel evaporation rate (arid or semi-



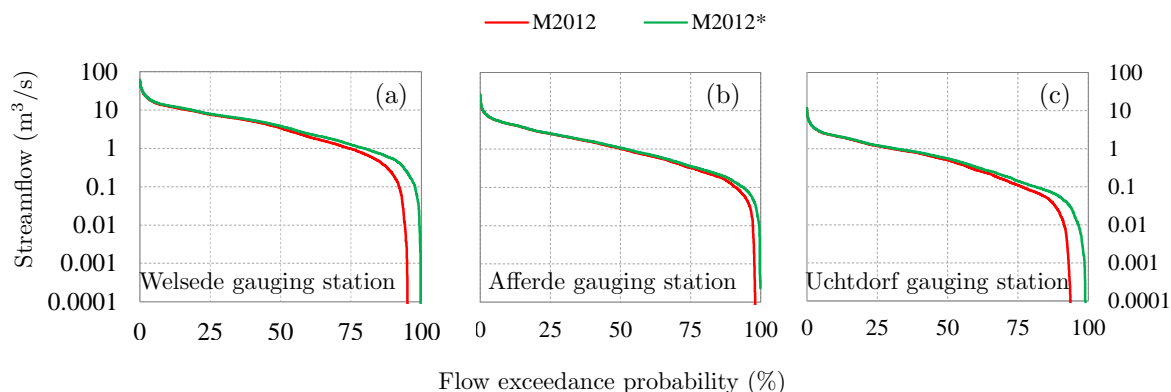


Figure 2.3: Flow duration curves of the simulated streamflow (logarithmic scale) at the (a) Welsede, (b) Afferde, and (c) Uchtdorf gauging stations during 1990–2000 with M2012 and M2012\*.

arid areas), (3) river width/depth ratio, and (4) the number of sub-daily time steps used in the Muskingum routing subroutine.

## 2.5 Conclusions and Recommendations

In this study, we validated and corrected the hydrologic routing subroutines of different SWAT revisions. Results show that there are major issues in both routing subroutines of SWAT, the variable storage and Muskingum. In case of simulation with the variable storage method, (1) SWAT2012 (Revision 664) does not perform hydrologic routing, and (2) unphysical oscillation of simulated flow was observed with SWAT2009 due to the assumption of the flood plain geometry and the use of the Manning’s equation. In case of simulation with the Muskingum subroutine (SWAT2009 Revision 528 and SWAT2012 Revision 664), (1) a high portion if not all of streamflow volume in low flow periods could be lost due to overestimation of channel evaporation, (2) unphysical results could be obtained due to violating the numerical stability condition, and (3) channel transmission loss is underestimated if it is activated. A corrected Muskingum subroutine from SWAT2012 (Revision 664), here called M2012\*, shows a good estimation of the two flood waves in our simulation period and a reduced channel evaporation loss.

Based on the results of this study, we suggest that the SWAT user community check and upgrade their existing SWAT models, which used the aforementioned affected SWAT versions. It is recommended that whether the updated result supports their methods and conclusions be checked. This is especially important for studies focused on (1) basins



with short reaches, and/or (2) low flow simulation, (3) event-based simulation, and/or (4) basins in (semi-) arid regions, where evaporation is high but channel transmission losses can be significant. A bias contribution of streamflow in an order of 5% is considered significant for the calibration of other components of the model, in particular during low flow periods, where soil and groundwater parameters might be estimated wrongly due to the error in channel routing. Although SWAT+ is announced as the next generation of SWAT, there are still many SWAT users working with existing SWAT models. Therefore, verifications of other functions of SWAT are also suggested in order to decrease the model structure uncertainty.

## **Author Contributions:**

V.T.N. and J.D. designed the study. V.T.N. carried out the simulation. V.T.N., D.A.T., and B.U. reviewed the SWAT codes. All authors wrote the draft and contributed to the final version of the manuscript.

## **2.6 Funding**

This research received no external funding. The APC was funded by the Open Access fund of Leibniz Universität Hannover.

## **2.7 Acknowledgments**

The authors thank three anonymous reviewers for their constructive comments which improved the quality of the manuscript.

## **2.8 Conflicts of Interest**

The authors declare no conflict of interest.

## Bibliography

- Arnold, J. G., Fohrer, N., 2005. SWAT2000: Current capabilities and research opportunities in applied watershed modelling. *Hydrol. Process.* 19, 563-572.
- Arnold, J.G., Kiniry, J.R., Srinivasan, R., Williams, J.R., Haney, E.B., Neitsch, S.L., 2012. Soil and Water Assessment Tool Input/Output Documentation 2012, Texas Water Resources Institute Technical Report No. 439, Texas A&M University System: College Station, TX, USA.
- Arnold, J.G., Srinivasan, R., Muttiah, R.S., Williams, J.R., 1998. Large area hydrologic modeling and assessment Part I: Model development. *Trans. ASABE* 34, 73-89.
- Arnold, J.G., Williams, J.R., Maidment, D.R., 1995. Continuous-time water and sediment-routing model for large basins. *J. Hydraul. Eng.* 121, 171-183.
- Chow, V.T., 1964. *Handbook of Applied Hydrology*. McGraw-Hill, New York, NY, USA, 1964.
- Cunge, J.A., 1969. On the subject of a flood propagation computation method (Muskingum method). *J. Hydraul. Res.* 7, 205-230.
- Diskin, M.H., 1967. On the solution of the Muskingum flood routing equation. *J. Hydrol.* 5, 286-289.
- Gassman, P., Reyes, M., Green, C., Arnold, J., 2007. The soil and water assessment tool: Historical development, applications, and future research directions. *Trans. Am. Soc. Agric. Biol. Eng.* 50, 1211-1250.
- Kim, N.W., Lee, J., 2010. Enhancement of the channel routing module in SWAT. *Hydrol. Process.* 24, 96-107.
- Krysanova, V., Arnold, J.G., 2008. Advances in ecohydrological modelling with SWAT—A review. *Hydrolog. Sci. J.* 53, 939-947.
- Nash, J.E., Sutcliffe, J.V., 1970. River flow forecasting through conceptual models. Part 1: A discussion of principles. *J. Hydrol.* 10, 282-290.
- Neitsch, S.L., Arnold, J.G., Kiniry, J.R., Williams, J.R. Soil and Water Assessment Tool Theoretical Documentation Version 2009, Texas Water Resources Institute, Texas A&M University, College Station, TX, USA, 2011.

- Neitsch, S.L., Arnold, J.G., Kiniry, J.R., Williams, J.R., 2005. Soil and Water Assessment Tool Theoretical Documentation Version 2005, Texas Water Resources Institute, Texas A& M University: College Station, TX, USA.
- Neitsch, S.L., Arnold, J.G., Kiniry, J.R., Williams, J.R., King, K.W., 2002. Soil and Water Assessment Tool, Theoretical Documentation, Version 2000, Texas Water Resources Institute, Texas A&M University, College Station, TX, USA.
- Pati, A., Sen, S., Perumal, M., 2018. Modified channel-routing scheme for SWAT model. *J. Hydrol. Eng.* 23, 04018019.
- United States Department of Agriculture—Natural Resources Conservation Service 2004.. *National Engineering Handbook: Part 630—Hydrology*, USDA Soil Conservation Service: Washington, DC, USA.
- Williams, J.R., 1969. Flood routing with variable travel time or variable storage coefficients. *Trans. ASABE* 12, 100-0103.

## Chapter 3

# Modification of the SWAT Model to Simulate Regional Groundwater Flow Using A Multi-Cell Aquifer

Nguyen, V. T., Dietrich, J., 2018. Modification of the SWAT model to simulate regional groundwater flow using a multicell aquifer. *Hydrological Processes*, 32 (7), 939 - 953.

### Abstract

The soil and water assessment tool (SWAT) has been widely used and thoroughly tested in many places in the world. The application of the SWAT model has pointed out that 2 of the major weaknesses of SWAT are related to the nonspatial reference of the hydrologic response unit concept and to the simplified groundwater concept, which contribute to its low performance in baseflow simulation and its inability to simulate regional groundwater flow. This study modified the groundwater module of SWAT to overcome the above limitations. The modified groundwater module has 2 aquifers. The local aquifer, which is the shallow aquifer in the original SWAT, represents a local groundwater flow system. The regional aquifer, which replaces the deep aquifer of the original SWAT, represents intermediate and regional groundwater flow systems. Groundwater recharge is partitioned into local and regional aquifer recharges. The regional aquifer is represented by a multicell aquifer (MCA) model. The regional aquifer is discretized into cells using the Thiessen polygon method, where centres of the cells are locations of groundwater observation wells. Groundwater flow between cells is modelled using Darcy's law. Return flow from cell to

stream is conceptualized using a non-linear storage–discharge relationship. The SWAT model with the modified aquifer module, the so-called SWAT-MCA, was tested in 2 basins (Wipperau and Neetze) with porous aquifers in a lowland area in Lower Saxony, Germany. Results from the Wipperau basin show that the SWAT-MCA model is able (a) to simulate baseflow in a lowland area (where baseflow is a dominant source of streamflow) better than the original model and (b) to simulate regional groundwater flow, shown by the simulated groundwater levels in cells, quite well.

*Keywords:* Baseflow, Groundwater flow, Hydrological connectivity, multicell aquifer, SWAT-MCA

### 3.1 Introduction

Hydrological models are often used to gain understanding of the surface and subsurface hydrologic processes within the interested region. Furthermore, they can be applied as systems analytic tools in water resources management. Hydrological models can be classified into lumped, semidistributed, and fully distributed models (Jajarmizadeh et al., 2012; Pechlivanidis et al., 2011). Lumped models consider a basin as a single unit. Fully distributed models, especially the ones with physically based approach, discretize the basin into grid cells and simulate surface and subsurface flow between these grid cells. However, the use of fully distributed models at the basin scale is often restricted due to extensive data requirements and high computational cost. Semidistributed models appear as compromise models between lumped models and fully distributed models even though semidistributed models often neglect groundwater flow between subbasin units, for example, HBV (Bergström, 1992), SLURP (Kite, 1997), and TOPMODEL (Beven and Kirkby, 1979).

The soil and water assessment tool (SWAT) is a semidistributed hydrological model used to assess the impact of land management practices on water, sediment, and agricultural chemical yields (Neitsch et al., 2011). The SWAT model (a) operates at a basin scale, (b) is continuous in time, (c) is computationally efficient, (d) uses readily available inputs, and (e) is a free and open-source software. SWAT can simulate most aspects of the hydrologic cycle in agricultural catchments and has been widely used and thoroughly tested worldwide (Arnold and Fohrer, 2005; Bieger et al., 2017; Francesconi et al., 2016; Gassman et al., 2007; Strauch et al., 2013; Wagner et al., 2016). Although there exist numerous semidistributed models, few of them can simulate groundwater flow between subbasin units (Efstratiadis et al., 2008; Joodavi et al., 2016; Lindström et al., 2010; Rozos

et al., 2004). However, it is hardly to find a model, which has all of the aforementioned advantages like the SWAT model in agricultural water management at catchment scale. Therefore, the SWAT model was selected for further modification in this study in order to improve its horizontal subsurface hydrological connectivity.

Applications of the SWAT model showed that one of the major weaknesses of SWAT is related to the nonspatial reference of the hydrologic response unit (HRU) concept (Arnold and Fohrer, 2005; Bieger et al., 2017; Bosch et al., 2010; Gassman et al., 2007). HRUs are created by lumping all areas having the same combination of land use, soil type, and slope within a subbasin (Leavesley et al., 1983). The HRU concept is computationally efficient while representing the abovementioned landscape heterogeneity. However, the HRU has no explicit spatial information, which is required to simulate flows between HRUs.

Simulation of groundwater flows between HRUs, subbasins, or different landscape units (LUs) is considered as an important part of water resources management (Refsgaard et al., 2010). In many places, groundwater is considered as one of the main sources for domestic uses and/or irrigation (e.g., Hutson et al., 2004; Siebert et al., 2010; Wittenberg, 2003, 2015). Groundwater flow can alter the overall water budget or affect the subsurface and surface water quality of a region.

In recent years, some studies have been carried out to simulate groundwater flow between different LUs in the SWAT model. Volk et al. (2007) and Arnold et al. (2010) developed a SWAT landscape model by using a catena approach (Kirkby, 1998; Lane and Nearing, 1989) to delineate the basin into three different LUs, the so-called divide, hillslope, and flood plain (each LU can be further delineated into HRUs). Within this approach, groundwater is routed from the divide through the hillslope, the flood plain, and ultimately to the stream as flow through a series of linear storage elements (e.g., Brutsaert, 2005). Rathjens et al. (2015) developed a grid-based version of the SWAT landscape model. In this model, groundwater flow between grid cells is also modelled as flow through a series of linear storage elements. The model performance in streamflow simulation significantly depends on the grid size and the routing algorithm implemented. In addition, this model requires significant computation time (Pignotti et al., 2017). Sun et al. (2016) further developed the SWAT landscape model by delineating the flood plain into three smaller LUs corresponding to flooded areas with different flood return periods. Groundwater flow between LUs within the flood plain and the groundwater–surface water interaction were modelled using Darcy’s law. The model is capable of simulating groundwater levels in the flood plain LUs. Both the models (Sun et al., 2016; Volk et al., 2007), however, only considered groundwater flow driven by topographic gradient (from the di-

vide through the hillslope, the flood plain, and ultimately to the stream) and neglected groundwater flow at larger scales (at intersubbasin and interbasin scales). Groundwater flow at larger scales might not follow local topographic lows and highs (Tóth, 1963). In addition, in lowland areas, it is difficult to differentiate (a) between the divide, the hillslope, and the flood plain and (b) between groundwater and soil water.

The SWAT model also has a poor performance in baseflow simulation, which is normally associated with the return flow from groundwater (Bosch et al., 2010; Eckhardt et al., 2002; Guse et al., 2014; Kalin and Hantush, 2006; Luo et al., 2012; Lv et al., 2014; Pfannerstill et al., 2014a). This is not only due to the unaccounted effect of the flows between HRUs but also due to the simplified representation of the aquifer system and the return flow from groundwater. SWAT uses a two-layer aquifer model, shallow or unconfined aquifer (typically 2–20 m) and deep or confined aquifer (> 20 m), to represent the aquifer system in each HRU (Luzio et al., 2004; Neitsch et al., 2011). The deep aquifer in SWAT is inactive, which means that water entering the deep aquifer is considered a loss to the hydrological system (Neitsch et al., 2011). The contribution of groundwater from the shallow aquifer to streamflow is modelled using a linear aquifer storage–discharge relation approach.

Modifications of the SWAT model regarding the aquifer structure and the interaction between aquifer and stream have been made to improve baseflow simulation. For example, Luo et al. (2012) allowed groundwater from the deep aquifer to contribute to streamflow in a similar manner as of the shallow aquifer. Gan and Luo (2013) added another aquifer layer and used a non-linear aquifer storage–discharge relation approach to simulate return flow. Pfannerstill et al. (2014a) divided the shallow aquifers into active fast and active slow shallow aquifers to account for fast and slow response components, respectively, of the return flow. Wang and Brubaker (2014) used a non-linear aquifer storage–discharge relation approach instead of a linear aquifer storage–discharge relation approach to simulate return flow. Results from the abovementioned studies showed that the modified SWAT models are able to simulate baseflow better than the original SWAT model. However, these studies have not considered lateral groundwater flow.

Another approach, which enables a reasonable representation of streamflow, groundwater flow, and groundwater–surface water interaction, integrates SWAT with the modular three-dimensional finite-difference groundwater flow (MODFLOW) model (McDonald and Harbaugh, 1988). MODFLOW is a fully distributed physically based groundwater model. There have been several versions of integrated SWAT and MODFLOW models, for example, SWATMOD (Sophocleous et al., 1999), SWAT-MODFLOW (Bailey et al.,

2016; Kim et al., 2008), and SWATmf (Guzman et al., 2015). Results showed that these models are able to simulate streamflow, groundwater flow, and groundwater–surface water interactions at a basin scale (Guzman et al., 2015; Kim et al., 2008; Sophocleous et al., 1999) with satisfactory results. However, the integrated models are not always applicable because they require extensive computational time and input data. In addition, the aforementioned models are not easy to use for modellers, who are not familiar with the MODFLOW model.

There is also an ongoing development and testing of the next generation of the SWAT model called SWAT+ (Bieger et al., 2017). SWAT+ allows users to discretize the aquifer in a flexible way. Aquifers could be discretized into a number of aquifer units (also called spatial objects), which are no longer tied to HRUs. Although there is an option for flow routing between these aquifer units (as flow through a series of linear storage elements) with SWAT+, however, users have to manually define a connection between these aquifer units and also a connection between these aquifer units with other spatial objects (e.g., HRU, channel, and LUs). This could be problematic with many spatial objects in large basins. In addition, the groundwater height in these aquifer units has the same meaning with the groundwater height of the original SWAT model, which is not referenced to a physical datum.

The research objective of the present study is to develop a simple semidistributed, physically based groundwater module for SWAT. The developed model is expected to be capable of simulating streamflow (especially baseflow) and groundwater flow at a basin/regional scale with fast computational time, less input data requirement, and satisfactory results for porous aquifers. In order to achieve the abovementioned objective, we applied a different discretization technique to delineate the aquifer while keeping the surface discretization as in the original SWAT model. The multicell aquifer (MCA; Bear, 1979; Bear and Cheng, 2010) model was used as a replacement of the deep aquifer in the original SWAT model. The modified SWAT was applied in two lowland basins, where contribution of groundwater to streamflow is dominant.

## 3.2 Methodology

### 3.2.1 The original groundwater module of SWAT

As mentioned in the previous section, SWAT divides the aquifer system in each HRU into two types of aquifers, shallow and deep aquifers. Percolated water from the unsaturated



zone is partitioned into the shallow and deep aquifer recharges via a parameter, which is typically calibrated. Water entering the deep aquifer is considered a loss to the system (Neitsch et al., 2011). This makes SWAT more flexible to calibrate, especially when there is a substantial amount of groundwater storage in the shallow aquifer, which results in an overestimation of baseflow. Groundwater in the shallow aquifer can be “revaporated” ( $w_{revap}$ ) or contribute to streamflow as return flow ( $Q_{gw}$ ) or be removed by pumping ( $w_{pump,sh}$ ). The volumetric water balance equation for the shallow aquifer in the original SWAT model on each day (e.g., day  $i$ ) is as follows (Neitsch et al., 2011):

$$aq_{sh,i} = aq_{sh,i-1} + w_{rchrg,sh} - Q_{gw} - w_{revap} - w_{pump,sh}, \quad (3.1)$$

where  $aq_{sh,i}$  and  $aq_{sh,i-1}$  are the amount of water stored in the shallow aquifer on day  $i$  and on day  $i - 1$ , respectively,  $w_{rchrg,sh}$  is the groundwater recharge, and other variables were as described previously. SWAT can simulate groundwater height in the shallow aquifer in each HRU (Neitsch et al., 2011). However, this variable provides only information about the groundwater storage content and has limited physical meaning because (a) it is not referenced to any physical datum; hence, it does not represent the groundwater level (Vazquez-Amábile and Engel, 2005); and (b) it does not account for groundwater flow between adjacent HRUs. Moreover, this variable has a unique value for each HRU, whereas a single HRU can be scattered over different areas having different altitudes. It should be noted that there is no groundwater flow between HRUs, and return flow from each HRU is routed directly to the stream outlet of the respective subbasin. The groundwater module in SWAT was documented in more detail in Neitsch et al. (2011). Hereinafter, when the SWAT model is mentioned, we refer to the one documented in Neitsch et al. (2011) unless otherwise stated.

### 3.2.2 The modified groundwater module

In this section, a brief review of the natural groundwater flow systems and groundwater flow dynamics at the basin scale is first provided. Tóth (1963) suggested that groundwater flow can be classified into local, intermediate, and regional groundwater flows. The local groundwater flow originates from the recharge area (local topographic high) and ends in the discharge area (adjacent local topographic low). Therefore, local groundwater flow is strongly driven by the topographic gradient. The intermediate and regional groundwater flows have recharge and discharge areas separated by several topographic highs and lows. Tóth (1963) also pointed out that the aforementioned types of groundwater flow systems

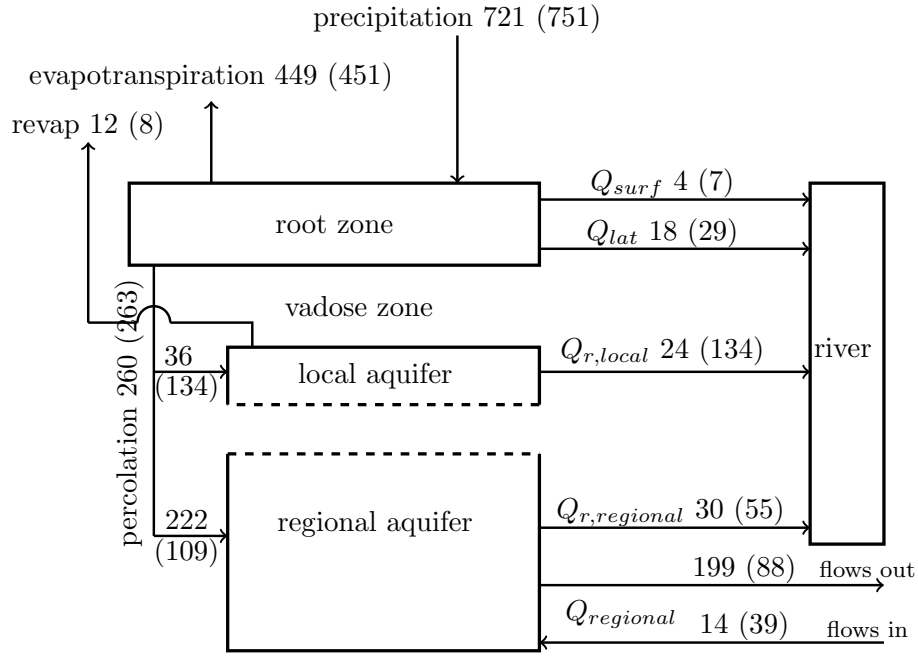


Figure 3.1: Schematic representation of the vertical structure of the modified groundwater module in SWAT.  $Q_{surf}$ ,  $Q_{lat}$ ,  $Q_{r,local}$ ,  $Q_{r,regional}$ , and  $Q_{regional}$  are the surface run-off, lateral flow, return flow from local aquifer, return flow from regional aquifer, and regional groundwater flow, respectively. The numbers indicate the average annual water balance components in millimeters per year in the Wipperau (numbers outside parentheses) and the Neetze (numbers inside parentheses) basins

might not exist simultaneously in all types of aquifers and the boundaries between them might not be well defined.

To mimic the groundwater flow systems as described above in the modified SWAT model, we modified the concept of the two-aquifer layer in the original SWAT model (Figure 3.1). The local aquifer layer in this study represents local groundwater flow, whereas the regional aquifer layer represents intermediate and regional groundwater flow. To be more precise, local groundwater flow in the modified SWAT model is restricted within a subbasin, which has a subbasin divide (topographic high) as recharge area and a stream of that subbasin (adjacent topographic low) as discharge area. In addition, the area between the subbasin divide and the stream is also considered as recharge area for the local groundwater flow system. Modelling local groundwater flow between local aquifers will not be the focus of our model. Therefore, we only model recharge and discharge and use a function to route local groundwater from recharge area to discharge area. Considering the above concept, the shallow aquifer in the original SWAT model will be considered as the local aquifer in our modified model. Therefore, discretization of the local aquifers is

identical to that of HRUs, and all simulations applied to the shallow aquifer in the original SWAT will be applied to the local aquifers in our modified model. The main differences between the modified SWAT model presented here with the original SWAT model lie in the regional aquifer layer. We used the MCA model to replace the deep aquifer in the original SWAT model and to represent intermediate and regional groundwater flows. The resulting model hereafter is referred to as the SWAT-MCA model. Delineation of the regional aquifer layer differs from that of the local aquifer because intermediate and regional groundwater flows are not restricted within a subbasin. The regional aquifer layer is discretized into cells (polygons) using Thiessen (1911) polygons constructed around the locations of the groundwater observation wells. Hence, one cell can be fully or partially overlaid by a single subbasin or several subbasins (Figure 3.2). It should be noted that the selected groundwater observation well must be representative for that cell and the screening depth must be within the unconfined aquifer. Groundwater flow between cells is modelled on the basis of Darcy's law. Considering the fact that there could be no clear boundary between local, intermediate, and regional groundwater flows and the local aquifer might only be filled after rainfall, flow in the regional aquifers in the SWAT-MCA model is assumed to be unconfined. This assumption is valid if the study area has discontinuous clay layers (lenses) or no distinct stratigraphic layers within the aquifer at the regional scale. Therefore, the volumetric water balance equation for each cell (e.g., cell  $i$ ) has the following form:

$$\sum_{j=1}^k Q_{ij} + W = SY_i \frac{\Delta h_i}{\Delta t} A_i, \quad (3.2)$$

where  $Q_{ij}$  ( $L^3T^{-1}$ ) is the total inflow (+) and outflow (-), which is calculated by using Darcy's law,  $k$  is the number of the neighbouring cells of cell  $i$ ,  $W$  ( $L^3T^{-1}$ ) represents sources (+) and sinks (-),  $SY_i$  (-) is the specific yield of cell  $i$ ,  $\Delta h_i$  (L) is the change in groundwater level at cell  $i$ ,  $\Delta t$  (T) is the time step size, which is 1 day in this study, and  $A_i$  ( $L^2$ ) is the surface area of cell  $i$ . In finite-difference form with implicit time-stepping scheme, Equation 3.2 has the following form:

$$\sum_{j=1}^k K_{ij} a_{ij} \frac{h_j^t - h_i^t}{L_{ij}} + W^t = SY_i \frac{h_i^t - h_i^{t-1}}{\Delta t} A_i, \quad (3.3)$$

where  $K_{ij}$  ( $LT^{-1}$ ) is the harmonic mean hydraulic conductivity between cells  $i$  and  $j$ ,  $a_{ij}$  ( $L^2$ ) is the average saturated area between cells  $i$  and  $j$ ,  $a_{ij}$  is a function of  $h_i^t$  (L) and  $h_j^t$  (L), which are the hydraulic heads of cells  $i$  and  $j$ , respectively, on the current day,  $L_{ij}$  (L) is the distance between centres of cells  $i$  and  $j$ , and  $h_i^{t-1}$  (L) is the hydraulic head of

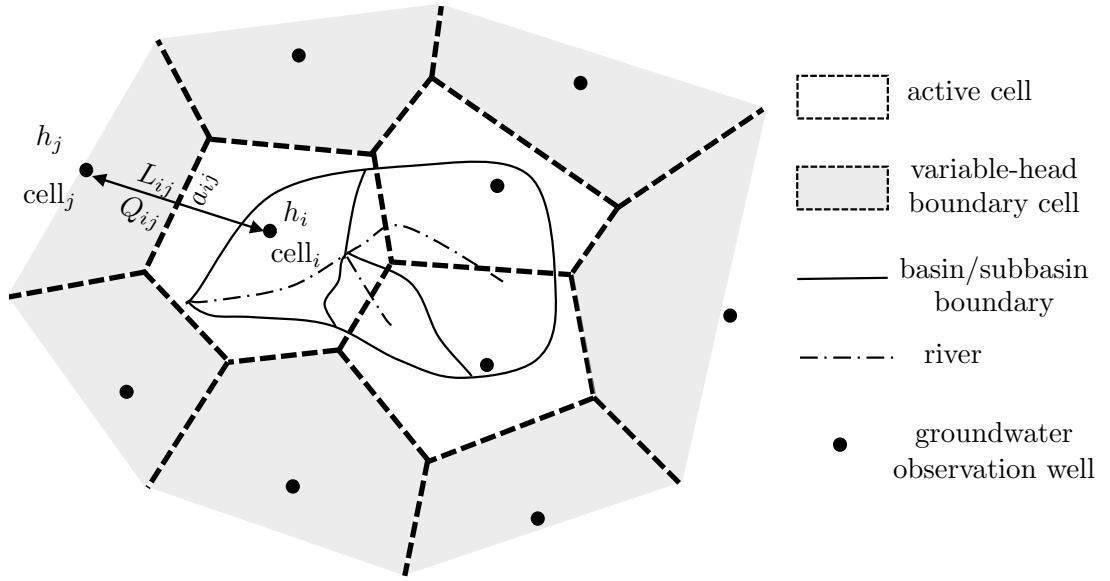


Figure 3.2: Schematic representation of the multicell aquifer model

cell  $i$  on the previous day.

Sources (+) and sinks (-) can be a portion of recharge from the unsaturated soil zone (+), return flow (-), and pumping for irrigation (-). We applied the HRU cell conversion technique used by [Kim et al. \(2008\)](#) to assign a spatial linkage between HRUs and cells. The amount of recharge from an HRU to a cell is proportional to the overlapping area between that HRU and that cell. To calculate recharge from an HRU to a cell, the overlapping area matrix between HRUs and cells is needed (Table 3.1). The total amount of recharge to a cell, which is not overlaid completely by the basin, is assumed to be area proportional to the recharge from the overlapping area.

Return flow from cell to stream is conceptualized using the non-linear storage-discharge relation suggested by [Wang and Brubaker \(2014\)](#). The total amount of return flow from each cell is calculated as follows:

$$Q_{r,regional} = (\alpha(S - S_{min}))^{1/\beta}, \quad (3.4)$$

where  $Q_r$ , regional ( $L^3T^{-1}$ ) is the total amount of return flow,  $S$  ( $L^3$ ) is the total groundwater storage,  $S_{min}$  ( $L^3$ ) is the minimum groundwater storage for return flow to occur (if  $S < S_{min}$ , then  $Q_{r,regional} = 0$ ), and  $\alpha$  ( $T^\beta L^{3(1-\beta)}$ ) and  $\beta$  (-) are coefficient parameters. Return flow from one cell can contribute to streamflow in several subbasins.

Table 3.1: The overlapping area matrix between HRUs and cells

	hru <sub>1</sub>	hru <sub>2</sub>	hru <sub>m</sub>
cell <sub>1</sub>	cell <sub>1</sub> _hru <sub>1</sub>	cell <sub>1</sub> _hru <sub>2</sub>	cell <sub>1</sub> _hru <sub>m</sub>
cell <sub>2</sub>	cell <sub>2</sub> _hru <sub>1</sub>	cell <sub>2</sub> _hru <sub>2</sub>	cell <sub>2</sub> _hru <sub>m</sub>
-	-	-	-
cell <sub>n</sub>	cell <sub>n</sub> _hru <sub>1</sub>	cell <sub>n</sub> _hru <sub>2</sub>	cell <sub>n</sub> _hru <sub>m</sub>

Conversely, one subbasin can receive return flow from several cells. This concept represents the recharge and discharge area of intermediate and regional groundwater flows. The amount of return flow from a cell to a subbasin is proportional to the overlapping area between the respective cell and subbasin (Table 3.1).

### 3.2.3 Input data preparation

In addition to the input data as described by Arnold et al. (2013), input data for the SWAT-MCA model must be prepared in ASCII text files. They are named “parameters.txt,” “hru.txt,” and “cell.txt.” The “parameters.txt” file contains information regarding the cell’s number, cell’s geometry (coordinates of the cell’s centre, bottom and top elevations of the cell, and ID of the neighbouring cells), cell’s hydrogeological characteristics (saturated hydraulic conductivity and specific yield), cell’s initial condition (initial groundwater level), and the parameters to control the amount of return flow ( $\alpha$ ,  $\beta$ , and  $S_{min}$ ). If the cell is used as a variable-head boundary cell, the name of the file, which contains observed daily groundwater levels of that cell during the simulation time, must be provided. Other types of boundary conditions could be also implemented with minor modification of the code. The “hru.txt” and “cell.txt” files are used to assign a spatial linkage between HRUs and cells and to calculate the overlapping area matrix between HRUs and cells (Table 3.1). The “hru.txt” and “cell.txt” files can be created using geographic information system (GIS) tools.

### 3.2.4 Model integration framework

The MCA model was integrated into SWAT (SWAT2012 rev. 664) by using two main subroutines. The first subroutine, “read\_process,” reads and processes input data for MCA. This subroutine is called only once (at the beginning of the simulation). The second subroutine, “simulate\_gw,” simulates groundwater flow between cells, groundwater levels,

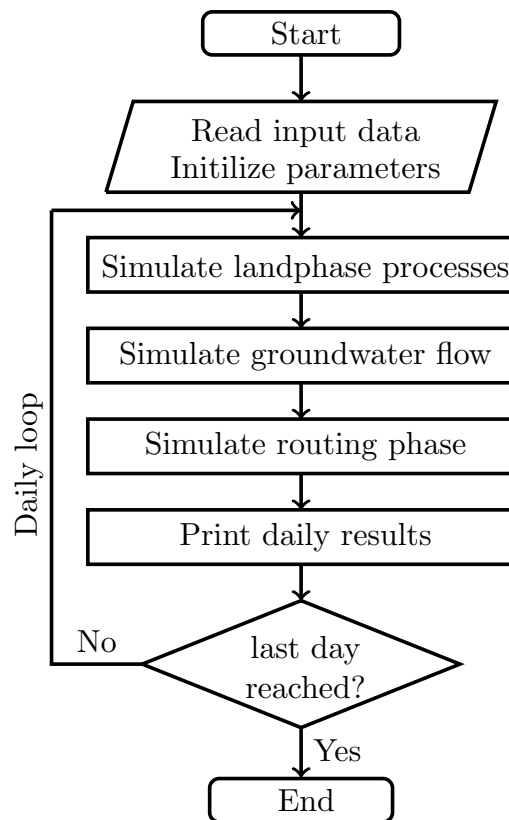


Figure 3.3: Integration framework of the soil and water assessment tool–multicell aquifer model

and return flow from the regional aquifer (Equations 3.3 and 3.4). This subroutine is called each time step after the subroutine “subbasin,” which simulates all land phase processes for each HRU, and before the subroutines “route,” “add,” and other subroutines, which simulate the routing phase of the hydrologic cycle. After each simulation day, results are printed out. For more information regarding the subroutines “subbasin,” “route,” and “add,” one could refer to [Arnold et al. \(2013\)](#). Minor modifications in the SWAT code were also made to transfer variable values between subroutines of SWAT and MCA and to print out daily results, resulting in only one executable program (Figure 3.3). The source code of the SWAT-MCA model could be available upon request.

## 3.3 Case Study

### 3.3.1 Study areas and data

The study areas, the Wipperau and the Neetze basins, are located in a lowland area within the Lüneburger Heide region in Lower Saxony, Germany (Figure 3.4). The two

Table 3.2: Characteristics of the study areas

	Wipperau basin	Neetze basin
Total area (km <sup>2</sup> )	200.4	172.8
Agricultural land (% total area)	65.6	56.0
Forest (% total area)	31.2	39.3
Average annual precipitation (mm)	721	751
Average annual water yield (mm)	66.3	173.4
Average annual baseflow (mm)	49.4	151.8
(% average annual water yield)	75	88

basins are part of the Ilmenau basin, which drains to the Elbe River in the north-west. The digital elevation model of 10-m resolution was provided by the Lower Saxony Water Management, Coastal Defence and Nature Conservation Agency (NLWKN). The study areas are relatively flat with elevation ranges from 19 to 139 m above mean sea level (Figure 3.4). Daily weather data (precipitation, wind speed, sunshine hours, and relative humidity) from 1976 to 2007 were obtained from the German Weather Service (DWD). Weather data were interpolated for all subbasins using the inverse distance weighting method. Daily sunshine hours were converted to solar radiation using the formulae suggested by Ångström (1924). The average annual precipitation values of the two basins from interpolated data are of similar magnitude (Table 3.2). Daily streamflow records at the outlets of the Wipperau basin (Oetzmühle gauging station) and the Neetze basin (Süttoorf gauging station) from 1976 to 2007 were obtained from NLWKN. Streamflow data show that the average annual water yields of the two basins are significantly different (Table 3.2). Baseflow analysis using the baseflow filter program (Arnold et al., 1995) indicates that (a) return flow from groundwater is a dominant source of streamflow in both basins and (b) return flow from the Neetze basin is much higher than return flow from the Wipperau basin (Table 3.2).

Land use/land cover map and soil map 1:200000 (BÜK200) were taken from the CORINE Land Cover project and the Federal Institute for Geosciences and Natural Resources (BGR), respectively. The dominant land cover types in both basins are agricultural land and forest (Table 3.2). The majority of the agricultural land (about 90%) is irrigated with an average annual amount of groundwater extraction for irrigation of around 73 mm (Riediger et al., 2014; Wittenberg, 2015). The dominant soils in the Wipperau basin are (a) podzols and brown podzolic soils, 43.4% of the total area, and (b) brown earth and podzolic-brown earth soils, 32.4% of the total area. In the Neetze basin,

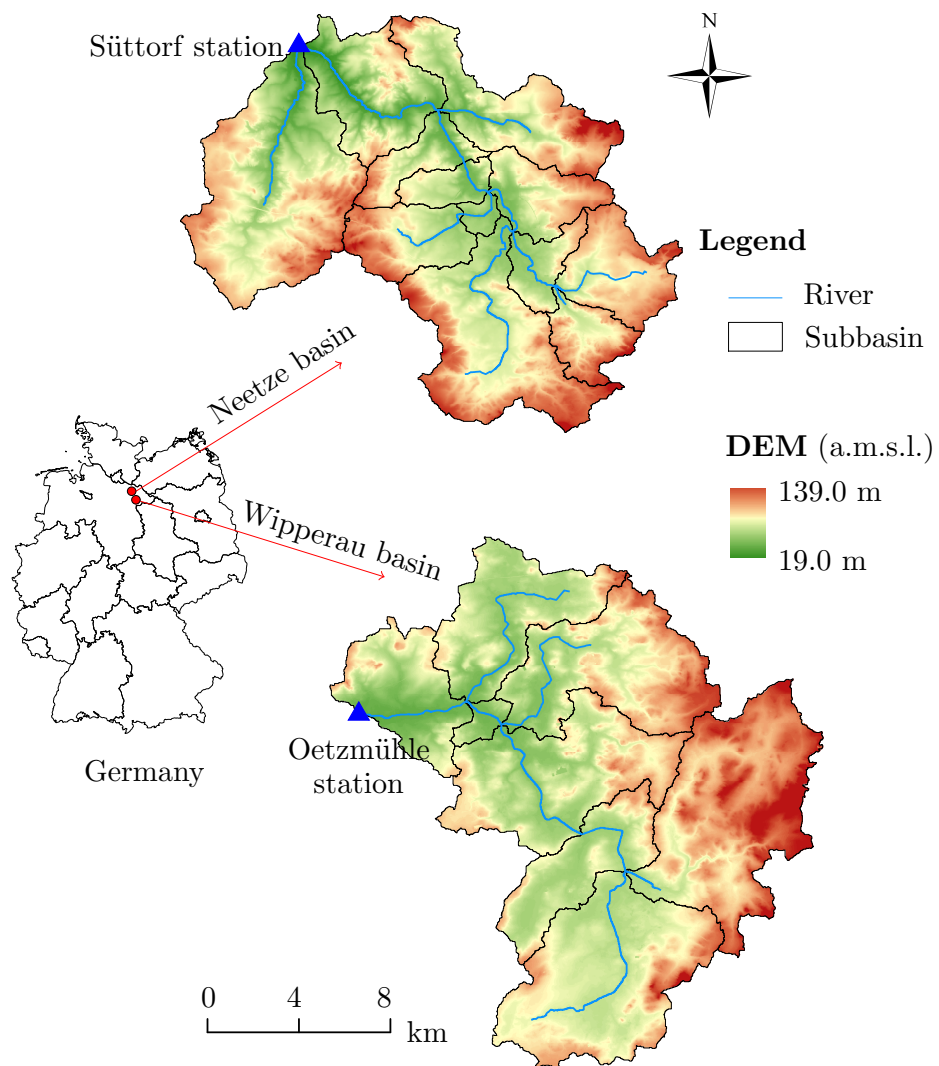


Figure 3.4: Location and digital elevation model (DEM) of the Neetze and Wipperau basins



the dominant soils are (a) podzols and brown podzolic soils, 47.2% of the total area, and (b) brown earth soil, 23.2% of the total area. Soil hydraulic properties were derived by using the pedotransfer functions/tables from [Wessolek et al. \(2009\)](#).

Average annual groundwater recharge recorded at the lysimeters at Hohenzethen, which are operated by the Landesamt für Bergbau, Energie, und Geologie, in the Wipperau catchment from 2001 to 2015 varied between 328 and 347 mm. However, simulated annual groundwater recharge from [Lemke et al. \(2008\)](#) was around 225 mm. These values along with the estimated return flow from groundwater (Table 3.2) indicate that in both basins, the majority of groundwater recharge does not become return flow.

Hydrogeological cross sections of the area published by Landesamt für Bergbau, Energie, und Geologie indicate that aquifers and aquitards are sandwiched and the aquitards are discontinuous at regional scale. Thus, the assumption that the regional aquifer is unconfined in the SWAT-MCA model is valid in this case. The dominant hydrogeological layers of the underlying aquifer are aquifers of classes L3 to L6 according to the classification given by [Manhenke et al. \(2001\)](#). This means that the hydraulic conductivity of the underlying aquifers varies between 0.86 and 86.4 m/day.

Observed groundwater levels from 1980 to 2007 within and nearby the study areas (Figure 3.5) were obtained from NLWKN. Groundwater levels were observed at different time steps, from monthly to daily time steps. Linear-in-time interpolation was applied to get daily groundwater levels at the boundary cells.

### 3.3.2 Spatial discretization

Figure 3.5 shows the spatial discretization of the surface and subsurface of the Wipperau and Neetze basins. The Wipperau basin was divided into 8 subbasins and 221 HRUs, whereas the Neetze basin was discretized into 12 subbasins and 213 HRUs. Discretization of the subbasins into HRUs was not shown because HRUs are not easy to recognize visually. The local aquifers within the two basins were delineated identically with the delineation of their HRUs, resulting in 221 local aquifer units in the Wipperau basin and 213 local aquifer units in the Neetze basin. The regional aquifers of the Wipperau and the Neetze basins were delineated into 33 and 26 cells, respectively, using Thiessen polygon method with locations of the groundwater observation wells as cell's centre.

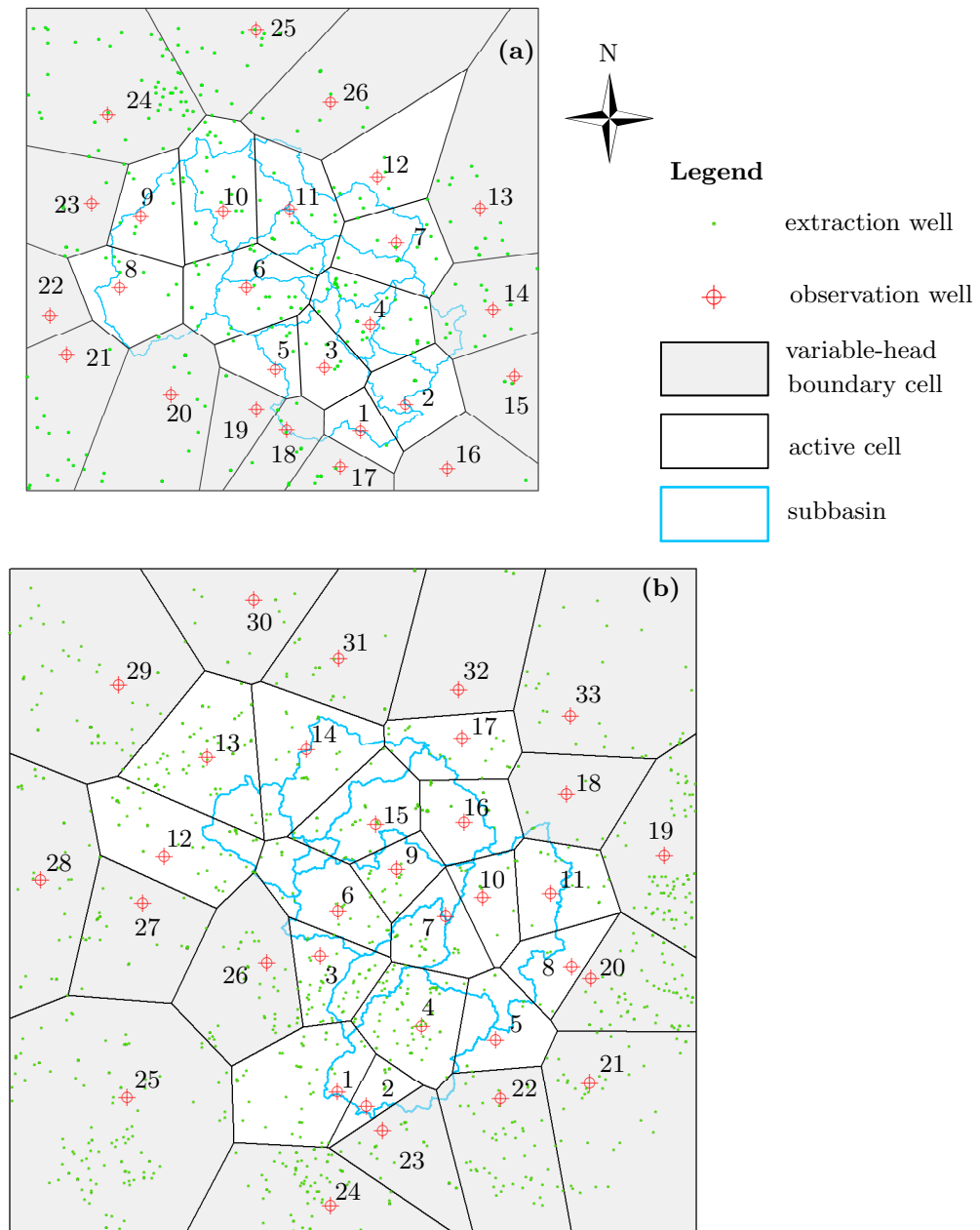


Figure 3.5: Delineation of the subbasin and the regional groundwater aquifer of (a) the Neetze basin and (b) the Wipperau basin

### 3.3.3 Calibration and validation strategy

The SWAT and SWAT-MCA models were run for 32 years (1976–2007) with 4 years for warm-up (1976–1979), 14 years for calibration (1980–1993), and 14 years for validation (1994–2007). The regional groundwater module was activated after the warm-up period with initial groundwater levels obtained from observed groundwater levels. By doing that, the groundwater recharge is expected to be reasonably estimated when the regional groundwater module is activated. Similar with [Guzman et al. \(2015\)](#), we first calibrated and validated the original SWAT model against the observed streamflow to ensure that the surface processes are adequately represented and the amount of groundwater recharge is reasonably estimated. Parameters used for calibrating the original SWAT were selected on the basis of the dominant conditions in the basin, sensitivity analysis, and literature review of the most commonly used parameters ([Arnold et al., 2013](#)). The selected parameters are shown in Table 3.3. Assuming the aquifer recharge is satisfactorily estimated by the original SWAT, the best calibrated parameter values from the original SWAT model will be kept unchanged during the calibration of the SWAT-MCA model, except the RCHRG\_DP, GW\_DELAY, and ALPHA\_BF. In the SWAT-MCA model, RCHRG\_DP represents the portion of groundwater recharge percolating to the regional aquifer. Parameters used for calibrating the SWAT-MCA model are RCHRG\_DP, GW\_DELAY, ALPHA\_BF,  $K$ ,  $SY$ ,  $\alpha$ ,  $\beta$ , and  $S_{min}$ .

Daily streamflow at the basin outlet was used to calibrate and validate the original SWAT model. To calibrate and validate the SWAT-MCA model, however, both time series of observed daily streamflow at the basin outlets and observed groundwater levels at active cells were used. As the numbers of subbasins and cells are small, calibration of both models was performed manually by adjusting one parameter at a time until satisfactory model performance is achieved.

The common parameters of the SWAT and SWAT-MCA models (Table 3.3) were adjusted in the ranges suggested by [Arnold et al. \(2013\)](#) and other studies in lowland basins in Germany (e.g., [Kiesel et al., 2010](#); [Uniyal et al., 2017](#)), whereas  $K$  was varied within the range mentioned in the previous section, from 0.864 to 86.4 m/day.  $SY$  was varied between 0.5 and 0.3, which is the range for various geologic materials ([Morris and Johnson, 1967](#)). The constant value of  $\beta = 2$  was taken for all cells to represent the non-linear behaviour of the baseflow as pointed out by other studies (e.g., [Pfannerstill et al., 2014a](#)).  $S_{min}$  and  $\alpha$  were varied cell to cell. It should be noted that for each active cell, five parameters need to be calibrated ( $K$ ,  $SY$ ,  $S_{min}$ ,  $\alpha$ , and  $\beta$ ). However, only one

Table 3.3: Best calibrated parameter values of the original SWAT and SWAT-MCA models

Variables	Wiperau basin			Neetze basin	
	SWAT	SWAT-MCA	SWAT	SWAT-MCA	
r_CN2	-15%	-	-10%	-	
v_SURLAG (days)	0.1	-	0.1	-	
r_SOL_AWC (mm H <sub>2</sub> O)	-20%	-	-15%	-	
r_SOL_K (mm/hr)	-3%	-	-10%	-	
v_RCHRG_DP	0.75	0.86	0.15	0.45	
v_ALPHA_BF (days)	0.15	0.25	0.2	0.2	
v_GW_DELAY (days)	175	75	750	500	

Note. “r\_” and “v\_” mean relative change and replacement of the default values, CN2 is the SCS curve number for moisture condition II, SURLAG is the surface run-off lag coefficient in the HRU, SOL\_AWC is available soil water content, SOL\_K is soil saturated hydraulic conductivity, RCHRG\_DP is deep aquifer percolation coefficient, ALPHA\_BF is baseflow recession constant, and GW\_DELAY is delay time for aquifer recharge. MCA = multicell aquifer; SWAT = soil and water assessment tool.

parameter ( $K$ ) needs to be calibrated for each boundary cell. With these parameters, there could be a problem of equifinality because  $K$  and  $SY$  were varied in a wide range and the actual return flow from the deep aquifer to stream is unknown.

Model performance in terms of simulated streamflow and simulated groundwater levels was evaluated qualitatively and quantitatively. Qualitative evaluation of simulated streamflow was based on time series plots and the flow–duration curve, whereas qualitative evaluation of simulated groundwater levels was done on the basis of time series plots. Quantitative evaluation of both simulated streamflow and groundwater levels was based on three statistical indices: the Nash–Sutcliffe efficiency (NSE), the percent bias (PBIAS), and the ratio of the root mean square error to the standard deviation of measured data (RSR, [Moriassi et al., 2007](#); [Sun et al., 2016](#)). In addition, the boxplot of the absolute differences between observed and simulated groundwater levels was used to qualitatively evaluate simulated groundwater levels. The logarithmic NSE ( $\ln$ NSE) index was used to quantitatively evaluate the quality of simulated low flow (e.g., [Pushpalatha et al., 2012](#)). To enable the calculation of  $\ln$ NSE, all time steps with zero values of streamflow were excluded.

## 3.4 Results and Discussion

### 3.4.1 Calibrated parameter values

The best calibrated parameter values of the original SWAT and SWAT-MCA models are listed in Table 3.3. It is seen from this table that RCHRG\_DP was increased from 0.75 and 0.15 in the original SWAT model to 0.86 and 0.45 in the SWAT-MCA model. This is because in the original SWAT model, more water needs to be stored in the shallow aquifer to sustain adequate baseflow. In the SWAT-MCA model, however, baseflow is sustained by both local and regional aquifers. Therefore, less water needs to be stored in the local aquifer. In contrast, the best calibrated GW\_DELAY value was decreased from 175 and 750 days in the original SWAT model to 75 and 500 days in the SWAT-MCA model. The reason is that the GW\_DELAY value in the original SWAT model should represent both fast flow and slow flow responses of the baseflow to precipitation. In the SWAT-MCA model, the GW\_DELAY value was reduced to represent the fast flow response of the baseflow. The slow flow response of the baseflow is controlled by  $\alpha$  and  $\beta$  of the regional aquifer. Additional parameters, which were used to calibrate the new groundwater module of the SWAT-MCA model, and their best calibrated values were varied within the ranges given in Section 3.3, except the best calibrated K values were varied in a smaller range, from 1 to 40 m/day.

### 3.4.2 Overall water balance

Figure 3.1 provides a schematic representation of the overall water balance from the calibrated SWAT-MCA model for the Wipperaue and the Neetze basins. It clearly shows that there is a substantial amount of groundwater flow out of the two study areas. Results from both calibrated models show that (a) the simulated average annual groundwater recharge in the Wipperaue and the Neetze basins is 258 and 243 mm, respectively, (b) a considerable amount of groundwater recharge, about 222 mm, in the Wipperaue basin percolates to the deep aquifer compared with only 109 mm in the Neetze basin, and (c) the contribution of groundwater to streamflow (return flow) is dominant. About 71% and 84% of streamflow of the Wipperaue basin and Neetze basin, respectively, are baseflow. The simulated groundwater recharge in this study is lower than the observed percolation at the lysimeter, but higher than the simulated value from Lemke et al. (2008). The model currently underestimated irrigation demand compared with the reported values from Riediger et al. (2014). The incorporation of crop species could be done to improve the

estimation of irrigation water demand. The amount of baseflow is close to the estimated values from the baseflow filter program (Table 3.2). In the original SWAT model, all baseflow is from the shallow aquifer, whereas in the SWAT-MCA model, about 44% of the baseflow of the Wipperaue basin and 71% of the baseflow of the Neetze basin are from the local aquifer and the rest is from the regional aquifer.

### 3.4.3 Stream discharge

Figure 3.6a,b shows the observed and simulated daily streamflow at the outlet of the Wipperaue basin with the original SWAT model and the SWAT-MCA model, respectively. The streamflow hydrographs were plotted in log scale to emphasize the quality of simulated low flow because improvement in high-flow simulation is not the focus of this present study. Visual assessment shows that low flows are poorly simulated with the original SWAT model, whereas with the SWAT-MCA model, low flows are better simulated. For example, simulated streamflow with the original SWAT sometimes dropped to zero, whereas observed low flows during the respective periods were much higher (Figure 3.6a), which is not observed with the SWAT-MCA model (Figure 3.6b). Better simulation of low flows with the SWAT-MCA model is also shown in the flow–duration curve, where low flows are underestimated with the original SWAT model (Figure 3.7), and in the lnNSE efficiency (Table 3.4), where there is a significant improvement in the lnNSE with the SWAT-MCA. The changes in NSE, PBIAS, and RSR indices between the two models are minor (Table 3.4) because these indices are more sensitive to high flows, which were underestimated in both models (Figure 3.7). The medium range of streamflow values was overestimated in both models (Figure 3.7). However, all statistical index values (Table 3.4) are within the “satisfactory” range according to Moriasi et al. (2007), meaning that the SWAT and SWAT-MCA models for the Wipperaue basin were successfully calibrated against streamflow and the simulated groundwater recharge can be considered as reasonable.

Figure 3.6c,d shows the observed and simulated daily streamflow of the Neetze basin with the original SWAT model and the SWAT-MCA model, respectively. Visual assessment shows that there is no significant difference between simulated streamflow from the original SWAT and the SWAT-MCA models. NSE and lnNSE values show that there are only minor improvements of simulated streamflow with the SWAT-MCA model (Table 3.4). However, NSE, lnNSE, and RSR indices show that the SWAT and SWAT-MCA models were less well calibrated against observed streamflow compared with Wipperaue. This could indicate that the surface processes were not sufficiently represented. Never-

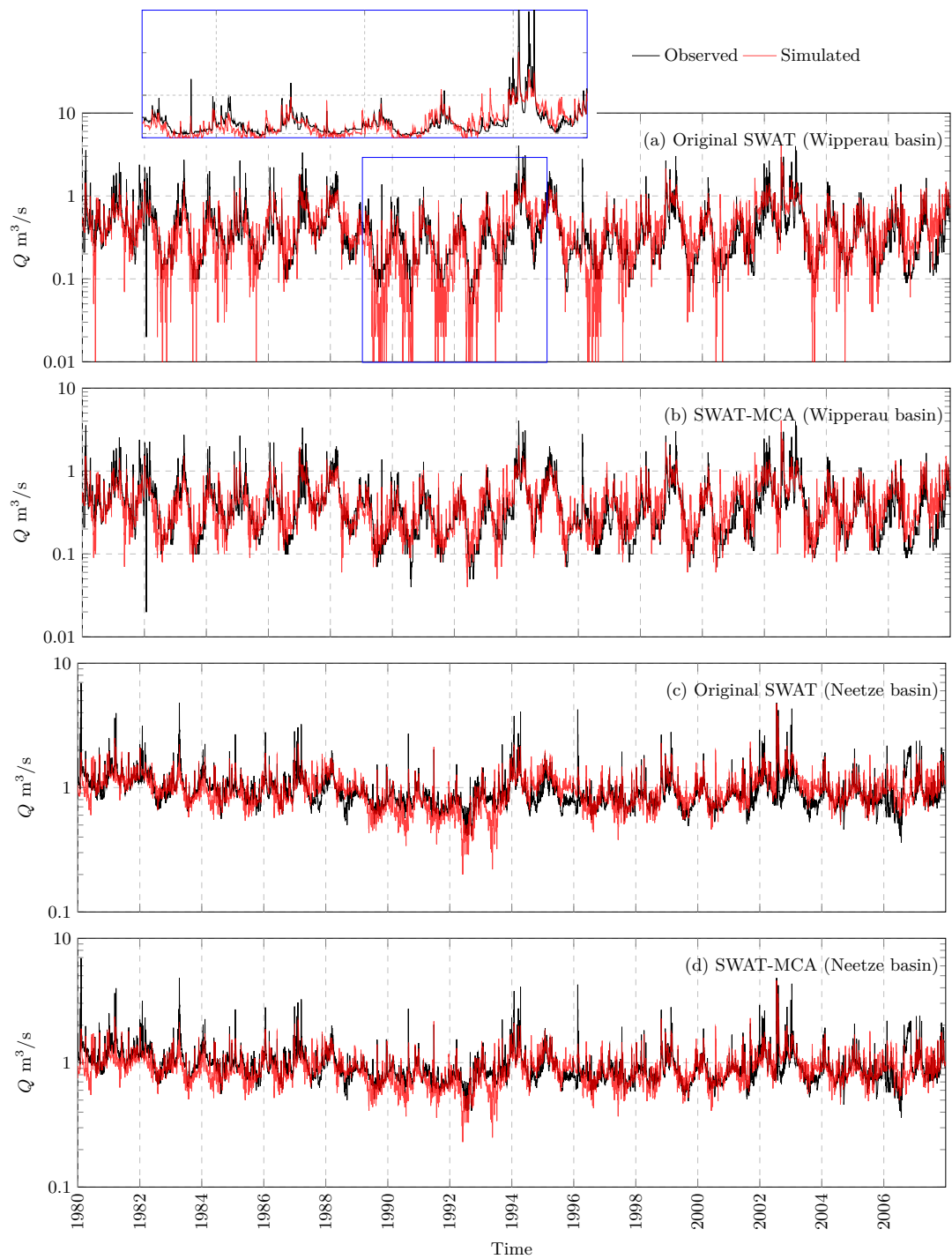


Figure 3.6: Observed and simulated streamflows from (a, c) the original SWAT models and (b, d) the SWAT-MCA model at the Oetzmühle (Wipperau basin) and Süttrorf (Neetze basin) gauging stations during 1980–2007. A portion of the semi-log plot was shown in normal plot (a) to show that it is difficult to see the quality of the simulated low flow with normal plot. SWAT = soil and water assessment tool; MCA = multicell aquifer



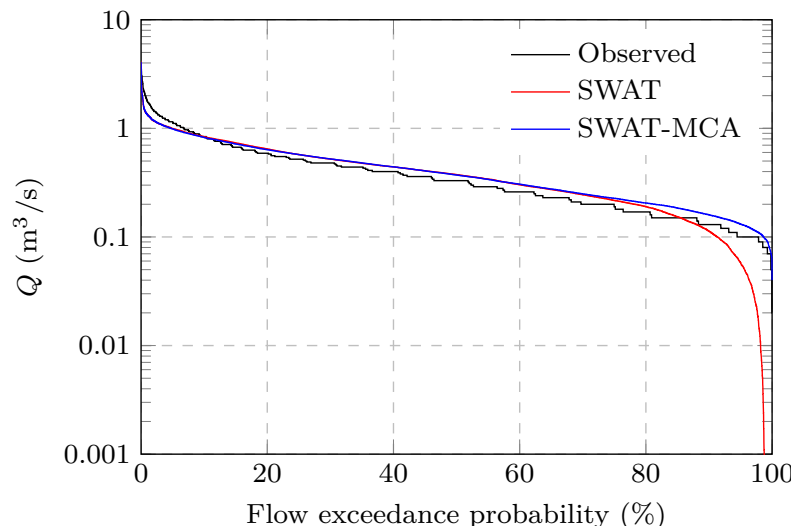


Figure 3.7: Flow duration curves of the observed and simulated streamflows at the Oetzmühle gauging station from the SWAT and SWAT-MCA models during 1980–2007. SWAT = soil and water assessment tool; MCA = multicell aquifer

theless, the simulated groundwater recharge is considered as acceptable because of the following reasons: (a) The annual simulated groundwater recharge of the Neetze basin is similar with that of the Wipperau basin, (b) the Neetze and Wipperau basins are located close to each other and have similar climate and physical characteristics (Table 3.2), (c) the contribution of baseflow to streamflow in the Neetze basin is much larger than that in the Wipperau basin. This could be an explanation why the simulated streamflow in the Neetze basin is less satisfactorily calibrated than that in the Wipperau basin.

### 3.4.4 Groundwater levels

Figure 3.8a–c shows the time series plots of simulated and observed groundwater levels with the NSE, PBIAS, and RSR indices and the boxplots of the absolute differences between observed and simulated groundwater levels. In these figures, observed groundwater levels fluctuated quite smoothly without sudden increases and decreases, indicating that observed groundwater levels in these cells were not or only minor affected by extraction wells located nearby (Figure 3.5). Observed groundwater levels in other cells (Figure 3.9), however, were disturbed by extraction wells located nearby (Figure 3.5). This is shown by the sudden increases and decreases in observed groundwater levels (Figure 3.9). Therefore, only time series plots were used to evaluate simulated groundwater levels in these cells.

Figure 3.8a illustrates that in cells where there are no sharp increases and decreases



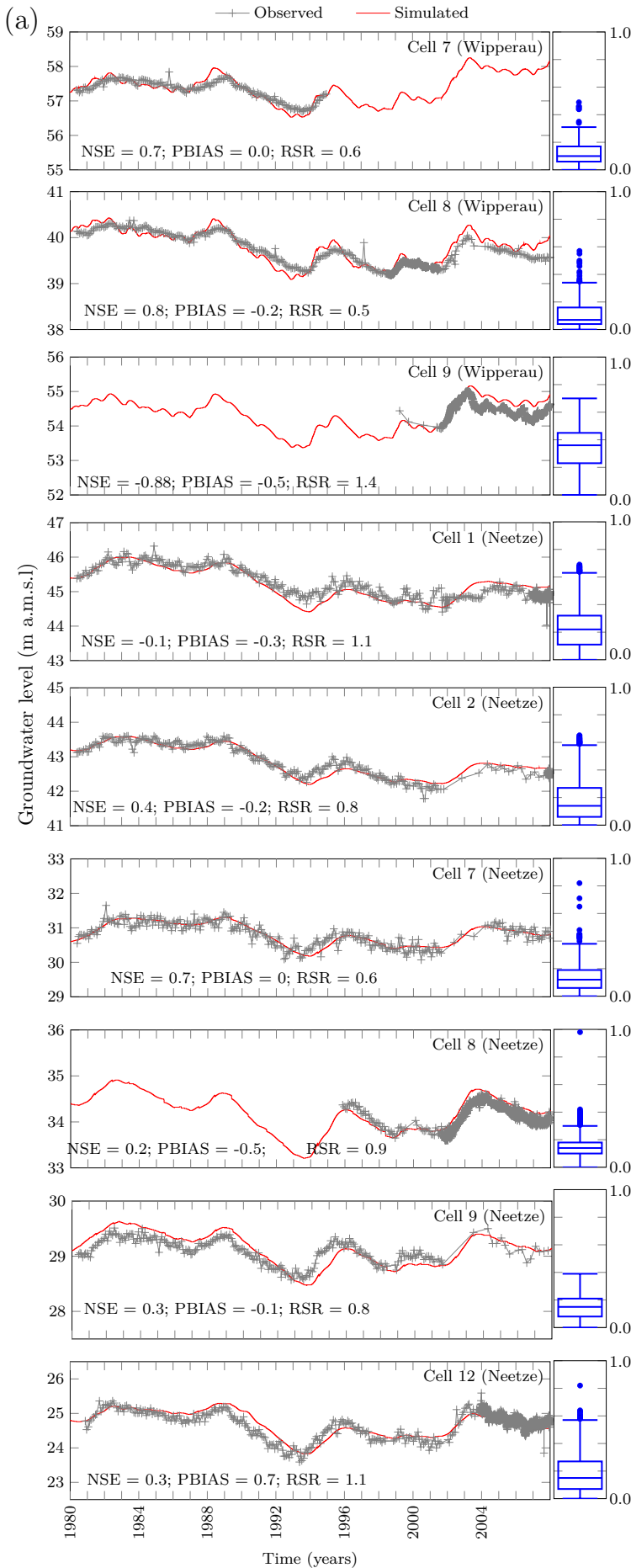


Figure 3.8: Time series plots of the observed and simulated groundwater levels during 1980–2007 and statistical indices (Nash–Sutcliffe efficiency [NSE], percent bias [PBIAS], and ratio of the root mean square error to the standard deviation of measured data [RSR]): (a) good match between observed and simulated groundwater levels, (b) mismatch between the time of occurrences of the high and low groundwater levels between observed and simulated groundwater levels, and (c) well reproduced of short- and long-term groundwater fluctuations. Boxplots of the absolute differences between simulated and observed groundwater levels are attached to the right of the time series plots

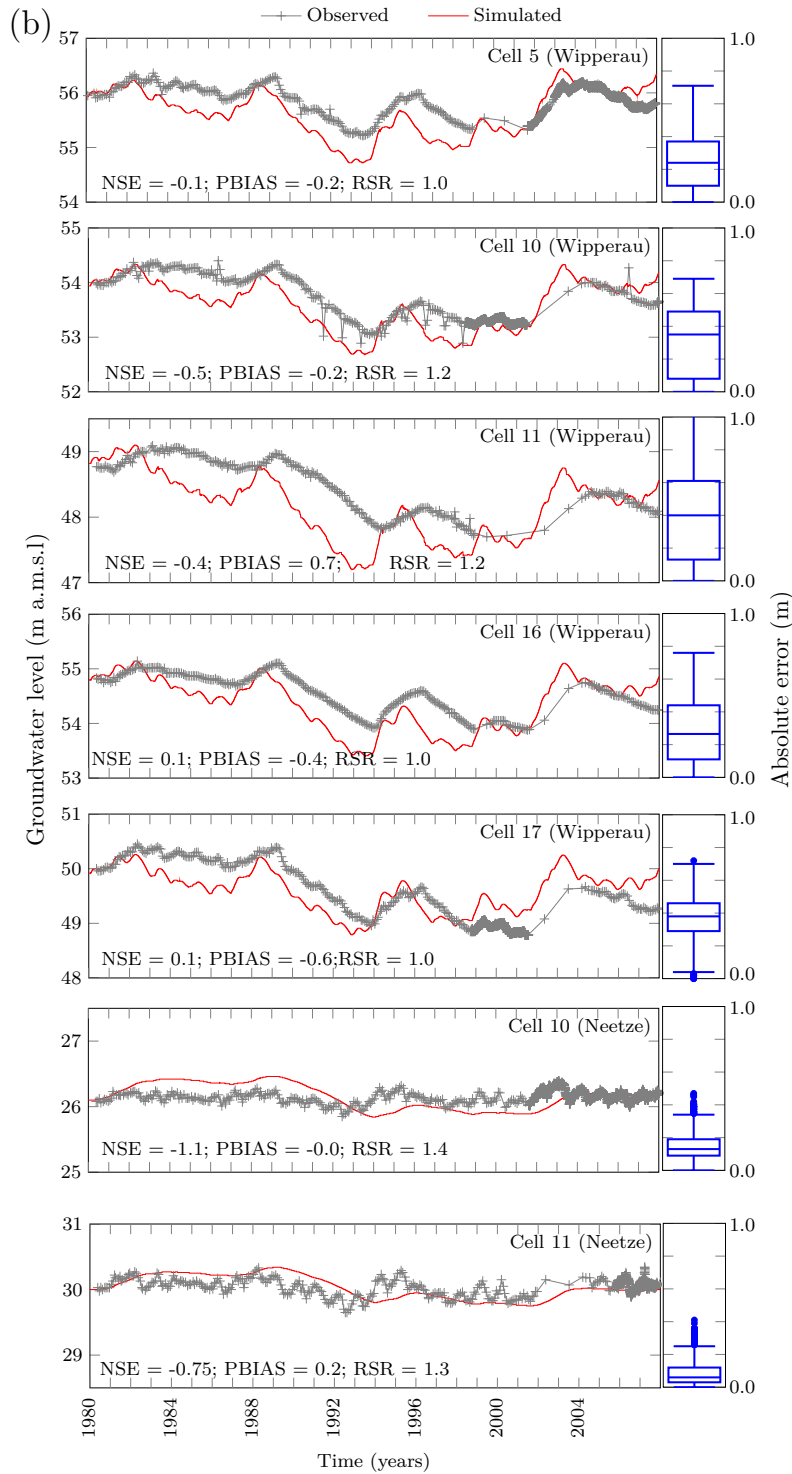


Figure 3.8: Continued

Table 3.4: Performance of the calibrated SWAT and SWAT-MCA model (in terms of streamflow at the Oetzmühle and Süttorf gauging stations)

	Oetzmühle station (Wipperau basin)		Süttorf station (Neetze basin)	
	SWAT	SWAT-MCA	SWAT	SWAT-MCA
NSE	0.62 (0.65)	0.64 (0.65)	0.50 (0.27)	0.46 (0.42)
lnNSE	-0.07 (0.38)	0.63 (0.60)	0.38 (0.29)	0.39(0.46)
PBIAS	9.5 (-13.8)	2.8 (-11.8)	4.4 (-10.5)	8.7 (-3.8)
RSR	0.61 (0.59)	0.59 (0.60)	0.70 (0.86)	0.73 (0.76)

Note. According to [Moriiasi et al. \(2007\)](#), model performance is considered as satisfactory if  $NSE > 0.50$ ,  $PBIAS < \pm 25\%$ , and  $RSR < 0.7$ . Numbers outside parentheses indicate values of the calibration period, whereas numbers inside parentheses indicate values of the validation period. MCA = multicell aquifer; SWAT = soil and water assessment tool; NSE = Nash–Sutcliffe efficiency; lnNSE = logarithmic NSE; PBIAS = percent bias; RSR = ratio of the root mean square error to the standard deviation of measured data.

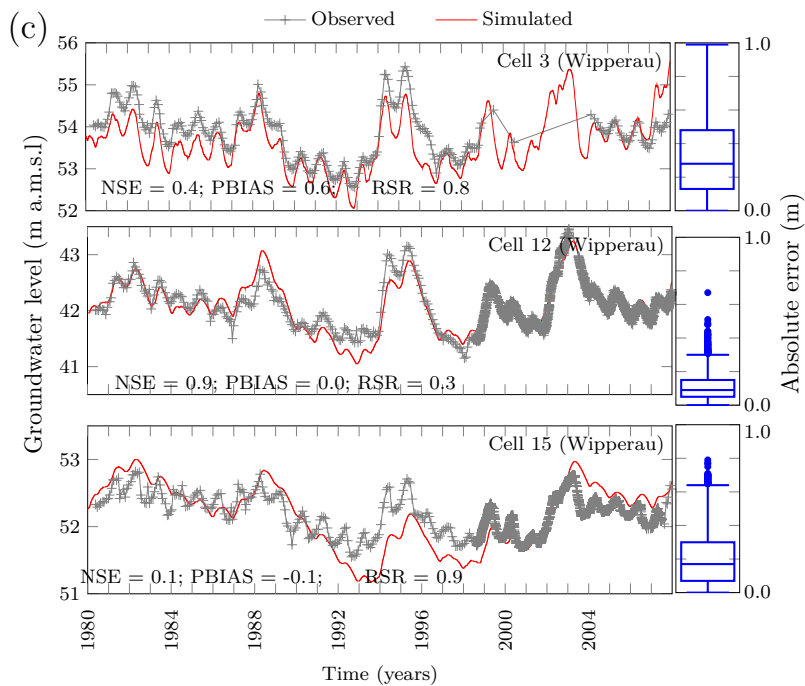


Figure 3.8: Continued

of the observed groundwater levels, the simulated groundwater levels match well with the observed. Especially the long-term fluctuations are well reproduced by the SWAT-MCA model. It is interesting to note that the quality of the simulated groundwater levels in Cells 7 and 9 in the Neetze basin, which are located in the middle of the modelling domain, is comparable with the simulated groundwater levels at other cells, which are neighbours of boundary cells. The boxplots (which were attached to the right of the time series plots) show that the third quartile varies from less than 0.2 to about 0.4 m, meaning that 75% of the simulated groundwater level errors are within this range. The statistical indices NSE, PBIAS, and RSR vary from -0.88 to 0.7, from -0.5% to 0.7%, and from 0.6 to 1.4, respectively.

Figure 3.8b presents cells, where the observed groundwater levels fluctuate quite smoothly similar to Figure 3.8a. Although the SWAT-MCA model here reproduces the long-term fluctuations as well, the time of occurrence of the simulated low and high groundwater levels mismatch with that of the observed. This problem could be due to the delay time for groundwater recharge to reach the regional aquifer, which is controlled by the GW\_DELAY parameter. The GW\_DELAY parameter was assigned as the same value for both the local and regional aquifers. The boxplots (except the boxplots of Cells 10 and 11 in the Neetze basin) and the statistical indices (NSE, PBIAS, and RSR) also indicate higher errors compared with that of the cells shown in Figure 3.8a. The boxplots of Cells 10 and 11 in the Neetze basin show that the third quartile is quite small mainly because the simulated and observed groundwater levels in these cells fluctuate in a narrow range (less than 0.5 m).

Figure 3.8c shows a group of cells where variations of observed groundwater levels were in a wider range and a shorter time compared with that of cells in Figure 3.8a,b. However, results show that the SWAT-MCA model can reproduce both long-term (multiannual) and short-term (annual) groundwater fluctuations quite well. For example, it is seen that although observed groundwater levels in Cell 12 of the Wipperaue basin varied more than 2 m, the time series plot of simulated groundwater levels is almost identical to the observed and the third quartile is less than 0.2 m with NSE, PBIAS, and RSR are 0.9, 0%, and 0.3, respectively.

Figure 3.9 shows a group of cells, where observed groundwater levels in these cells decrease and increase sharply within a short time period. This can be explained by the effect of extraction wells for irrigation located nearby (Figure 3.5), which has not been incorporated directly into the model. Depression cones cannot be simulated by the SWAT-MCA model because of the model concept. The groundwater level is simulated

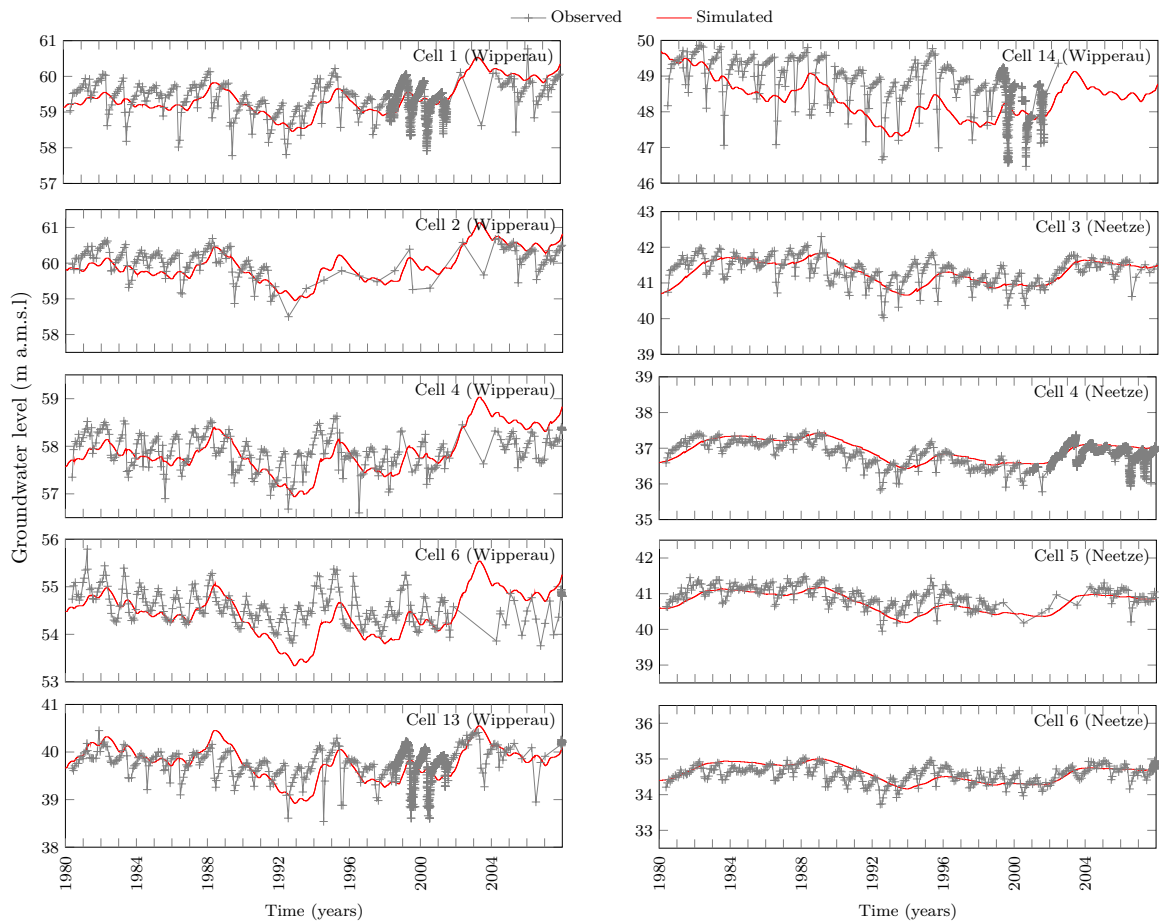


Figure 3.9: Time series plots of the observed and simulated groundwater levels during 1980–2007 in cells that are strongly affected by the cones of depression of the extraction wells located nearby

for polygons, which are assumed to be homogenous and cover an area larger than a depression cone from a single well. It is seen in these wells that the long-term fluctuations were reproduced by the model; however, the short-term fluctuations cannot be reproduced. Although the extracted amount of groundwater was incorporated into the model indirectly by activating auto irrigation, however, the effect of extracted water for irrigation on the simulated groundwater level is weakened because the cell size is large.

### 3.5 Conclusion and Recommendations

In this study, the SWAT model was modified to account for regional groundwater flow by replacing the deep aquifer with an MCA, resulting in the SWAT-MCA model. SWAT-MCA was tested in two basins in Niedersachsen, Germany. Results showed that SWAT-MCA is able to simulate groundwater levels (which was previously impossible with the original SWAT model) and baseflow better than the original SWAT model. The SWAT-MCA model (a) requires less input data regarding the subsurface than fully distributed groundwater models (e.g., MODFLOW), (b) is computationally efficient due to its semidistributed characteristic (using big cell size), and (c) is simple and easy to use. The delineation of the regional aquifer and the flow direction between these aquifer units with the SWAT-MCA model are flexible. The delineation of the regional aquifer does not necessarily have to follow HRU or basin delineation and flow direction between the aquifer units is automatically defined by hydraulic gradient. If a dense network of groundwater observation wells is not available, SWAT-MCA can work with even a single cell with given boundary conditions, but the advantage over the original SWAT is minimal. The SWAT source code is open and available for download via its official website (<http://swat.tamu.edu/>). Additional source codes from the SWAT-MCA model could be also provided upon request.

In this study, model calibration was done against observed daily streamflow and groundwater levels. More advanced calibration and evaluation techniques could be applied to improve the model performance by including more constraints and criteria (Yilmaz et al., 2008), for example, satellite-based soil moisture and evapotranspiration products (López et al., 2017), and by applying signature metrics (Pfannerstill et al., 2014b; Pokhrel et al., 2012).

Further works with the SWAT-MCA model are suggested to overcome its limitations. At the present, the SWAT-MCA model is only applied to areas with porous and unconfined aquifers. Discretization of cells with the MCA model can be more flexible. Cells could have

a rectangular shape while representing any subsurface reservoir with equivalent storage and hydraulic conductivity. Although the SWAT-MCA model cannot capture drawdown cones at individual pumping wells because of the large cell size, reducing the cell size and having more data about the pumping well could solve this problem. However, it should be noted that this is not the objective of the MCA model, which is developed to use a small number of cells in order to make a clear difference with fully distributed subsurface models (Bear, 1979). In addition, the interaction between the regional aquifer and the river in the SWAT-MCA was simplified using a conceptual non-linear storage–discharge relationship. A more physically based approach, which is based on the hydraulic head in the river and the underlying aquifer, could be used to model the aquifer–river interactions. However, it should be noted that increasing the model complexity could require more computational time and input data and a more complex model does not always guarantee better performance.

## Acknowledgments

We thank the editor and two anonymous reviewers, whose constructive comments helped to improve this manuscript. We also thank Bhumika Uniyal for proofreading the original manuscript. Furthermore, we thank the providers of data.

## Bibliography

- Ångström, A., 1924. Solar and terrestrial radiation. Report to the international commission for solar research on actinometric investigations of solar and atmospheric radiation. *Quarterly Journal of the Royal Meteorological Society*, 50(210), 121–126.
- Arnold, J.G., Allen, P. M., Muttiah, R., Bernhardt, G., 1995. Automated base flow separation and recession analysis techniques. *Groundwater*, 33, 1010–1018.
- Arnold, J.G., Allen, P.M., Volk, M., Williams, J. R., Bosch, D.D., 2010. Assessment of different representations of spatial variability on SWAT model performance. *Transactions of the ASABE*, 53(5), 1433–1443.
- Arnold, J.G., Fohrer, N., 2005. SWAT2000: Current capabilities and research opportunities in applied watershed modelling. *Hydrological Processes*, 19(3), 563–572.

- Arnold, J.G., Kiniry, J.R., Srinivasan, R., Williams, J.R., Haney, E.B., Neitsch, S.L., 2013. Soil and water assessment tool input/output documentation version 2012. Texas Water Resources Institute. TR-439, Texas.
- Bailey, R.T., Wible, T.C., Arabi, M., Records, R.M., Ditty, J., 2016. Assessing regional-scale spatio-temporal patterns of groundwater–surface water interactions using a coupled SWAT-MODFLOW model. *Hydrological Processes*, 30, 4420–4433.
- Bear, J., 1979. *Hydraulics of groundwater*. New York, McGraw-Hill.
- Bear, J., Cheng, A.H.-D., 2010. *Modeling groundwater flow and contaminant transport*. Dordrecht, Netherlands, Springer.
- Bergström, S. (1992). *The HBV model: Its structure and applications* (Report hydrology no. 4. Norrköping: Swedish Meteorological and Hydrological Institute.
- Beven, K. J., Kirkby, M. J., 1979. A physically based, variable contributing area model of basin hydrology / Un modèle à base physique de zone d'appel variable de l'hydrologie du bassin versant. *Hydrological Sciences Journal*, 24(1), 43–69.
- Bieger, K., Arnold, J. G., Rathjens, H., White, M. J., Bosch, D. D., Allen, P. M., ... Srinivasan, R., 2017. Introduction to SWAT+, a completely restructured version of the soil and water assessment tool. *Journal of the American Water Resources Association*, 53(1), 115–130.
- Bosch, D. D., Arnold, J. G., Volk, M., Allen, P. M., 2010. Simulation of a low-gradient coastal plain watershed using the SWAT landscape model. *Transactions of the ASABE*, 53(5), 1445–1456.
- Brutsaert, W., 2005. *Hydrology: An introduction*. Cambridge, UK: Cambridge University Press.
- Eckhardt, K., Haverkamp, S., Fohrer, N., Frede, H.-G., 2002. SWAT-G, a version of SWAT99.2 modified for application to low mountain range catchments. *Physics and Chemistry of the Earth, Parts A/B/C*, 27(9), 641–644.
- Efstratiadis, A., Nalbantis, I., Koukouvinos, A., Rozos, E., Koutsoyiannis, D., 2008. HYDROGEIOS: A semi-distributed GIS-based hydrological model for modified river basins. *Hydrology and Earth System Sciences*, 12, 989–1006.



- Francesconi, W., Srinivasan, R., Pérez-Miñana, E., Willcock, S. P., Quintero, M., 2016. Using the soil and water assessment tool (SWAT) to model ecosystem services: A systematic review. *Journal of Hydrology*, 535, 625–636.
- Gan, R., Luo, Y., 2013. Using the nonlinear aquifer storage–discharge relationship to simulate the base flow of glacier- and snowmelt-dominated basins in northwest China. *Hydrology and Earth System Sciences*, 17, 3577–3586.
- Gassman, P. W., Reyes, M., Green, C. H., Arnold, J. G., 2007. The soil and water assessment tool: Historical development, applications, and future research directions. *Transactions of the ASABE*, 50, 1211–1250.
- Guse, B., Reusser, D. E., Fohrer, N., 2014. How to improve the representation of hydrological processes in SWAT for a lowland catchment—Temporal analysis of parameter sensitivity and model performance. *Hydrological Processes*, 28, 2651–2670.
- Guzman, J. A., Moriasi, D. N., Gowda, P. H., Steiner, J. L., Starks, P. J., Arnold, J. G., Srinivasan, R., 2015. A model integration framework for linking SWAT and MODFLOW. *Environmental Modelling & Software*, 73, 103–116.
- Hutson, S. S., Barber, N. L., Kenny, J. F., Linsey, K. S., Lumia, D. S., Maupin, M. A., 2004. Estimated use of water in the United States in 2000. Reston, United States: US geological survey circular 1268.
- Jajarmizadeh, M., Harun, S., Salarpour, M., 2012. A review on theoretical consideration and types of models in hydrology. *Journal of Environmental Science and Technology*, 5(5), 249–261.
- Joodavi, A., Zare, M., Raeisi, E., Ahmadi, M. B., 2016. A multi-compartment hydrologic model to estimate groundwater recharge in an alluvial-karst system. *Arabian Journal of Geosciences*, 9(3), 195.
- Kalin, L., Hantush, M. H., 2006. Hydrologic modeling of an eastern Pennsylvania watershed with NEXRAD and rain gauge data. *Journal of Hydrologic Engineering*, 11, 555–569.
- Kiesel, J., Fohrer, N., Schmalz, B., White, M. J., 2010. Incorporating landscape depressions and tile drainages of a northern German lowland catchment into a semi-distributed model. *Hydrological Processes*, 24, 1472–1486.

- Kim, N. W., Chung, I. M., Won, Y. S., Arnold, J. G., 2008. Development and application of the integrated SWAT–MODFLOW model. *Journal of Hydrology*, 356, 1–16.
- Kirkby, M. J., 1998. Modelling across scales: The MEDALUS family of models. In J. Boardman, & D. Favis-Mortlock (Eds.), *Modelling soil erosion by water* (pp. 161-173. Berlin: Springer.
- Kite, G. W., 1997. *Manual for the SLURP hydrological model V. 11*. National Hydrology Research Institute, Saskatoon, Canada.
- Krysanova, V., White, M., 2007. Advances in water resources assessment with SWAT—An overview. *Hydrological Sciences Journal*, 60(5), 771–783.
- Lane, L. J., Nearing, M. A., 1989. *USDA water erosion prediction project: Hillslope profile model documentation*. USDA-ARS National Soil Erosion Research Laboratory, NSERL Report No. 2.
- Leavesley, G. H., Lichty, R. W., Troutman, B., Saindon, L. G., 1983. *Precipitation-runoff modelling system. User's manual*. USGS Water Resour. Inst., report 83-4238.
- Lemke, D., Elbracht, J., 2008. *Grundwasserneubildung in Niedersachsen: eine vergleich der Methoden Dörhöfer & Josopait und GROWA06V2*. GeoBerichte 10. Landesamt für Bergbau, Energie und Geologie, Hannover.
- Lindström, G., Pers, C. P., Rosberg, R., Strömqvist, J., Arheimer, B., 2010. Development and test of the HYPE (hydrological predictions for the environment) model—A water quality model for different spatial scales. *Hydrology Research*, 41(3–4), 295–319.
- López, P. L., Sutanudjaja, E. H., Schellekens, J., Sterk, G., Bierkens, M., 2017. Calibration of a large-scale hydrological model using satellite-based soil moisture and evapotranspiration products. *Hydrology and Earth System Sciences*, 21, 3125–3144.
- Luo, Y., Arnold, J. G., Allen, P., Chen, X., 2012. Baseflow simulation using SWAT model in an inland river basin in Tianshan mountains, Northwest China. *Hydrology and Earth System Sciences*, 16, 1259–1267.
- Luzio, M. D., Srinivasan, R., Arnold, J. G., 2004. A GIS-coupled hydrological model system for the watershed assessment of agricultural nonpoint and point sources of pollution. *Transactions in GIS*, 8(1), 113–136.
- Lv, M., Hu, T., Dan, L., 2014. Daily streamflow simulation in a small-scale farmland catchment using modified SWAT model. *Transactions of the ASABE*, 57(1), 31–41.

- Manhenke, V. O., Reutter, E., Hübschmann, M., Limberg, A., Lückstedt, M., Nommensen, B., ... Voigt, H. J., 2001. Hydrostratigrafische Gliederung des nord-und mitteleuropäischen känozoischen Lockergesteinsgebietes. *Zeitschrift für Angewandte Geologie*, 47(3–4), 146–152.
- McDonald, M. G., Harbaugh, A. W., 1988. A modular three-dimensional finite-difference ground-water flow model. US Geological Survey, Techniques of Water Resources Investigation Book 6/A1. Washington: United States Government Printing Office.
- Moriasi, D. N., Arnold, J. G., Van Liew, M. W., Bingner, R. L., Harmel, R. D., Veith, T. L., 2007. Model evaluation guidelines for systematic quantification of accuracy in watershed simulations. *Transactions of the ASABE*, 50(3), 885–900.
- Morris, D. A., Johnson, A. I., 1967. Summary of hydrologic and physical properties of rock and soil materials as analyzed by the Hydrologic Laboratory of the U.S. Geological Survey. U.S. Geological Survey Water-Supply Paper 1839-D.
- Neitsch, S. L., Arnold, J. G., Kiniry, J. R., Williams, J. R., 2011. Soil and water assessment tool theoretical documentation version 2009. Tex. Water Resour. Inst.. TR-406
- Pechlivanidis, I. G., Jackson, B. M., McIntyre, N. R., Wheeler, H. S., 2011. Catchment scale hydrological modelling: A review of model types, calibration approaches and uncertainty analysis methods in the context of recent developments in technology and applications. *Global NEST Journal*, 13(3), 193–214.
- Pfannerstill, M., Guse, B., Fohrer, N., 2014a. A multi-storage groundwater concept for the SWAT model to emphasize nonlinear groundwater dynamics in lowland catchments. *Hydrological Processes*, 28(22), 5599–5612.
- Pfannerstill, M., Guse, B., Fohrer, N., 2014b. Smart low flow signature metrics for an improved overall performance evaluation of hydrological models. *Journal of Hydrology*, 510, 447–458.
- Pignotti, G., Rathjens, H., Cibin, R., Chaubey, I., Crawford, M., 2017. Comparative analysis of HRU and grid-based SWAT models. *Water*, 9(4), 272.
- Pokhrel, P., Yilmaz, K. K., Gupta, H. V., 2012. Multiple-criteria calibration of a distributed watershed model using spatial regularization and response signatures. *Journal of Hydrology*, 418-419, 49–60.

- Pushpalatha, R., Perrin, C., Le Moine, N., Andréassian, V., 2012. A review of efficiency criteria suitable for evaluating low-flow simulations. *Journal of Hydrology*, 420-421, 171–182.
- Rathjens, H., Oppelt, N., Bosch, D. D., Arnold, J. G., Volk, M., 2015. Development of a grid-based version of the SWAT landscape model. *Hydrological Processes*, 29, 900–914.
- Refsgaard, J. C., Hjbørg, A. L., Møller, I., Hansen, M., Søndergaard, V., 2010. Groundwater modeling in integrated water resources management—Visions for 2020. *Groundwater*, 48(5), 633–648.
- Riediger, J., Breckling, B., Nuske, R. S., Schröder, W., 2014. Will climate change increase irrigation requirements in agriculture of Central Europe? A simulation study for Northern Germany. *Environmental Sciences Europe*, 26, 18.
- Rozos, E., Efstratiadis, A., Nalbantis, I., Koutsoyiannis, D., 2004. Calibration of a semi-distributed model for conjunctive simulation of surface and groundwater flows/Calage d'un modèle semi-distribué pour la simulation conjointe d'écoulements superficiels et souterrains. *Hydrological Sciences*, 49(5), 819–842.
- Siebert, S., Burke, J., Faures, J. M., Frenken, K., Hoogeveen, J., Döll, P., Portmann, F. T., 2010. Groundwater use for irrigation—A global inventory. *Hydrology and Earth System Sciences*, 14, 1863–1880.
- Sophocleous, M. A., Koelliker, J. K., Govindaraju, R. S., Birdie, T., Ramireddygari, S. R., Perkins, S. P., 1999. Integrated numerical modeling for basin-wide water management: The case of the Rattlesnake Creek basin in south-central Kansas. *Journal of Hydrology*, 214, 179–196.
- Strauch, M., Lima, J. E. F. W., Volk, M., Lorz, C., Makeschin, F., 2013. The impact of best management practices on simulated streamflow and sediment load in a Central Brazilian catchment. *Journal of Environmental Management*, 127, S24–S36.
- Sun, X., Bernard-Jannin, L., Garneau, C., Volk, M., Arnold, J. G., Srinivasan, R., ... Sánchez-Pérez, J. M., 2016. Improved simulation of river water and groundwater exchange in an alluvial plain using the SWAT model. *Hydrological Processes*, 30(2), 187–202.
- Thiessen, A. H., 1911. Precipitation averages for large areas. *Monthly Weather Review*, 39(7), 1082–1089.

- Tóth, J., 1963. A theoretical analysis of groundwater flow in small drainage basins. *Journal of Geophysical Research*, 68, 4795–4812.
- Uniyal, B., Dietrich, J., Vasilakos, C., Tzoraki, O., 2017. Evaluation of SWAT simulated soil moisture at catchment scale by field measurements and Landsat derived indices. *Agricultural Water Management*, 193, 55–70.
- Vazquez-Amábile, G. G., Engel, B. A., 2005. Use of SWAT to compute groundwater table depth and streamflow in the Muscatatuck River watershed. *Transactions of the ASABE*, 48(3), 991–1003.
- Volk, M., Arnold, J. G., Bosch, D. D., Allen, P. M., Green, C. H., 2007. Watershed configuration and simulation of landscape processes with the SWAT model. In L. Oxley, & D. Kulasiri (Eds.), *MODSIM 2007 international congress on modelling and simulation* (pp. 2382–2389. Christchurch: Modelling and Simulation Society of Australia and New Zealand.
- Wagner, P. D., Bhallamudi, S. M., Narasimhan, B., Kantakumar, L. N., Sudheer, K. P., Kumar, S., . . . Fiener, P., 2016. Dynamic integration of land use changes in a hydrologic assessment of a rapidly developing Indian catchment. *Science of Total Environment*, 539, 153–164.
- Wang, Y., Brubaker, K., 2014. Implementing a nonlinear groundwater model in the soil and water assessment tool (SWAT). *Hydrological Processes*, 28(9), 3388–3403.
- Wessolek, G., Kaupenjohann, M., Renger, M., 2009. *Bodenphysikalische Kennwerte und Berechnungsverfahren für die Praxis* (Bodenökologie und Bodengeneese, Heft 40. Berlin: Technische Universität.
- Wittenberg, H., 2003. Effects of season and man-made changes on baseflow and flow recession: Case studies. *Hydrological Processes*, 17, 2113–2123.
- Wittenberg, H., 2015. Groundwater abstraction for irrigation and its impacts on low flows in a watershed in northwest Germany. *Resources*, 4(3), 566–576.
- Yilmaz, K. K., Gupta, H. V., Wagener, T., 2008. A process-based diagnostic approach to model evaluation: Application to the NWS distributed hydrologic model. *Water Resources Research*, 44(9).

## Chapter 4

# Modeling Interbasin Groundwater Flow in Karst Areas: Model Development, Application, and Calibration Strategy

Nguyen, V. T., Dietrich, J., Uniyal, B., 2020. Modeling Interbasin Groundwater Flow in Karst Areas: Model Development, Application, and Calibration Strategy. *Environmental Modelling & Software*, 124, 104606.

### Abstract

Karstification is considered as one of the most common reasons for interbasin groundwater flow (IGF). IGF in some karst areas could be significant such that it must be accounted for in hydrologic modeling. In this study, the Soil and Water Assessment Tool (SWAT) was modified to explicitly account for IGF in karst areas. The modified model uses two conceptual models to simulate hydrologic processes in karst and non-karst regions. The modified model was applied in the karst-dominated region in the southwest Harz Mountains, Germany. Multisite streamflow data and satellite-derived actual evapotranspiration (ETa) were used for model calibration. Results show that (1) the modified model can be satisfactorily calibrated and validated for streamflow and ETa (2) the model performance for ETa and streamflow at some gauging stations are highly correlated, and (3) the use of satellite-derived ETa does not affect the model performance.

Keywords: Modified SWAT, Karst, Interbasin groundwater flow, Calibration, Satellite-derived evapotranspiration.

## Software availability

Name of software: SWAT\_IGF

Developer and contact address: Van Tam Nguyen (nguyen@iww.uni-hannover.de), Institute of Hydrology and Water Resources Management, Leibniz Universität Hannover, Appelstraße 9A, 30167 Hannover, Germany

Year available: 2019

Availability and cost: the source code is freely available at <http://doi.org/10.5281/zenodo.3574312>

Language: Fortran

## 4.1 Introduction

The term “karst” refers to a region with distinct landscape features (e.g., sinking streams, sinkholes, and springs) and underground features (e.g., underground conduits and caves). In some karst regions, the karst landscape features could be absent or subtle, but their aquifers could be heavily karstified (Ford and Williams, 2007). Karst aquifers are developed as a result of the dissolution of karstifiable rocks (e.g., limestone, dolomite, gypsum, and rock salt), the so-called karstification (Bögli, 1980; Ford and Williams, 2007; Howard, 1963). Karst aquifers account for about 10% to 15% of the continental area and karst groundwater is one of the sources of drinking water for approximately a quarter of the world’s population (Ford and Williams, 2007). However, karst groundwater is particularly vulnerable to contamination due to their distinct hydrogeologic characteristics (Doerfliger et al., 1999; Drew and Hötzl, 1999; Goldscheider, 2005). Therefore, understanding the hydrogeologic characteristics of karst aquifers plays an important role in water resources management in karst regions.

Hydrogeologic characteristics of karst aquifers are different from other aquifers (Bakalowicz, 2005). Karst aquifers often exhibit a duality of recharge, infiltration, porosity, flow and storage (Goldscheider and Drew, 2007; Gun, 1986; White, 2002). Karst

aquifers also show a high degree of spatial heterogeneity in hydraulic properties (Bonacci et al., 2006). Especially, the surface drainage basin in karst aquifers usually does not coincide with the groundwater basin (Dar et al., 2014; Spangler, 2001). Karstification is considered as one of the most common causes of interbasin groundwater flow (IGF) (Le Moine et al., 2007). Water recharged to karst aquifers could flow through an underground conduit system spanning over several basins and emerge at springs located at distant sites (e.g., Anderson et al., 2006; Belcher et al., 2006; Le Moine et al., 2008). It should be noted that IGF could also occur in porous aquifer in the form of regional groundwater flow (Danapour et al., 2019; Nguyen and Dietrich, 2018; Tóth, 1963), however, in this study we focus on IGF in karst areas. The term IGF in this study could be also understood as regional groundwater flow across surface topographic divides. IGF in karst areas could significantly alter the water budget of a basin (e.g., Anderson et al., 2006; Le Moine et al., 2008). Considering the aforementioned facts, IGF in karst areas should be accounted for in hydrological modeling, especially in the context of transboundary or interbasin groundwater management.

Various models have been used to simulate IGF in karst aquifers with varying model complexity, ranging from physically based distributed to conceptual lumped models. Physically based distributed models simulate groundwater flow based on hydraulic head gradient, therefore, groundwater could flow across topographic divide units, which are normally considered as isolated groundwater units in surface hydrology. Conceptual models can simulate IGF by allowing the simulation (or routing) of groundwater flow between topographical basins. Some models of these types are the Modular Three-Dimensional Finite-Difference Ground-Water Flow Model (MODFLOW, Scanlon et al., 2003), the modified WetSpa model (Liu et al., 2005), the modified Soil and Water Assessment Tool (SWAT, Arnold et al., 1998; Malagó et al., 2016; Nerantzaki et al., 2015; Palanisamy and Workman, 2014), modèle du Génie Rural à 4 paramètres Journalier (GR4J, Le Moine et al., 2007, 2008; Perrin and Michel, 2003), the tank model (Anaya and Wanakule, 1993), and the multi-cell aquifer model (Barrett and Charbeneau, 1997; Rozos and Koutsoyianis, 2006). SWAT is one of the most widely-used models to simulate the effect of land use, agricultural management practices and climate change on water and chemical yields in non-karst areas (Arnold et al., 2005; Gassman et al., 2007; Krysanova and White, 2007; Molina-Navarro et al., 2017). Therefore, the modified SWAT versions which account for IGF in karst areas could potentially help to explore these effects in karst regions.

The aforementioned modified SWAT models, the so-called KarstSWAT (Palanisamy and Workman, 2014) and KSWAT (Malagó et al., 2016; Nerantzaki et al., 2015), simulate



IGF in karst regions. The KarstSWAT model was specifically developed for watersheds dominated by sinkholes and springflow, which is mainly fed by the water from sinkholes (Palanisamy and Workman, 2014). The KSWAT model combines the *adapted SWAT model* (Fig. 3, Malagó et al., 2016) and the *karst-flow model* (Nikolaidis et al., 2013). The *adapted SWAT model* assumes that all water entering the soil profile is karst groundwater recharge (Fig. 3, Malagó et al., 2016). However, part of the infiltrated water could contribute to the streamflow as lateral flow and baseflow if the underlying aquifer of a subbasin is not entirely a karst aquifer (e.g., Palanisamy and Workman, 2014). The *adapted SWAT model* does not differentiate between concentrated recharge and diffuse recharge. The *karst-flow model* is the two-linear-storage reservoir model, which receives the recharge simulated from the *adapted SWAT model* (or from the original SWAT model, Nikolaidis et al., 2013) and routes it to spring. Outflows from the two reservoirs of the *karst-flow model* represent flow from wide conduits and narrow fractures (Kourgialas et al., 2010; Malagó et al., 2016). Because of the lumped feature of deep recharge from the *adapted SWAT model*, the KSWAT model does not explicitly differentiate between (1) the diffuse recharge and concentrated recharge, (2) between matrix storage and conduit storage. This is important because these recharges and storages are different in terms of travel time and storage. In addition to the aforementioned disadvantages, the recharge area of the karst aquifer in the KarstSWAT and KSWAT models follows the subbasin delineation of SWAT.

In addition to the model development, parameter identification in karst regions is also subject to higher uncertainty compared to other regions (Brenner et al., 2018; Hartmann et al., 2017, 2013). This is because the karst aquifer is highly heterogeneous and the upper flux (actual evapotranspiration, ET<sub>a</sub>) and the lower flux (karst groundwater recharge) are usually unknown. In order to develop a robust model and to minimize the parameter uncertainty, especially in karst regions, multi-variable calibration is suggested. ET<sub>a</sub> is one of the main components of the hydrologic cycle. About 60% of the annual precipitation on the global land surface returns to the atmosphere as evapotranspiration (Jung et al., 2010; Oki and Kanae, 2006). Considering the aforementioned facts, observed ET<sub>a</sub> should be used for calibrating the model. However, direct observation of ET<sub>a</sub> is very scarce.

In non-karst areas, many studies have used satellite-derived ET<sub>a</sub> for model calibration (e.g., Droogers et al., 2010; Franco and Bonumá, 2017; Immerzeel and Droogers, 2008; Muthuwatta et al., 2009; Rajib et al., 2018; Rientjes et al., 2013; Vervoort et al., 2014; Zhang et al., 2009). In these studies, satellite-derived ET<sub>a</sub> was either used as an independent calibration data set or as input data. Results showed that the model performance for

streamflow could decrease when constraining model calibration with satellite-derived ETa as an additional variable (Vervoort et al., 2014). However, the above-mentioned studies showed that using satellite-derived ETa in combination with observed streamflow for calibrating a hydrologic model could (1) better reproduce the catchment's water balance, (2) reduce the parameter uncertainty, (3) increase the model robustness, and (4) detect the structural model issues. In karst areas, the use of satellite-derived ETa as an additional calibration variable has not been given enough attention.

In this study, we developed a conceptual model which is able to (1) simulate surface and subsurface flows in both karst and non-karst areas, (2) apply for a region where the karst aquifer boundaries do not coincide with the surface subbasin boundaries, and (3) represent different recharges (diffuse recharge and concentrated recharge) and storages (matrix storage and conduit storage) in karst areas. The proposed concept was implemented in the SWAT model. The modified SWAT model was tested in the karst-dominated area in Lower Saxony, Germany. The effects of using satellite-derived ETa for model calibration on the model performance was examined in detail. The Moderate Resolution Imaging Spectroradiometer (MOD16 ETa, Mu et al., 2013) was used for the model calibration.

## 4.2 Methodology

### 4.2.1 The original SWAT model

In SWAT, a basin can be divided into subbasins, which are further divided into Hydrologic Response Units (HRUs). HRUs are created by lumping all areas having the same combination of land use, soil type and slope within a subbasin. The HRU concept is computationally efficient while incorporating the aforementioned landscape properties. SWAT simulates two phases of the hydrologic cycle, the land phase and the routing phase. The land phase includes HRU-related processes such as surface processes (e.g., evapotranspiration, surface runoff, vegetation-related processes) and subsurface processes (e.g., percolation, lateral flow, groundwater recharge, return flow) (Fig. 4.1A). The routing phase includes stream-related processes (e.g., flood routing, nutrient transport) and reservoir routing. In SWAT, groundwater recharge is partitioned into shallow and deep aquifer recharge. Recharge into the shallow aquifer ultimately returns to stream as base-flow while recharge into the deep aquifer is considered as a loss. SWAT is not capable of simulating groundwater flow between HRUs (or subbasins) due to the non-spatial characteristic of the HRU concept. A more detailed description of the SWAT model is given

by Neitsch et al. (2011).

## 4.2.2 The modified SWAT model for IGF

In this section, after a summary of the general hydrogeologic characteristics of karst areas, the modified SWAT for karst areas is presented. The modified SWAT model for modeling IGF, hereafter referred to as the SWAT\_IGF model, is comprised of two conceptual models. The original conceptual model of SWAT is applied for non-karst areas (Fig. 4.1A) while modified conceptual model of SWAT is applied for karst areas (Fig. 4.1B). The two conceptual models were combined into a single program, resulting in a single executable file. An aquifer classification map is used as an additional criterion for the delineation of HRUs (Fig. 4.3C). This aquifer classification map contains information about the aquifer type and the extended recharge area of each spring. Then, the SWAT\_IGF will assign the appropriate conceptual model for the karst and non-karst HRUs automatically (Fig. 4.3C) and recharge from the extended karst area will be routed to the corresponding spring. The user needs to assign the amount of recharge to each spring (in case multiple springs are fed by the same recharge area).

Recharge into the karst aquifer could either be classified as (1) autogenic or allogenic recharge or (2) concentrated or diffuse recharge (Ford and Williams, 2007; Gun, 1986; Taylor and Greene, 2008). Autogenic recharge originates from precipitation falling on the karst areas while allogenic recharge originates from runoff on non-karst areas. Concentrated recharge can occur via sinkholes, losing streams, closed depressions, and well-developed fissures. Diffuse recharge is a areal recharge through the unsaturated soil zone. Recharge into the karst aquifer is often drained by a well-developed solution-conduit system and discharged via one or several springs. Flow in the conduit is often fast and turbulent while flow in the rock matrix is slow and laminar (Hartmann et al., 2014; White, 2002). However, the majority of karst groundwater is stored in the rock matrix. Due to the fast flow and small storage of the conduit system compared to that of the rock matrix, the response of discharge to recharge from the conduit system is often faster than that from the matrix storage.

In this study, the SWAT\_IGF is proposed for the cases where (1) the recharge area and discharge points (springs) are located in different subbasins and (2) the discharge points are located in one subbasin. Further modifications could be done for other cases. A two-reservoir model is proposed to represent the duality of and storage and discharge of the karst area (Fig. 4.1B). The first reservoir, hereinafter referred to as the matrix storage

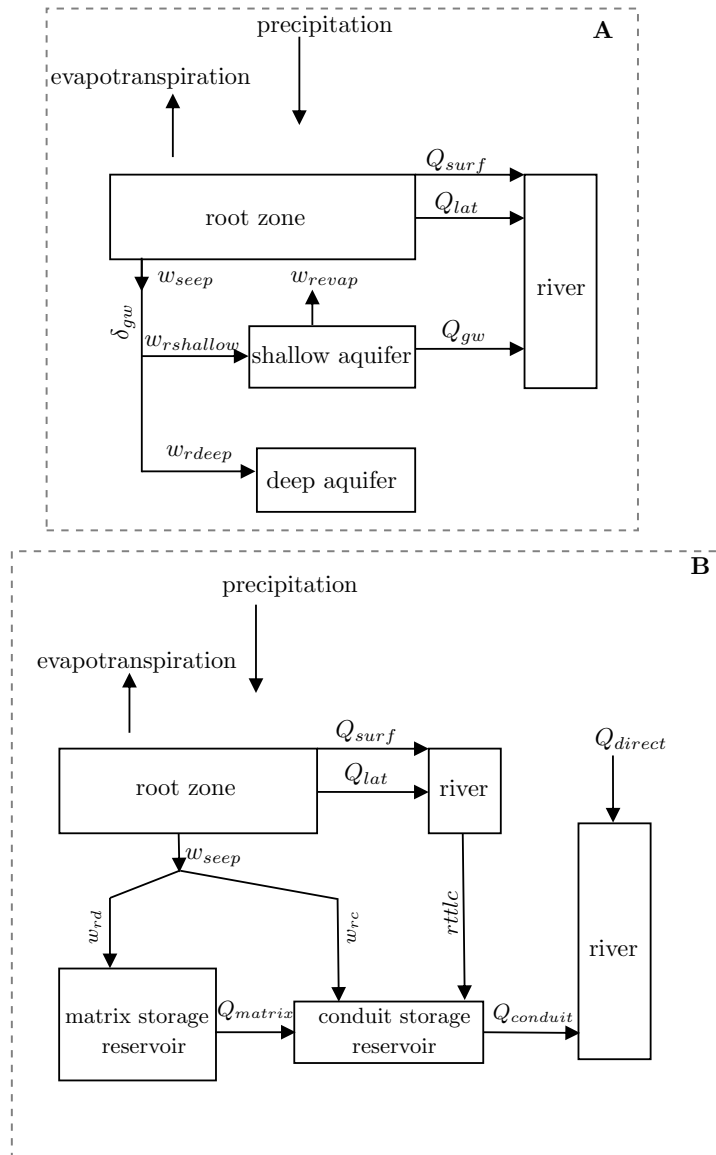


Figure 4.1: Conceptual models of the SWAT\_IGF model. (A) the conceptual model for the non-karst area (the original conceptual model of SWAT), (B) the conceptual model for the karst area (modified from SWAT).  $Q_{surf}$  is the surface runoff,  $Q_{lat}$  is the lateral flow,  $w_{revap}$  is the groundwater revap,  $w_{rshallow}$  and  $w_{rdeep}$  are the shallow and deep groundwater recharge, respectively, other variables were described in text.

reservoir, represents groundwater storage in the rock matrix. The matrix storage reservoir receives diffuse recharge from the overlying zone. The second reservoir, hereinafter referred to as the conduit storage reservoir, represents groundwater storage in the conduit system. The conduit storage reservoir receives (1) concentrated recharge from closed depressions, infiltration losses from streams, fractures and dolines and (2) diffuse discharge from the matrix storage reservoir. It should be noted that there could be flow from the conduit storage reservoir to the matrix reservoir (e.g., [Screaton et al, 2004](#)), however, it is not explicitly considered in this study. We consider flow from the matrix to the conduit as net flow, which already takes into account flow from the conduit to the rock matrix.

Diffuse recharge from the bottom of the soil profile to the matrix storage reservoir on day  $i$ , taking into account the delay time in the unsaturated zone, is calculated using the exponential decay weighting function ([Sangrey et al, 1984](#); [Venetis, 1969](#)):

$$w_{rd,i} = (1 - e^{-1/\delta_{gw}}) \cdot \beta \cdot w_{seep,i} + e^{-1/\delta_{gw}} \cdot w_{rd,i-1} \quad (4.1)$$

where  $w_{rd,i}$  and  $w_{rd,i-1}$  (mm H<sub>2</sub>O) is the amount of diffuse recharge to the matrix reservoir on day  $i$  and  $i - 1$ , respectively,  $\delta_{gw}$  (days) is the delay time for infiltrated water to reach the matrix storage reservoir,  $\beta$  (-) is the recharge separation factor, ranging from 0 to 1,  $w_{seep}$  (mm H<sub>2</sub>O) is the total amount of water exiting the bottom of the soil profile on day  $i$ .

Outflow from the matrix storage reservoir is simulated using the linear storage-discharge relationship (e.g., [Neitsch et al., 2011](#); [Nikolaidis et al., 2013](#)):

$$Q_{matrix,i} = e^{-\alpha_{matrix} \cdot \Delta t} \cdot Q_{matrix,i-1} + (1 - e^{-\alpha_{matrix} \cdot \Delta t}) \cdot \sum_{j=1}^{nhrus} w_{rd,i,j} \cdot a_j \cdot 10^{-3} \quad (4.2)$$

where  $Q_{matrix,i}$  and  $Q_{matrix,i-1}$  (m<sup>3</sup> H<sub>2</sub>O) are the outflows from the matrix storage reservoirs on day  $i$  and  $i - 1$ , respectively,  $\alpha_{matrix}$  (1/day) is the recession constant of the matrix storage reservoir, respectively,  $\Delta t$  is the time step ( $\Delta t = 1$  day),  $w_{rd,i,j}$  (mm H<sub>2</sub>O) and  $a_j$  (m<sup>2</sup>) are the diffuse recharge and area of the hydrologic response unit  $j$ , respectively,  $10^{-3}$  is the unit conversion factor (from mm H<sub>2</sub>O to m H<sub>2</sub>O),  $nhrus$  is the number of HRUs in the recharge area.

Concentrated recharge from closed depressions, fractures, and sinkholes to the conduit storage reservoir on day  $i$ ,  $w_{rc,i}$  (mm H<sub>2</sub>O), is calculated as follows:

$$w_{rc,i} = (1 - \beta) \cdot w_{seep,i} \quad (4.3)$$

The total amount of recharge to the conduit storage reservoir on day  $i$ ,  $W_{rconduit,i}$  ( $\text{m}^3 \text{H}_2\text{O}$ ), is expressed as follows:

$$W_{rconduit,i} = \sum_{j=1}^{nhrus} w_{rc,i,j} \cdot a_j \cdot 10^{-3} + rttlc_i + Q_{matrix,i} \quad (4.4)$$

where  $rttlc_i$  ( $\text{m}^3 \text{H}_2\text{O}$ ) is the amount of recharge from losing streams on day  $i$ . Outflow from the conduit storage reservoir is simulated using the linear storage-discharge relationship:

$$Q_{conduit,i} = e^{-\alpha_{conduit} \cdot \Delta t} \cdot Q_{conduit,i-1} + (1 - e^{-\alpha_{conduit} \cdot \Delta t}) \cdot W_{rconduit,i} \quad (4.5)$$

where  $Q_{conduit,i}$  and  $Q_{conduit,i-1}$  ( $\text{m}^3 \text{H}_2\text{O}$ ) are outflows from the conduit storage reservoir on day  $i$  and  $i - 1$ , respectively,  $\alpha_{conduit}$  (1/day) is the recession constant of the conduit storage reservoir.

The total runoff of a basin where the springs are located,  $Q_{river,i}$  ( $\text{m}^3 \text{H}_2\text{O}$ ), is calculated as follows:

$$Q_{river,i} = Q_{conduit,i} + Q_{direct,i} \quad (4.6)$$

where  $Q_{direct,i}$  ( $\text{m}^3 \text{H}_2\text{O}$ ) is the direct runoff (the sum of surface runoff and lateral flow) from the basin where the spring is located.

It should be noted that the conduit and matrix reservoirs proposed in this study correspond to the upper and lower reservoirs of the *karst-flow model* (Nikolaidis et al., 2013), respectively. The conduit and the matrix reservoirs are arranged in series while the upper and lower reservoirs are arranged in parallel. The lower reservoir receives recharge from the upper reservoir while the conduit receives recharge from the matrix reservoir. Springflow in the *karst-flow model* is directly fed by the upper and lower reservoirs while it is only directly fed by the conduit reservoir in the SWAT\_IGF model. Outflows from both reservoirs in both models are simulated using a linear storage-discharge relationship.

## 4.3 Case Study

### 4.3.1 Study area and data

The study area is located in the southwest Harz Mountains (non-karst area) and the southern Harz rim (karst-dominated area) in Northern Germany with a drainage basin of about 384 km<sup>2</sup> (Fig. 4.2). The study area has two outlets located at the Rhume spring and Lindau gauging stations. The study area receives inflow from the Odertalsperre reservoir. The Digital Elevation Model (DEM) obtained from the Niedersächsische Landesbetrieb für Wasserwirtschaft, Küsten- und Naturschutz (NLWKN) shows that the elevation of the study area varies from 142 m to 929 m above mean sea level (a.m.s.l). Land use/land cover (LULC) map was taken from the Copernicus Land Monitoring Service. The soil map (BÜK 200) and soil profile data were obtained from the Bundesanstalt für Geowissenschaften und Rohstoffe (BGR) (Fig. 4.3). Initial soil hydraulic conductivity and soil available water content were derived by using the pedotransfer functions/tables (Wessolek et al., 2009). The dominant land use/land cover classes are forest and agricultural, accounting for about 55% and 31% of the study area, respectively. The most dominant soil type in the southwest Harz Mountains is spodic Cambisols from acid igneous and metamorphic rocks, covering 46% of the study area. In the southern Harz rim, most of the soils were developed from gypsum with low water-holding capacity (Schnug et al, 2004). Observed groundwater level data at three wells located within and nearby the Pöhlder Becken were collected from the NLWKN (Fig. 4.2).

Daily weather data (precipitation, wind speed, temperature, solar radiation, and relative humidity) from 1997-2010 were obtained from Deutscher Wetterdienst (DWD). Weather data from observed stations were interpolated for all subbasins using the inverse distance weighting (IDW) method. The study area has an average annual precipitation of 1242 mm/yr with high spatial variability. The annual precipitation is up to 1619 mm/yr in the southwest Harz Mountains, whereas that in the southern Harz rim is 862 mm/year. Temperature in the study area decreases with an increase in elevation. Daily observed streamflow and reservoir outflow were obtained from the NLWKN and the Harzwasserwerke (HWW). The MOD16 ETa at 8-day time step and 1 km<sup>2</sup> spatial resolution was downloaded using the MODISTools (Tuck et al., 2014).

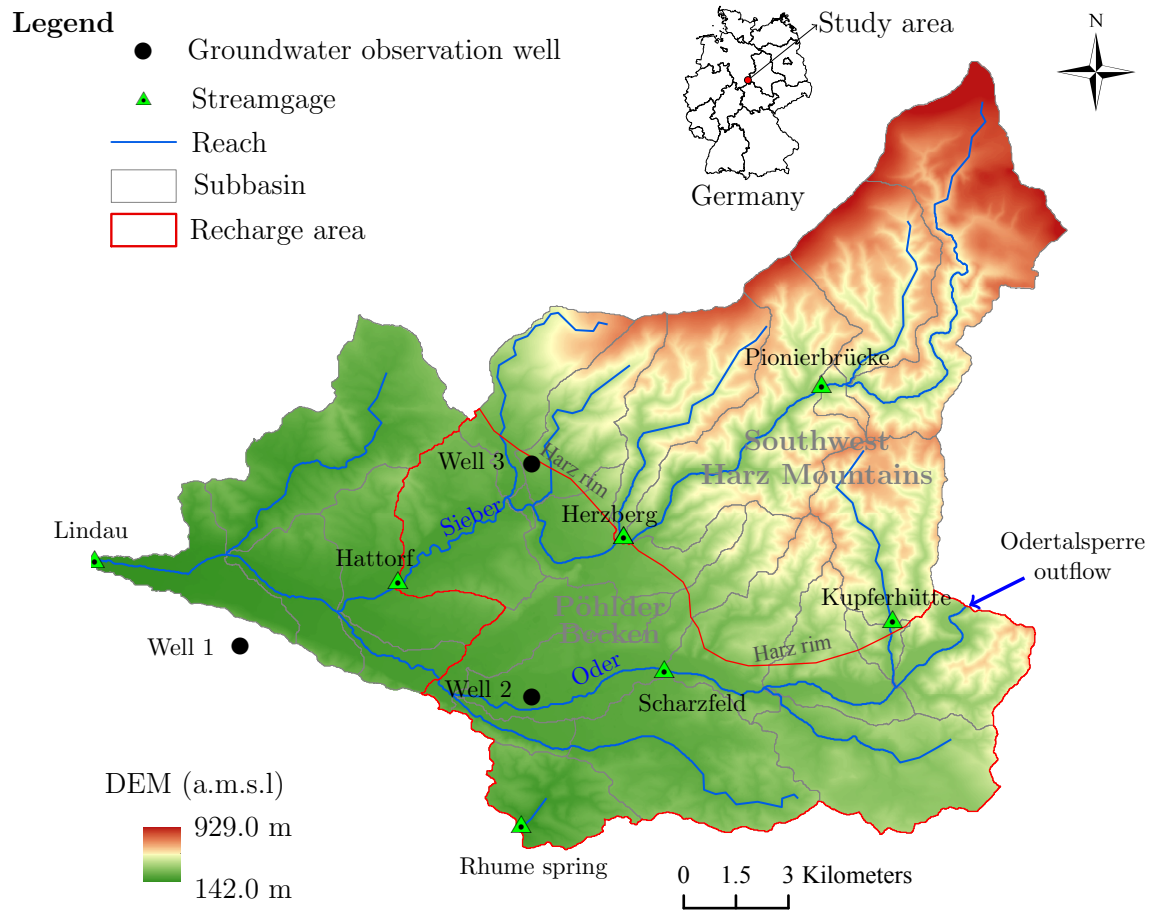


Figure 4.2: The study area with the Digital Elevation Model.



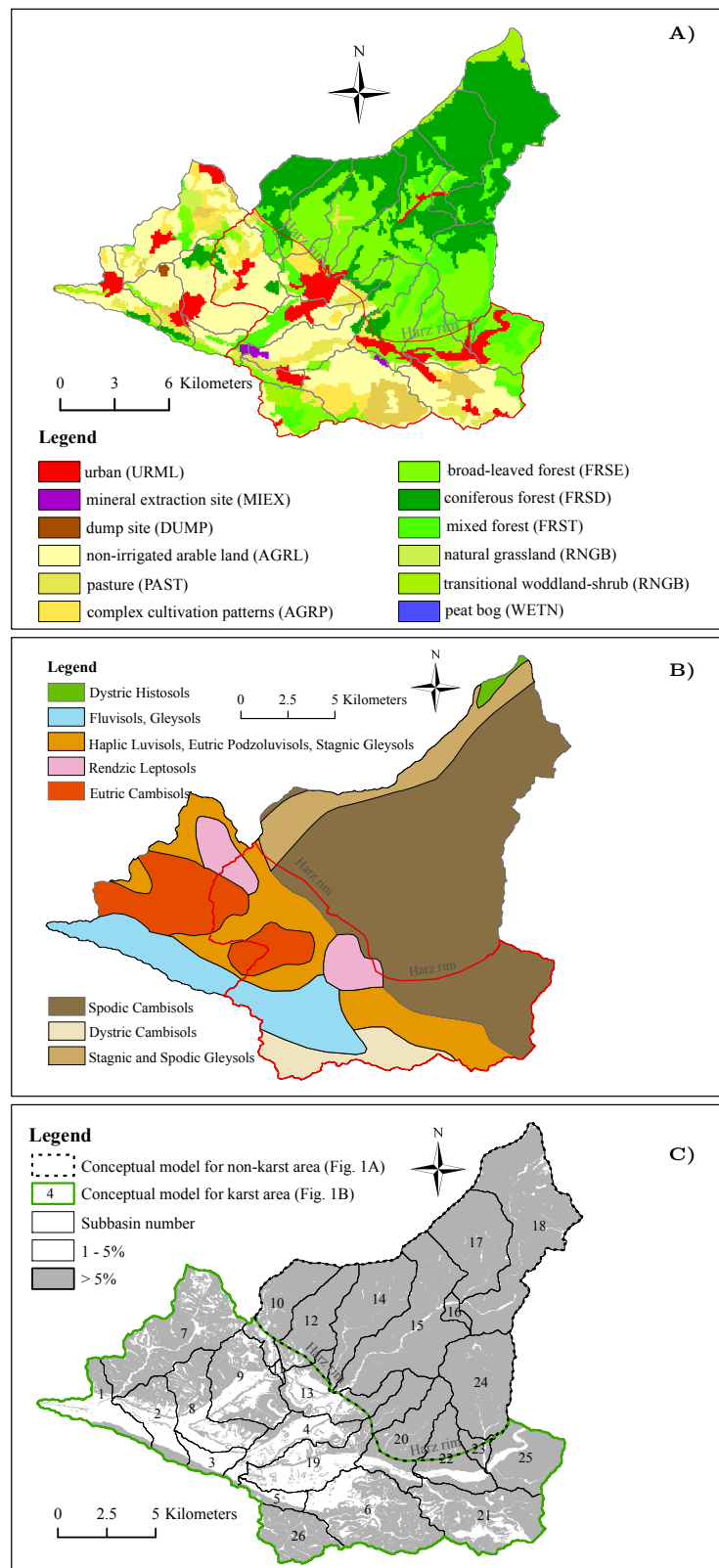


Figure 4.3: Distribution of (A) land use/land cover, (B) soil, and (C) slope with subbasin numbers in the study area.

### 4.3.2 Geology

The study area consists of two distinct geologic areas, the southwest Harz Mountains and the southern Harz rim (Grimmelmann, 1992). The Harz Mountains were part of the European Variscan fold belt formed by the collision of Africa, Baltica, Laurentia and other microplates in the early Paleozoic Era (Haggett, 2002; Tait et al., 1997). The Harz Mountains were later eroded and a large part of it was inundated by the Zechstein Sea (Haggett, 2002; Koster, 2005). Under hot and dry climatic conditions of the late Permian period, a large amount of evaporites was formed in the inundated area after several evaporation cycles (Böttcher, 1999; Kramm and Wedepohl, 1991; Schnug et al, 2004; Taylor, 1998; Tucker, 1991).

After other geologic processes, the underlying geology of the southern Harz Mountains nowadays mainly consists of Palaeozoic greywacke, shale, and conglomerate (Fig. 4.4) while in the southern Harz rim, the Permian Zechstein (dolomite, gypsum, anhydrite) was exposed to the surface and subjected to the karstification process (Böttcher, 1999; Paul and Vladi, 2001; Schnug et al, 2004; Voigt et al., 2008). There is a 2- to 6-km-wide strip of exposed Permian Zechstein in the southern Harz rim with various karst features such as sinking streams, sink holes, caves, and springs (Liersch, 1987). The karst area in this region is subjected to a continuous karstification process. About 7092 tons of sulfur bound to gypsum are washed from this karst-dominated area each year (Herrmann, 1969; Schnug and Haneklaus, 1998). Geological cross-sections in the area show that the Permian Zechstein rocks are exposed to the surface near the southern Harz rim and overlaid by non-karstifiable rocks in the south. At the Oder and Sieber rivers, it was overlaid by a Quaternary fluvial deposit layer originated from the Harz Mountains (Fig. 4.4). Detailed geologic maps and geologic cross-sections of the study area can be found in Herrmann (1969), Grimmelmann (1992), Liersch (1987), Voigt et al. (2008), and NIBIS®Kartenserver (<http://nibis.lbeg.de/cardomap3/?TH=647>).

### 4.3.3 Hydrogeology

The main Rhume spring outlet is located in a NW-SE trending fault, where flow in the underground conduit of the Zechstein deposits is blocked by a low permeability Lower Buntsandstein stratum (Herrmann, 1969; LaMoreaux and Tanner, 2001). Besides the main outlet with a diameter of about 20 m, there are about 360 small outlets located nearby (Herrmann, 1969). They altogether release an average discharge of about 2.2 m<sup>3</sup>/s via a small stream with a minimum of 1.5 m<sup>3</sup>/s during low flow periods. This indicates

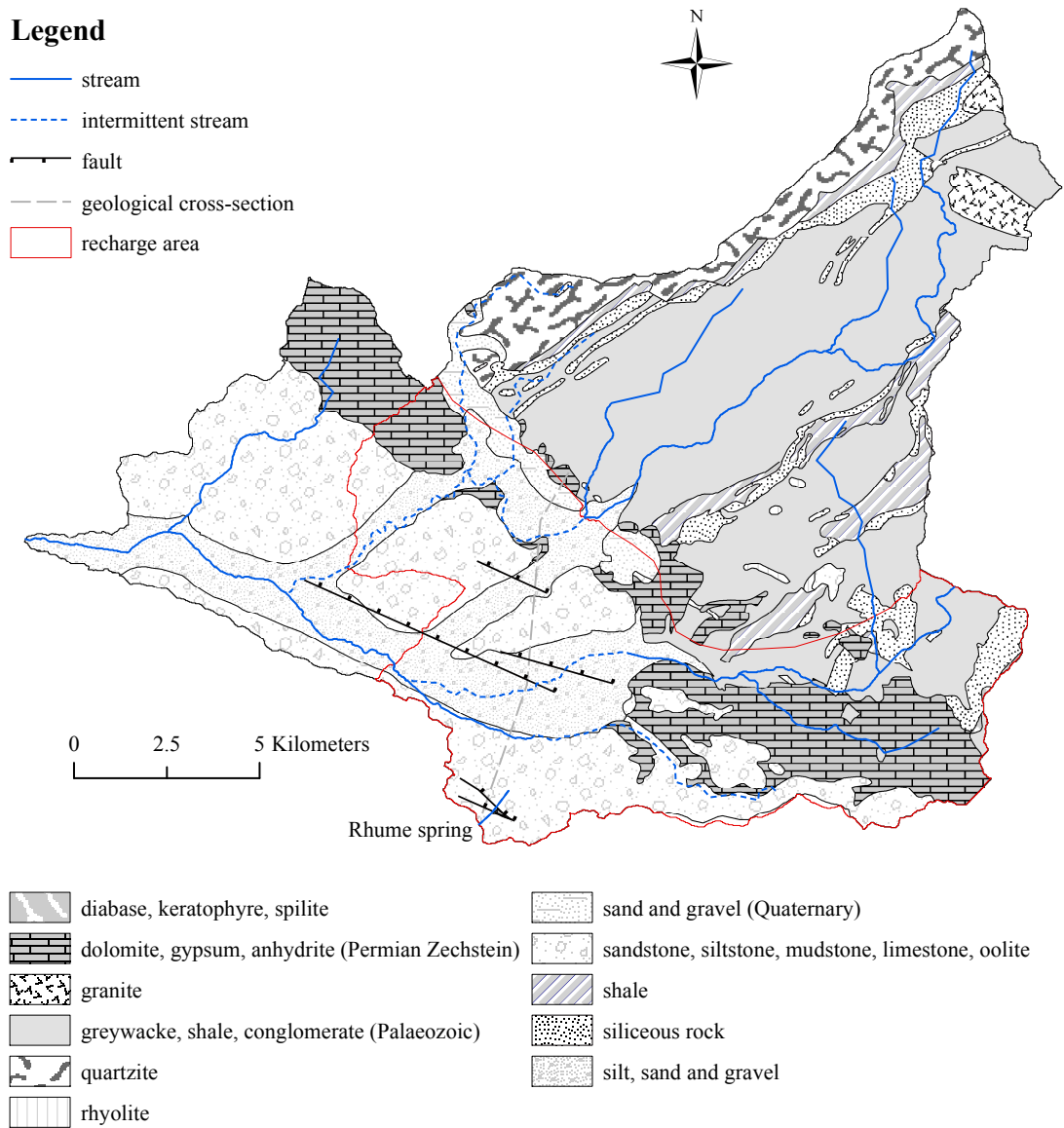


Figure 4.4: Geological map of the study area (BGR). Location of the faults and different types of streams were identified according to Thürnaeu (1913) and Grimmelmann (1992). More information about the geological cross-section could be found in Grimmelmann (1992).

that there could be a relatively big subsurface matrix storage in the area compared to the Rhume spring subbasin. The sum of discharge from the main Rhume spring outlet and its neighboring outlets is hereafter referred to as the Rhume spring discharge. Many studies have been conducted to explain the origin of the water from the Rhume spring discharge since the early 20th century.

Thürnaeu (1913) conducted tracer tests with Uranine and found that the infiltrated tracers from the area in the southern Harz rim, which were later known as the Pöhlder Becken, reappears at the Rhume spring (Fig. 4.2). Thürnaeu (1913) was also able to determine the main losing streams (Fig. 4.4) in the Pöhlder Becken as well as the travel time of tracers from the infiltration points to the Rhume spring. Haase et al. (1970) analyzed the water balance in the study area and found that there are significant infiltration losses in the Sieber and Oder rivers. In 1981, another tracer tests with about 12 kg of Uranine were carried out at sinkholes near Herzberg (Liersch, 1987). The injected tracers were detected at the Rhume spring about 78 hours after the injection and were almost undetectable after 25 days. From this experiment, a flow path of about 7500 m and a horizontal groundwater flow velocity of over 100 m/h were estimated (LaMoreaux and Tanner, 2001). A three-reservoir storage model was proposed to explain the breakthrough curve of tracer concentration at the Rhume spring (Liersch, 1987). Rienäcker (1987) found that the time-lag between peak discharges of the Sieber (at Hattorf gauging station), of the Oder (at Scharzfeld gauging station) and the Rhume spring varies between 24 to 72 hours, depending on the existing groundwater reservoir storage level. Results from various geophysical and tracer experiments showed that infiltrated water from the Pöhlder Becken, hereinafter referred to as the recharge area of the Rhume spring (Fig. 4.2), and transmission losses of the rivers located in this area are the main sources of the Rhume spring discharge (Goldmann, 1986; Liersch, 1987).

The recharge area of the Rhume spring receives allogenic recharge from upstream sub-basins via a connected river network in the area. In addition, it also receives groundwater inflow from the southwest Harz Mountains. However, the estimated amount is negligible,  $< 0.03 \text{ m}^3/\text{s}$  (Grimmelmann, 1992). The estimated contribution of flow from the Rhume basin (with an area of  $8 \text{ km}^2$ ) is about 4% of the Rhume spring discharge. About 96% of the Rhume spring discharge is from IGF, of which about 60% originates from the infiltration loss of the Oder and Sieber rivers (Goldmann, 1986; LaMoreaux and Tanner, 2001; Liersch, 1987). Therefore, the original SWAT\_IGF should be used instead of the original SWAT to explain 96% of the flow volume at the Rhume spring.

## 4.4 Model setup, calibration and validation

### 4.4.1 Model setup

The study area was divided into 26 subbasins and 1094 HRUs based on LULC, soil, DEM and aquifer map (Fig. 4.3). The thresholds for defining HRUs were set to zero to include all of the basin landscape. The SWAT-IGF model uses the conceptual model presented in Fig. 4.1A for the southwest Harz Mountains and the conceptual model presented in Fig. 4.1B for the southern Harz rim (Fig. 4.3C). Infiltration losses ( $w_{seep}$ ) and river transmission losses ( $rttlc$ ) from the karst area located outside the recharge area of the Rhume spring were considered as losses from the hydrologic system. The model was set to run for the period of 14 years (from 1997 to 2010) with 3 years of warm-up (1997-1999), 6 years of calibration (2000-2005), and 5 years of validation (2006-2010) at a daily time step. In order to have a comparable result with MOD16 ETa, the Penman-Monteith method (Allen, 1986; Allen et al., 1989; Monteith, 1965) (which was used for deriving MOD16 ETa) was used for calculating evapotranspiration in SWAT-IGF.

### 4.4.2 Calibration and validation strategy

In this study, the Sequential Uncertainty Fitting (SUFI-2) in the SWAT-Calibration and Uncertainty Programs (SWAT-CUP) was used for parameter sensitivity, model calibration, validation and uncertainty analysis (Abbaspour, 2013; Abbaspour et al, 2007, 2004). The selected parameters and their initial ranges (Tab. 4.1) were chosen based on local expertise and literature review (Arnold et al., 2012; Lam et al., 2012; Maier and Dietrich, 2016; Nguyen and Dietrich, 2018; Rajib et al., 2018; Uniyal et al., 2017; White and Chaubey, 2005). Global sensitivity analysis was used to identify the important influencing factors and to reduce the number of parameters for model calibration. SUFI-2 uses multiple regression and  $t$ -test to identify the relative sensitivity of each parameter. Within this approach, a higher absolute value of  $t$ -stat and a smaller  $p$ -value indicate a higher sensitivity of the parameter (Abbaspour et al, 2018).

Several multi-criteria objective functions were proposed and tested. The following form of the multi-criteria objective function was found to be appropriate for this study:

$$OF = \max\left(\frac{w_1 \cdot \sum_{i=1}^5 NSE_{Q_i} + w_2 \cdot NSE_{Q_{Lindau}} + w_3 \cdot NSE_{Q_{Rhumespring}} + w_4 \cdot NSE_{ETa}}{5 \cdot w_1 + w_2 + w_3 + w_4}\right) \quad (4.7)$$

where  $OF$  is the multi-criteria objective function,  $NSE_{Q_i}$  is the Nash-Sutcliffe efficiency (Eq. 4.8, Nash and Sutcliffe, 1970) for streamflow at five streamgauging stations inside the catchment (Hattorf, Scharzfeld, Herzberg, Kupferhütte, and Pionierbrücke),  $NSE_{Q_{Lindau}}$ ,  $NSE_{Q_{Rhumespring}}$  and  $NSE_{ETa}$  are the NSE for streamflow at the catchment outlets (Rhume spring and Lindau gauging stations) and the NSE for ETa, respectively,  $w$  is the weight. For sensitivity analysis, the weights in the objective function were assigned as follows:  $w_1 = 1$ ,  $w_2 = 5$ ,  $w_3 = 5$ ,  $w_4 = 5$ . Therefore, the model performances for streamflow at the Lindau, Rhume spring, five aforementioned gauging stations inside the catchment, and for ET are considered equally important in the objective function.

Table 4.1: Selected parameter for sensitivity analysis and sensitivity ranking

Parameter	Initial range	Description	Ranking
Surface runoff and channel processes			
1) CN2	[-0.25, 0.25]	SCS runoff curve number	1
2) SURLAG	[0.05, 10]	Surface runoff lag time (days)	15
3) SOL_K	[-0.2, 0.2]	Soil hydraulic conductivity (mm/h)	18
4) SOL_AWC	[-0.2, 0.2]	Soil available water capacity	6
5) CH_K2(sub <sup>4-6,19,21,26</sup> )	[1, 15]	Riverbed hydraulic conductivity (mm/h)	3
6) CH_K2(sub <sup>9,11,13</sup> )	[10, 40]		2
Evapotranspiration and plant water uptake			
7) ESCO	[0, 1]	Soil evaporation compensation factor	7
8) EPCO	[0, 1]	Plant uptake compensation factor	13
9) REVAPMN	[0, 500]	Threshold for groundwater revap to occur	5
Snow fall and snow melt			
10) SFTMP	[-1.5, 1]	Snowfall temperature (T °C)	9
11) SMTMP	[0, 3]	Snowmelt base temperature (T °C)	8
12) TIMP	[0, 1]	Snowpack temperature lag factor	4
Groundwater and karst processes			
13) GW_DELAY	[1, 9]	Groundwater delay (days)	21
14) GWQMN	[0, 1000]	Threshold for return flow to occur	12
15) ALPHA_BF	[0, 1]	Baseflow recession constant	10
16) RCHRG_DP(sub <sup>15</sup> )	[0, 1]	Deep aquifer percolation factor	15
17) RCHRG_DP(sub <sup>24</sup> )	[0, 1]		17
18) RCHRG_DP(sub <sup>10,12,14</sup> )	[0, 1]		11
19) $\beta$	[0.7, 0.9]		19
20) $\alpha_{conduit}$	[0.05, 0.015]	Karst parameters	16
21) $\alpha_{matrix}$	[0.002, 0.003]		20

CN2, SOL\_K, and SOL\_AWC are changed by relative change, all other parameters are changed by replacing.

All parameters are changed at the basin scale except otherwise mentioned (e.g., sub<sup>9,11,13</sup> means changes are only applied to subbasins 9, 11, and 13).

Table 4.2: List of calibration scenarios and the corresponding weights in the objective function

Scenario	Calibrated variable	Weight values in the objective function
S1	Only $Q_{Rhumespring}$	$w_1 = 0, w_2 = 0, w_3 = 5, w_4 = 0$
S2	All Q	$w_1 = 1, w_2 = 5, w_3 = 5, w_4 = 0$
S3	All Q and ETa	$w_1 = 1, w_2 = 5, w_3 = 5, w_4 = 5$

Three calibrations scenarios were carried out with an increase in the number of calibrated variables from calibration scenarios S1 to S3 (Tab. 4.2). If a variable is not calibrated, its corresponding weight in the objective function is set to zero (Tab. 4.2). The objective of these calibration scenarios is to examine the effects of using multi-site streamflow and MOD16 ETa for model calibration on the model performance. For model calibration, 1000 parameter sets were generated using Latin hypercube sampling. These parameter sets were used for all three calibration scenarios.

Although only the NSE was considered in the objective function, the Kling-Gupta efficiency (KGE, Gupta et al., 2009) and percent bias (PBIAS) was also calculated for the best simulation as follows:

$$NSE = 1 - \frac{\sum_{i=1}^n (x_i^{obs} - x_i^{sim})^2}{\sum_{i=1}^n (x_i^{obs} - \bar{x}^{obs})^2} \quad (4.8)$$

$$KGE = 1 - \sqrt{(r - 1)^2 + (\alpha - 1)^2 + (\beta - 1)^2} \quad (4.9)$$

$$PBIAS(\%) = 100 \cdot \frac{\sum_{i=1}^n (x_i^{obs} - x_i^{sim})}{\sum_{i=1}^n x_i^{obs}} \quad (4.10)$$

where  $x_i^{obs}$  and  $x_i^{sim}$  are the observed and simulated values, respectively, at time step  $i$ ,  $\bar{x}^{obs}$  is the mean of observed values,  $n$  is the number of simulated values,  $r$  is the linear regression coefficient between observed and simulated values,  $\alpha$  ( $\beta$ ) is the ratio of standard deviation (mean) of observed over standard deviation (mean) of simulated values.

In SUFI-2, parameter uncertainty, which is represented as a uniform distribution, integrates all types of uncertainties (e.g., uncertainty in input data, model concept, model parameter, and measured variables). All of these uncertainties ultimately propagate into the model output uncertainty, which is expressed by the 95% prediction uncertainty band (95PPU). The  $p$ -factor (the percentage of measured data bracketed by the 95PPU band)



and *r-factor* (the average thickness of the 95PPU band divided by the standard deviation of the measured data) are used to characterize the 95PPU band (Abbaspour et al, 2018).

## 4.5 Results and discussion

### 4.5.1 Sensitivity analysis and best calibrated parameter set

Tab. 4.1 shows the results of global sensitivity analysis for 21 model parameters. Parameter sensitivity ranking was based on the values of *t-stat* and *p-value*. It is seen that CN2 is the most sensitive parameter. This indicates that streamflow, karst groundwater recharge, and evapotranspiration are strongly affected by the surface runoff generation process. The parameter CH\_K2 (riverbed hydraulic conductivity) is listed among the most sensitive parameters. This is because river transmission losses in the karst area could infiltrate into the conduit network and formulate interbasin groundwater flow, ultimately affect the catchment water balance. The high sensitivity ranking of ESCO is because this parameter controls the amount of evaporation from the soil.

Table 4.3: Selected parameters for calibration and the best parameter values

Parameter	Scenario S1	Scenarios S2 and S3
CN2	0.06	-0.03
CH_K2(sub <sup>9,11,13</sup> )	26.06	25.65
CH_K2(sub <sup>4-6,19,21,26</sup> )	14.35	14.01
TIMP	0.48	0.89
REVAPMN	247.25	140.75
SOL_AWC	-0.11	0.05
ESCO	0.87	0.27
$\beta$	0.81	0.77
$\alpha_{conduit}$	0.0136	0.0084
$\alpha_{matrix}$	0.0021	0.0023

It is seen that the parameter which controls the amount of deep groundwater recharge (RCHRG\_DP) was found insignificant. This is because this parameter only exists in the conceptual model for the non-karst area. The non-karst area in this case is the Harz Mountains with a high topographic gradient. In this area, the runoff coefficient is expected to be high, therefore, the amount of deep groundwater recharge is expected to



be minor compared to surface runoff. The newly introduced parameters for the karst area ( $\beta$ ,  $\alpha_{conduit}$ ,  $\alpha_{matrix}$ ) are not identified as sensitive parameters. This could be due to the fact that these parameters only affect the Rhume spring discharge, which plays a minor role in the objective function (Eq. 4.7 and Tab. 4.2). However, one-at-time sensitivity analysis shows that these parameters significantly affect the dynamic of the simulated Rhume spring hydrograph and they should be taken into account for successful model calibration.

Based on the result of sensitivity analyses and the process-based evaluation as aforementioned, the seven most sensitive parameters and the three parameters of the karst model were selected for model calibration. The best parameter values obtained from automatic calibration were shown in Tab. 4.3.

### 4.5.2 The role of using MOD16 ETa and multi-site streamflow data and for model calibration

Calibration results show that the calibration scenarios S2 and S3 have the same best parameter values (Tab. 4.3) and the same number of behavioral simulations (71 behavioral simulations with a behavioral threshold of 0.5). As a result, the model performance statistics between the calibration scenarios S2 and S3 are identical (Tab. 4.4). This indicates that using MOD16 ETa for model calibration does not affect the model performance in this case study. A detailed examination of the results shows that simulated ETa from the calibration scenario S2 fits well with MOD16 ETa despite MOD16 ETa was not used for model calibration (Fig. 4.5 and Tab. 4.4). In addition, the model performance for ETa tends to be improved with improvement of the model performance for streamflow at the Lindau, Scharzfeld, and Kupferhütte gauging stations. This was shown by a strong positive correlation ( $r \geq 0.78$ ) between  $NSE_{ETa}$  and  $NSE_Q$  at these gauging stations in the calibration scenario S2 (Fig. 4.6). As a result, the best model performance for streamflow in these gauging stations is likely to be among the “best” model performances for ETa and the use of MOD16 ETa for model calibration might not have any effect (or only minor effects) on the model performance. The results indicate that if there is a strong positive correlation in the model performances between two different variables in a multi-variable calibration, one variable can be dropped out of the objective function without having much influence on the model performance. For multi-site calibration, the selected stream gauges should be located in different rivers unless there are some major changes in the river segment.

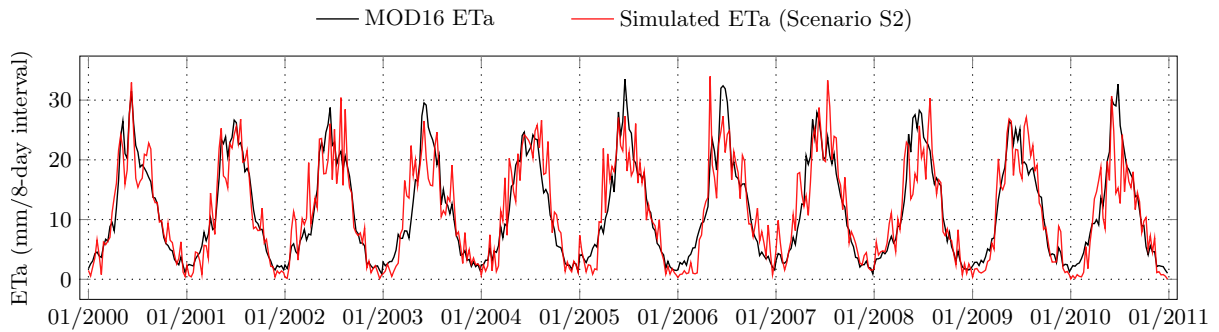


Figure 4.5: Time series plot of MOD16 ETa and simulated ETa from the calibration scenario S2.

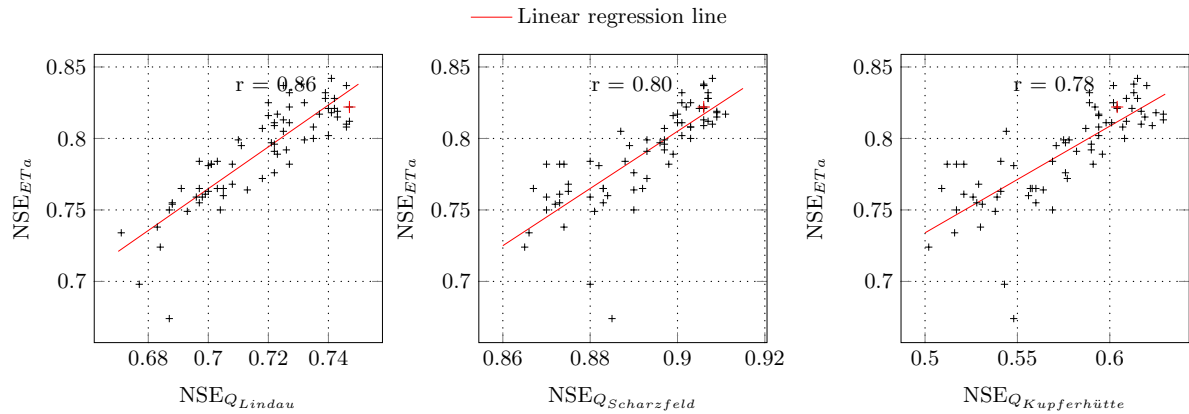


Figure 4.6: Scatter plots of  $NSE_{ETa}$  versus  $NSE_{Q_{Lindau}}$ ,  $NSE_{Q_{Scharzfeld}}$  and  $NSE_{Q_{Kupferhütte}}$  for behavioral simulations in the calibration scenario S2 (from 2000-2005). The red cross indicates the simulation corresponding to the best parameter set.

Table 4.4: Model performance statistics and characteristics of the 95PPU band. Numbers outside parentheses indicate values of the calibration period while numbers inside parentheses indicate values of the validation period.

Variable	NSE	PBIAS	KGE	<i>p-factor</i>	<i>r-factor</i>
Calibration scenario S1					
$Q_{Rhumespring}$	0.75 (0.48)	-0.2 (-2.6)	0.83(0.76)	0.96	1.10
Calibration scenarios S2 and S3					
$Q_{Lindau}$	0.75 (0.74)	0.1 (-3.6)	0.75(0.76)	0.45	0.24
$Q_{Hattorf}$	0.58 (0.70)	-7.5 (1.3)	0.68(0.78)	0.29	0.21
$Q_{Scharzfeld}$	0.91 (0.91)	3.3 (5.0)	0.90(0.82)	0.74	0.16
$Q_{Herzberg}$	0.61 (0.67)	2.6 (5.8)	0.76(0.78)	0.36	0.18
$Q_{Kupferhütte}$	0.60 (0.70)	9.9 (8.4)	0.72(0.72)	0.39	0.25
$Q_{Pionierbrücke}$	0.54 (0.60)	4.8 (5.4)	0.73(0.77)	0.32	0.19
$Q_{Rhumespring}$	0.69 (0.62)	0.5 (-0.9)	0.79(0.80)	0.96	1.01
ETa	0.82 (0.79)	-1.0 (2.12)	0.91(0.89)	0.58	0.36

The aforementioned results, however, should be considered along with the weights used in the objective function (Tab. 4.2). It should be noted that differences between the calibration results of scenarios S2 and S3 occur if the weight for  $NSE_{ETa}$  accounts for more than 70% of all weights in the objective function,  $w_4 \geq 0.7 \cdot (5 \cdot w_1 + w_2 + w_3 + w_4)$ . It means that improving the model performance for ETa is the main objective, which is not the objective in this study.

It is seen from the Tab. 4.4 that the model performance for streamflow at the Rhume spring was reduced, from  $NSE = 0.75$  (scenario S1) to  $NSE = 0.69$  (scenario S2), when streamflow data at additional stream gauges were used for model calibration. However, the model prediction uncertainty was reduced and the model robustness was increased. This is shown by a decrease in the *r-factor* (from 1.10 to 1.01) and a decrease in the difference of NSE between the calibration and validation periods (from 0.27 to 0.07, Tab. 4.4). In the calibration scenario S2, the model performance for streamflow at all gauging stations (except at the Rhume spring) and for ETa are improved compared to that in the calibration scenario S1. The results indicate that in a karst-dominated region, multi-gauge calibration should be done in order to have a better model performance. Therefore, only results from the calibration scenario S2 were discussed in detail in the remaining sections.

### 4.5.3 Simulated streamflow

Fig. 4.7A-G presents the observed and simulated streamflow hydrographs and their respective flow duration curves during the calibration period with the best calibrated parameters. It is seen that the SWAT\_IGF tends to underestimate high flows (Fig. 4.7A-G) and low flows (Fig. 4.7D, E and F). The underestimation of high flows and low flows is inherited from the original SWAT (e.g., [Nguyen and Dietrich, 2018](#); [Nguyen et al., 2018](#); [Uniyal et al., 2017](#)). This could be a reason for the small *p-factor* observed from the model calibration outputs (Tab. 4.4). The good fit between simulated low flows at the Lindau and Scharzfeld gauging stations with observed data (Fig. 4.7A-G) is due to the effect of using observed outflow from the Oder dam (Odertalsperre, Fig. 4.2) as input data to the model. At the Hattorf gauging station, low flows were overestimated by the model (Fig. 4.7B). This is due to a non-linear relationship between discharge and transmission losses of the Sieber river, which cannot be represented in the current SWAT\_IGF model. In this river, transmission losses are reported to be higher (more than 70% of the river discharge) with smaller discharges ([Thürnaeu, 1913](#)). At the Rhume spring gauging station, the observed flow duration curve is well reproduced by the model and the 95PPU band covers most of the observed values (*p-factor* = 96). Simulated results show that runoff generated from the Rhume spring basin accounts for about 4% of the Rhume spring discharge, whereas the remainder (96%) is from IGF. The results match well with the ones reported by [Goldmann \(1986\)](#). Simulated results from the SWAT\_IGF also show that annual transmission losses from the Sieber and Oder river systems contribute about 59% of the Rhume spring discharge, which is similar to the previously estimated value of 60% ([LaMoreaux and Tanner, 2001](#)).

Due to a significant contribution of IGF to the Rhume spring as aforementioned, the original SWAT model failed to simulate flow at this gauging station (Fig. 4.7G). It should be noted that simulated streamflows in the karst area (Lindau, Hattorf, and Scharzfeld gauging stations) from the original SWAT could be better than the SWAT\_IGF. This is because parameters of the SWAT\_IGF model in the karst region are further constrained to match the simulated streamflow at the Rhume spring with observed data. Therefore, we did not compare the simulated streamflow from the original SWAT and the SWAT\_IGF at these gauging stations. In the validation period (2006-2010), similar results were also observed (Fig. 4.8A-G).

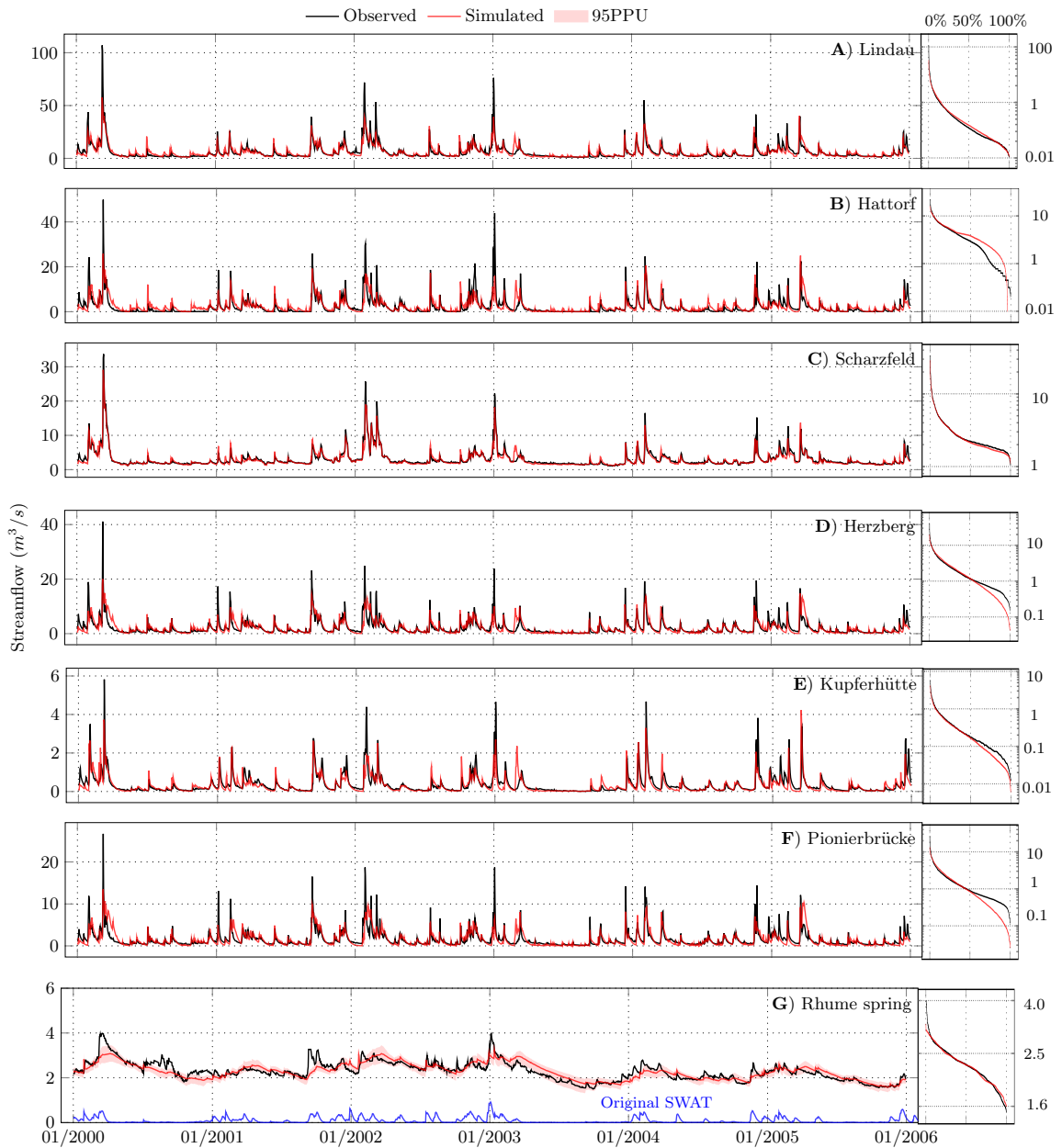


Figure 4.7: Times series plots of streamflows and flow duration curves (attached to the right of the respective time series plot) of the observed and the simulated streamflow from SWAT IGF during the calibration period (2000-2005). The simulated streamflow at the Rhume spring (blue line) using the original SWAT was added in (G). For a better visualization, only the 95PPU band for the Rhume spring was shown.

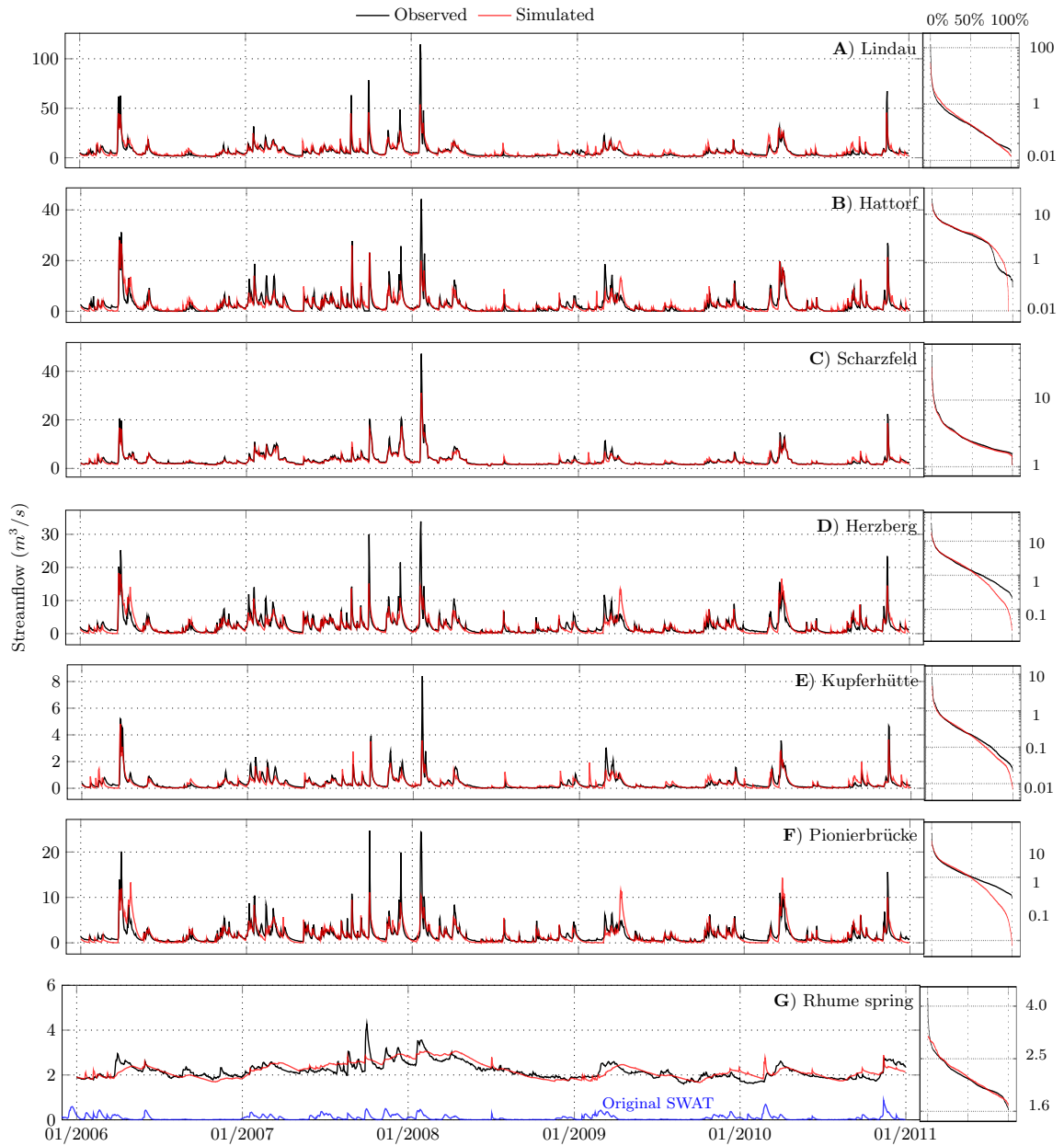


Figure 4.8: Times series plots of streamflows and the flow duration curves (attached to the right of the respective time series plot) of the observed and the simulated streamflow from SWAT IGF during the validation period (2006-2010). The simulated streamflow at the Rhume spring (blue line) using the original SWAT was added in (G).

#### 4.5.4 Simulated karst groundwater storage variation

Fig. 4.9A-C shows 1) the variations of simulated karst groundwater storage (the total groundwater storage in the matrix and conduit storage reservoirs) in the recharge area of the Rhume spring and 2) changes in the observed groundwater levels in three wells (Fig. 4.2). It is expected that changes in the groundwater levels reflect the variations in karst groundwater storage. In three wells, it is seen that the annual variations in the simulated karst groundwater storage agree well with the observed groundwater levels. Especially with well 1, a high correlation coefficient ( $r = 0.93$ ) between the simulated groundwater storage and the observed groundwater levels was found (Fig. 4.9A). At wells 2 and 3 (Fig. 4.9B-C), lower correlation coefficients ( $r = 0.73$  and  $r = 0.47$ , respectively) were found. The simulated karst groundwater storage varies from 35 to 67 million  $\text{m}^3$  with an average value of about 48 million  $\text{m}^3$ .

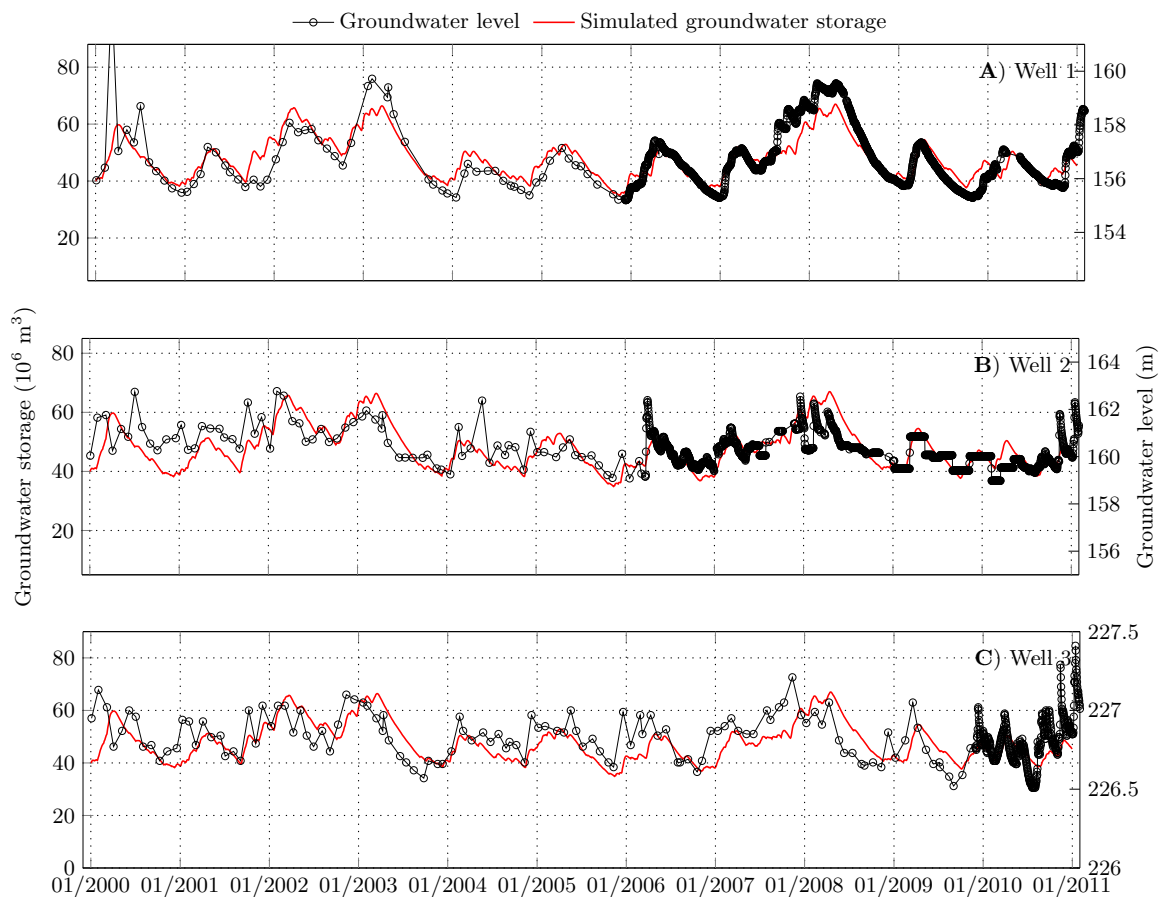


Figure 4.9: Variations of the simulated karst groundwater storage (the matrix and conduit storage reservoirs) and the observed groundwater levels.

## 4.6 Conclusions and recommendations

Interbasin groundwater flow (IGF), especially in karst areas, could significantly alter the water budget of a region. In this study, the original SWAT model was modified for simulating IGF in karst areas, resulting in the SWAT\_IGF model. A two-linear-reservoir model was proposed to represent the duality of recharge, infiltration, storage, and discharge in the karst area. The study area is located in a karst-dominated region in the southwest Harz Mountains, Germany. The model was successfully calibrated at the Rhume spring and at multiple sites for streamflow, and for ETa by using MOD16 ETa.

Calibration results show that multi-site calibration is necessary to achieve a good model performance. Simulated ETa from the SWAT\_IGF model matches well with MOD16 ETa despite MOD16 ETa was not used for model calibration. The use of MOD16 ETa as an additional calibration variable does not affect the model performance. This is because the model performance for ETa tends to be improved with an improvement of the model performance for streamflow at some gauging stations. The conclusion regarding the use of MOD16 ETa for model calibration, however, should not be generalized to other satellite remote sensing products and to studies in other areas.

The SWAT\_IGF model was demonstrated as a robust model by further validating the model outputs with other data. The SWAT\_IGF is also highly flexible. It could be applied in both karst and non-karst areas where the surface subbasin boundaries do not coincide with the subsurface subbasin boundaries. The model uses a parsimonious approach for modeling IGF in karst systems while explicitly representing the duality of recharge, discharge, and storage in karst regions.

The SWAT\_IGF introduced in this study, however, has not been developed for modeling solute transport. Different solute transport models could be incorporated into the SWAT\_IGF model due to its flexible structure. For example, future studies could apply a well-mixed model for modeling solute transport in the conduit because flow in the conduit storage is fast and turbulent. For solute transport in the soil matrix, the catchment scale formulation of transport based on travel time distributions appears to be a promising tool (Benettin et al., 2013; Botter et al., 2011). The concept of travel time-based formulation of transport could be used to simulate (1) the delay between input and output solute concentration signals and (2) different selection schemes for outflow from the rock matrix. In addition, the recharge separation factor ( $\beta$ ) was assumed to be constant regardless of the rainfall event characteristics. Future studies could use different recharge separation factors depending on different rainfall event characteristics (Hartmann et al., 2015b).



## Acknowledgments

This research did not receive any specific grant from funding agencies in the public, commercial, or not-for-profit sectors. We thank the Editor and three anonymous reviewers for their constructive comments, which helped significantly improve quality of the manuscript. We also thank the DWD, HWW, BGR, and NLWKN for providing data.

## Bibliography

- Abbaspour, K.C., Vaghefi, S.A., Srinivasan, R. A., (2018). A guideline for successful calibration and uncertainty analysis for Soil and Water Assessment: A review of papers from the 2016 International SWAT Conference. *Water*, 2018, 10, 6.
- Abbaspour, K.C., 2013. SWAT-CUP 2012. SWAT Calibration and Uncertainty Program—A User Manual.
- Abbaspour, K.C., Yang, J., Maximov, I., Siber, R., Bogner, K., Mieleitner, J., Zobrist, J., Srinivasan, R. (2007). Modelling hydrology and water quality in the pre-alpine/alpine Thur watershed using SWAT. *J. Hydrol.*, 333(2-4), 413-430.
- Abbaspour, K.C., Johnson, C.A., Van Genuchten, M.T., 2004. Estimating uncertain flow and transport parameters using a sequential uncertainty fitting procedure. *Vadose Zone Journal*, 3(4), 1340–1352.
- Allen, R.G., 1986. A Penman for all seasons. *J. Irrig. Drain Eng. ASCE*, 112 (4), 348–368.
- Allen, R.G., Jensen, M.E., Wright, J.L., Burman, R.D., 1989. Operational estimates of reference evapotranspiration. *Agron. J.*, 81 (4), 650–662.
- Anaya, R., Wanakule N., 1993. A lumped parameter model for the Edwards Aquifer. Texas Water Resources Institute, Texas A&M University.
- Anderson, K., Nelson, S., Mayo, A., Tingey, D., 2006. Interbasin flow revisited: the contribution of local recharge to high-discharge springs, Death Valley, CA. *J. Hydrol.* 323, 276–302.
- Arnold, J. G., Fohrer, N., 2005. SWAT2000: Current capabilities and research opportunities in applied watershed modelling. *Hydrol. Process.*, 19 (3), 563–572.

- Arnold, J.G., Moriasi, D.N., Gassman, P.W., Abbaspour, K.C., White, M.J., Srinivasan, R., Santhi, C., van Harmel, R.D., Van Griensven, A., Van Liew, M.W., Kannan, N., Jha, M.K., 2012. SWAT: model use, calibration, and validation. *Trans. ASABE* 55 (4), 1491–1508.
- Arnold, J.G., Srinivasan, R., Muttiah, R.S., Williams, J.R., 1998. Large area hydrologic modeling and assessment. Part I: model development. *J. Am. Water Resour. Assoc.* 34, 73–89.
- Bakalowicz, M., 2005. Karst groundwater: a challenge for new resources. *Hydrogeol. J.* 13 (1), 148–160.
- Barrett, M.E., Charbeneau, R.J., 1997. A parsimonious model for simulating flow in a karst aquifer. *J. Hydrol.* 196 (1–4), 47–65.
- Benettin, P., Velde, Y., Zee, S. E. A. T. M., Rinaldo, A., and Botter, G., 2013. Chloride circulation in a lowland catchment and the formulation of transport by travel time distributions, *Water Resour. Res.* 49, 4619– 4632
- Belcher, W.R., Bedinger, M.S., Back, J.T., Sweetkind, D.S., 2009. Interbasin flow in the great basin with special reference to the southern Funeral Mountains and the source of Furnace Creek springs, Death Valley, California, US. *J. Hydrol.* 369 (1–2), 30–43.
- Bonacci, O., Ljubenkovic, I., Roje-Bonacci T., 2006. Karst flash floods: an example from the Dinaric karst (Croatia). *Nat. Hazards Earth Syst. Sci.* 6, 195–203.
- Botter, G., Bertuzzo, E., Rinaldo, A., 2011. Catchment residence and travel time distributions: The master equation. *Geophys. Res. Lett.*, 38, L11403.
- Bögli, A., 1980. *Karst Hydrology and Physical Speleology*. Springer, Berlin.
- Böttcher, M.E., 1999. The stable isotopic geochemistry of the sulfur and carbon cycles in a modern karst environment, *Isot. Environ. Health Stud.* 35 (1–2), 39–61.
- Brenner, S., Coxon, G., Howden, N. J. K., Freer, J., Hartmann, A. (2018). Process-based modelling to evaluate simulated groundwater levels and frequencies in a Chalk catchment in south-western England. *Nat. Hazards Earth Syst. Sci.*, 18, 445–46.1
- Danapour, M., Højberg, A.L., Jensen, K.H., Stisen, S. (2019). Assessment of regional inter-basin groundwater flow using both simple and highly parameterized optimization schemes. *Hydrogeol. J.* 27, 1929–1947.

- Dar, F. A., Perrin, J., Ahmed, S., Narayana, A. C., 2014. Review: carbonate aquifers and future perspectives of karst hydrogeology in India. *Hydrogeol. J.* 22 (7), 1493–1506.
- Doerfliger, N., Jeannin, P.-Y., Zwahlen, F., 1999. Water vulnerability assessment in karst environments: a new method of defining protection areas using a multi-attribute approach and GIS tools (EPIK method). *Environ. Geol.* 39 (2), 165–176.
- Drew, D., Hötzl, H., 1999. *Karst Hydrogeology and Human Activities. Impacts, Consequences and Implications*, Balkema, Rotterdam.
- Droogers, P., Immerzeel, W.W., Lorite, I.J., 2010. Estimating actual irrigation application by remotely sensed evapotranspiration observations. *Agric. Water Manage.* 97 (9), 1351–1359.
- Ford, D.C., Williams, P.W., 2007. *Karst Hydrogeology and Geomorphology*. John Wiley & Sons, Chichester.
- Franco, A.C.L., Bonumá, N.B., 2017. Multi-variable SWAT model calibration with remotely sensed evapotranspiration and observed flow. *Brazilian J. Water Resour.* 22, e35.
- Gassman, P. W., Reyes, M., Green, C. H., Arnold, J. G., 2007. The Soil and Water Assessment Tool: historical development, applications, and future research directions. *Trans. ASABE*, 50 (4), 1211–1250.
- Goldmann, A., 1986. *Die Wasserbilanz der Rhumequelle*. Bericht Wasserwirtschaftsamt Göttingen.
- Goldscheider, N., 2005. Karst groundwater vulnerability mapping: application of a new method in the Swabian Alb, Germany. *Hydrogeol. J.* 13 (4), 555–564.
- Goldscheider, N., Drew, D., 2007. *Methods in Karst Hydrogeology*. Taylor & Francis, London.
- Grimmelmann, W., 1992. *Hydrogeologisches Gutachten zur Bemessung und Gliederung des Trinkwasserschutzgebiets Pöhlder Becken*. Niedersächsischen Landesamtes für Bodenforschung, Hannover.
- Gun, J., 1986. A conceptual model for conduit flow dominated karst aquifers. In: Günay, G., Johnson, A.I. (Eds.), *Proc. Ankara Symp. “Karst water resources”*, July 1985, IAHS Publ. 161, 587–596.

- Gupta, H.V., Kling, H., Yilmaz, K.K., Martinez, G.F., 2009. Decomposition of the mean squared error and NSE performance criteria: Implications for improving hydrological modelling. *J. Hydrol.*, 377(1-2), 80–91.
- Haggett, P., 2002. *Encyclopedia of World Geography*. Vol. 12. Germany, Austria and Switzerland. Second ed. Marshall Cavendish Inc., New York.
- Haase, H., Schmidt, M., Lenz, J., 1970. Der Wasserhaushalt des Westharzes-Hydrologische Untersuchungen von 1941–1965. Veröff. Nieders. Inst. Landeskunde Landesentwicklung Univ. Göttingen, A91, 1–96.
- Hartmann, A., Barberá, J.A., Andreo, B., 2017. On the value of water quality data and informative flow states in karst modelling. *Hydrol. Earth Syst. Sci.* 21, 5971–5985.
- Hartmann, A., Gleeson, T., Rosolem, R., Pianosi, F., Wada, Y., Wagener, T., 2015. A large-scale simulation model to assess karstic groundwater recharge over Europe and the Mediterranean. *Geosci. Model Dev.*, 8 (6), 1729–1746.
- Hartmann, A., Mudarra, M., Andreo, B., Marín, A., Wagener, T., and Lange, J. (2014). Modeling spatiotemporal impacts of hydroclimatic extremes on groundwater recharge at a Mediterranean karst aquifer. *Water Resour. Res.*, 50, 6507–6521.
- Hartmann, A., Wagener, T., Rimmer, A., Lange, J., Brielmann, H., Weiler, M., 2013. Testing the realism of model structures to identify karst system processes using water quality and quantity signatures. *Water Resour. Res.* 49, 3345–3358.
- Hartmann, A., Goldscheider, N., Wagener, T., Lange, J. Weiler, M., 2014. Karst water resources in a changing world: review of hydrological modeling approaches. *Rev. Geophys.* 52, 218–242.
- Herrmann, A., 1969. Die geologische und hydrogeologische Situation der Rhumequelle am Südharz. *Jh. Karst-u. Höhlenkunde* 9, 107–112.
- Howard, A.D., 1963. The development of karst features. *Bull. Nat. Spel. Soc.* 25, 45–65.
- Immerzeel, W.W., Droogers, P., 2008. Calibration of a distributed hydrological model based on satellite evapotranspiration. *J. Hydrol.* 349 (3–4), 411–424.
- Jung, M., Reichstein, M., Ciais, P., Seneviratne, S.I., Sheffield, J., Goulden, M.L., Bonan, B., et al., 2010. Recent decline in the global land evapotranspiration trend due to limited moisture supply. *Nature* 467, 951–954.

- Koster, E.A., 2005. *The Physical Geography of Western Europe*. Oxford Univ. Press, New York.
- Kourgialas, N.N., Karatzas, G.P., Nikolaidis, N.P., 2010. An integrated framework for the hydrologic simulation of a complex geomorphological river basin. *J. Hydrol.*, 381 (3–4), 308–321.
- Kramm, U., Wedepohl, K.H., 1991. The isotopic composition of strontium and sulfur in seawater of Late Permian (Zechstein) age. *Chem. Geol.* 90 (3–4), 253–262.
- Krysanova, V., White, M., 2007. Advances in water resources assessment with SWAT – an overview. *Hydrol. Sci. J.*, 60 (5), 771–783.
- Lam, Q.D., Schmalz, B., Fohrer, N., 2012. Assessing the spatial and temporal variations of water quality in lowland areas, Northern Germany. *J. Hydrol.* 438–439, 137–147.
- LaMoreaux, P.E., Tanner, J.T., 2001. *Springs and bottled waters of the world. Ancient history, source, occurrence, quality and use*. Springer Verlag, Berlin
- Le Moine, N., Andreassen, V., Perrin, C., Michel, C., 2007. How can rainfall–runoff models handle intercatchment groundwater flows? Theoretical study based on 1040 French catchments. *Water Resour. Res.* 43, W06428.
- Le Moine, N., Andreassen, V., Mathevet, T., 2008. Confronting surface- and groundwater balances on the La Rochefoucauld-Touvre karstic system (Charente, France). *Water Resour. Res.* 44, W03403
- Liersch, K. M., 1987. Zur Wasserbilanz der Rhumequelle und ihres Einzugsgebietes, des Pöhlder Becken. *N. Arch. F. Nds.* 36, 293–305.
- Liu, Y.B., Batelaan, O., Smedt, F.D., Huong, N.T., Tam, V.T., 2005. Test of a distributed modelling approach to predict flood flows in the karst Suoimuoi catchment in Vietnam. *Environ. Geol.* 48 (7), 931–940.
- Maier, N., Dietrich, J., 2016. Using SWAT for strategic planning of basin scale irrigation control policies: a Case study from a humid region in northern Germany. *Water Resour. Manage.* 30, 3285–3298.
- Malagó, A., Efstathiou, D., Bouraoui, F., Nikolaidis, N.P., Franchini, M., Bidoglio, G., Kritsotakis, M., 2016. Regional scale hydrologic modeling of a karst-dominant geomorphology: the case study of the Island of Crete. *J. Hydrol.* 540, 64–81.

- Molina-Navarro, E., Andersen, H. E., Nielsen, A., Thodsen, H., Trolle, D., 2017. The impact of the objective function in multi-site and multi-variable calibration of the SWAT model. *Environ. Modell. Softw.* 93, 255–267.
- Monteith, J.L., 1965. Evaporation and environment. In: *The State and Movement of Water in Living Organisms*, Proc. 15th Symposium Society for Experimental Biology, Swansea, Cambridge University Press, London, 205–234.
- Mu, Q., Zhao, M., Running, S.W., 2013. MODIS global terrestrial evapotranspiration (ET) product (NASA MOD16A2/A3), Algorithm Theoretical Basis Document, Collection 5. NASA, Washington.
- Muthuwatta, L.P., Booij, M.J., Reintjes, T.H., Bos, M.G., Geiske, A.S., Ahmad, M. 2009. Calibration of a semi-distributed hydrological model using discharge and remote sensing data. In: Yilmaz, K.K. et al. (Eds.), *New Approaches to Hydrological Prediction in Data-Sparse Regions*. IAHS, Hyderabad, 52–58
- Nash, J.E., Sutcliffe, J.V., 1970. River flow forecasting through conceptual models. Part 1: a discussion of principles. *J. Hydrol.*, 10, 282–290.
- Neitsch, S.L., Arnold, J.G., Kiniry, J.R., Williams, J.R., 2011. Soil and Water Assessment Tool theoretical documentation version 2009. Grassland, Soil and Water Research Laboratory, Agricultural Research Service and Blackland Research Center, Texas Agricultural Experiment Station, Temple, Texas.
- Nerantzaki, S.D., Giannakis, G.V., Efstathiou, D., Nikolaidis, N.P., Sibetheros, I.A., Karatzas, G.P., Zacharias, I., 2015. Modeling suspended sediment transport and assessing the impacts of climate change in a karstic Mediterranean watershed. *Sci Total Environ.*, 538, 288–297.
- Nguyen, V.T., Dietrich, J., 2018. Modification of the SWAT model to simulate regional groundwater flow using a multicell aquifer. *Hydrol. Process.* 32(7), 939–953.
- Nguyen, V.T., Dietrich, J., Uniyal, B., Tran, D.A., 2018. Verification and correction of the hydrologic routing in the soil and water assessment tool. *Water* 10, 1419.
- Nikolaidis, N.P., Bouraoui, F., Bidoglio, G., 2013. Hydrologic and geochemical modeling of a karstic Mediterranean watershed. *J. Hydrol.* 477, 129–138.
- Oki, T., Kanae, S., 2006. Global hydrological cycles and world water resources. *Science* 313, 1068–1072.

- Palanisamy, B., Workman, S.R., 2014. Hydrologic modeling of flow through sinkholes located in streambeds of Cane Run stream, Kentucky. *J. Hydrol. Eng.* 20 (5), 04014066–1–12.
- Paul, J., Vladi, F., 2001. Zur Geologie der Einhornhöhle bei Scharzfeld am südwestlichen Harzrand. *Ber. Naturhist. Ges. Hannover* 143, 109–131.
- Perrin, C., Michel, C., Andréassian, V., 2003. Improvement of a parsimonious model for streamflow simulation, *J. Hydrol.*, 279, 275–289.
- Rajib, A., Evenson, G.R., Golden, H.E., Lane, C.R., 2018). Hydrologic model predictability improves with spatially explicit calibration using remotely sensed evapotranspiration and biophysical parameters. *J. Hydrol.*, 567, 668–683.
- Rientjes, T.H.M., Muthuwatta, L.P., Bos, M.G., Booij, M.J., Bhatti, H.a., 2013. Multi-variable calibration of a semi-distributed hydrological model using streamflow data and satellite-based evapotranspiration. *J. Hydrol.* 505, 276–290.
- Rienäcker, I., 1987. Bericht zum Forschungsprogramm “Pöhlder Becken und Rhumequelle”: “Hydrochemische und hydrologische Untersuchungen an der Rhumequelle und in ihrem Einzugsgebiet – Ein Beitrag zur Nutzung des Wassers für die Trinkwasserversorgung”. Bericht EEW Duderstadt.
- Rozos, E., Koutsoyiannis, D., 2006. A multicell karstic aquifer model with alternative flow equations. *J. Hydrol.* 325, 340–355.
- Sangrey, D.A., Harrop-Williams, K.O., Klaiber, J.A., 1984. Predicting ground-water response to precipitation. *J. Geotech. Eng.* 110 (7). 957–975.
- Scanlon, B.R., Mace, R.E., Barrett, M.E., Smith, B., 2003. Can we simulate regional groundwater flow in a karst system using equivalent porous media models? Case study, Barton Springs Edwards Aquifer, USA. *J. Hydrol.*, 276, 137–158.
- Schnug, E., Ernst., W.H.O., Kraztz S., Knolle F., Haneklaus S., 2004. Aspects of ecotoxicology of sulphur in the Harz region - a guided excursion *Landbauforschung Völkenrode*, 54 (3), 129–143.
- Schnug E., Haneklaus S., 1998. Diagnosis of sulphur nutrition. In: Schnug, E. (Ed.), *Sulphur in Agroecosystems*. Kluwer Academic Press, Dordrecht, 1–38.
- Screaton, E., Martin, J.B., Ginn, B., Smith, L., 2004. Conduit properties and karstification in the unconfined Floridan Aquifer. *Groundwater*, 42(3), 338–346.

- Spangler, L.E., 2001. Delineation of recharge areas for karst springs in Logan Canyon, Bear River Range, northern Utah. In: Kuniandy, E.L. (Ed.), U.S. Geological Survey Karst Interest Group Proceedings, Water Resour. Invest. Rep. 01-4011, 186-193.
- Tait, J.A., Bachtadse, V., Franke, W., Soffel, H.C., 1997. Geodynamic evolution of the European Variscan fold belt: paleomagnetic and geological constraints. *Geol. Rundsch.*, 86, 585-98.
- Taylor, J.C.M., 1998. Upper Permian-Zechstein, In: Glennie, K.W. (Ed.), *Petroleum Geology of the North Sea Basic Concepts and Recent Advances*, 4th ed. Blackwell Scientific Publications, Oxford, 174-211.
- Taylor, C.J., Greene, E.A., 2008. Hydrogeologic characterization and method used in the investigation of karst hydrology. In: Rosenberry, D.O., LaBaugh, J.W. (Eds.), *Field Techniques for Estimating Water Fluxes between Surface Water and Groundwater*, chap. 3. Techniques and Methods 4-D2. U.S. Department of the Interior, U.S. Geological Survey, 75-114.
- Thürschau, K., 1913. Der Zusammenhang der Rhumequelle mit der Oder und Sieber. *Jb. Gewässerkunde Norddeutschlands*, Bes. Mitt. 2 (6), 1-25.
- Tóth, J., 1963. A theoretical analysis of groundwater flow in small drainage basins. *J. Geophys. Res.* 68 (16), 4795-4812.
- Tuck, S.L., Phillips, H.R.P., Hintzen, R.E., Scharlemann, J.P.W., Purvis, A., Hudson, L.N., 2014. MODISTools - downloading and processing MODIS remotely sensed data in R. *Ecol. Evol.* 4, 4658-4668.
- Tucker, M.E., 1991. Sequence stratigraphy of carbonate evaporite basins: the Upper Permian (Zechstein) of northeast England and adjoining North Sea. *J. Geol. Soc.* 148, 1019-1036.
- Uniyal, B., Dietrich, J., Vasilakos, C., Tzoraki, O., 2017. Evaluation of SWAT simulated soil moisture at catchment scale by field measurements and Landsat derived indices. *Agric. Water Manage.* 193, 55-70.
- Venetis, C., 1969. A study on the recession of unconfined aquifers. *International Association of Scientific Hydrology. Bull. Int. Assoc. Sci. Hydrol.* 14 (4), 119-125.



- Vervoort, R.W., Mielchels, S.F., van Ogtrop, F.F., Guillaume, J.H.A., 2014. Remotely sensed evapotranspiration to calibrate a lumped conceptual model: Pitfalls and opportunities. *J. Hydrol.* 519, 3223–3236.
- Voigt, R., Gröger, E., Baier, J., Meischner, D., 2008. Seasonal variability of Holocene climate: a palaeolimnological study on varved sediments in Lake Jues (Harz Mountains, Germany). *J. Paleolimnol.* 40, 1021–1052.
- Wessolek, G., Kaupenjohann, M., Renger, M., 2009. Bodenphysikalische Kennwerte und Berechnungsverfahren für die Praxis. *Bodenökologie und Bodengeneese* (40). University of Technology, Berlin, Germany.
- White, W.B., 2002. Karst hydrology: recent developments and open questions. *Eng. Geol.* 65, 85–105.
- White, K.L., Chaubey, I., 2005. Sensitivity analysis, calibration, and validations for a multisite and multivariable SWAT model. *J. Am. Water Resour. Assoc.* 41 (5), 1077–1089.
- Zhang, Y., Chiew, F.H.S., Zhang, L., Li, H., 2009. Use of remotely sensed actual evapotranspiration to improve rainfall–runoff modeling in southeast Australia. *J. Hydrometeorol.* 10 (4), 969–980.

# Chapter 5

## Conclusion and Future Outlooks

### 5.1 Conclusions

Understanding hydrological connectivity plays a crucial role in understanding the transport water and its associated components between different landscape units. Therefore, it could help to have an appropriate water resource management strategy. Hydrological models have been proved to be an efficient tool for understanding hydrological connectivity. Conceptual distributed models have shown certain advantages compared to physically-based distributed models in terms of data requirement and computational time. However, the hydrological connectivity (lateral surface and subsurface flows) in conceptual distributed models is often not well represented.

In many conceptual (semi-)distributed models, the hydrological connectivity is often restricted within a basin. In these models, the hydrological connection between basins is only represented via hydrological routing in a river network. However, interbasin groundwater flow or regional groundwater flow could exist between these basins. Especially in karst-dominated areas, interbasin groundwater flow is likely to be occur. For example, recharge into the karst aquifer could enter the underground conduit system and emerge at other subbasins. This type of hydrological connectivity could be significant, therefore, it should be accounted for. In this study, the SWAT model was modified to have a better representation and simulation of hydrological connectivity at the regional scale. Although SWAT was specifically selected for this study, the methods presented here could be applied for other conceptual (semi-)distributed models.

SWAT is a distributed hydrological model used to simulate the effects of land use management practices on water, sediments, and chemical yields at a basin scale. SWAT

has been widely used and applied worldwide. The HRU concept used in SWAT has been identified as one of the main disadvantages for simulating hydrological connectivity. For example, the lack of subsurface connectivity between HRUs results in its inability to simulate regional groundwater flow in porous and karst-dominated aquifers. In addition, the hydrologic routing subroutine of SWAT was inappropriate in representing the hydrological connectivity in the river network. This study proposed different approaches for improving the representation and simulation of hydrological connectivity within SWAT. The main results of this research are summarized in the following sections.

### 5.1.1 Hydrological connectivity in the river network

The current Muskingum flood routing method used in SWAT results in a disconnectivity (no flow) or reduction in the magnitude of hydrological connectivity (flow rate) between subbasins. This is due to the overestimation of channel evapotranspiration in the Muskingum routing subroutine of SWAT. During a low-flow period, the overestimated evapotranspiration amount could be significant that it could result in no-flow between subbasins. In terms of interbasin water resources management, this could lead to an inappropriate measure to maintain the environmental flow (especially during low flow period). In addition, the channel transmission losses are underestimated when the Muskingum routing method is activated. The modified Muskingum routing subroutine was proposed for flood routing because of its robustness in simulating different flood waves.

The second flood routing method used in SWAT, the variable storage method, could cause unphysical oscillations in the simulated flow during the wetting to drying phase (or during the drying to wetting phase) of the flood plain. This is due to the assumption of the flood plain geometry and the use of Manning's equation in the variable storage method. This is because the step-wise increase (or decrease) in the wetting perimeter during the wetting to drying phase (or during the drying to wetting phase). Thus, it results in a step-wise decrease (or increase) in the flow velocity. In addition, the current variable storage routing technique used in SWAT does not transform the flood wave as it moves to a downstream section.

### 5.1.2 Subsurface hydrological connectivity in porous aquifer

Due to the HRU concept, SWAT is not able to simulate groundwater flow between HRUs or subbasins. Therefore, the simulated groundwater level in SWAT does not have a physical

meaning. Furthermore, the disconnected subsurface hydrological connectivity could not explain the return flow originated from the regional groundwater flow. The multicell aquifer model was incorporated into SWAT, resulting in the SWAT-MCA model. In the SWAT-MCA model, the delineation of the subsurface aquifer does not follow the HRU or subbasin delineation. Instead, it is delineated by the Thiessen polygon method based on the observed groundwater well network. Flow between cells (Thiessen polygons) was simulated based on the Darcy's law with the cell's hydrogeological properties.

The SWAT-MCA was proved to be a compromise solution between physically-based distributed groundwater model and conceptual lumped groundwater model. Results show that the simulated groundwater levels from the SWAT-MCA model match well with the observed groundwater levels, except at some cells which are strongly affected by anthropogenic activities (e.g., groundwater pumping). In addition, the simulated low flows from the SWAT-MCA model are also better than the original SWAT model.

### **5.1.3 Subsurface hydrological connectivity in karst-dominated aquifer**

Interbasin groundwater flow often occurs in karst-dominated aquifers. The original SWAT model is not able to simulate interbasin groundwater flow. This study proposed a new approach for incorporating interbasin groundwater flow into the SWAT model. The modified SWAT model, so-called the SWAT-IGF, uses two conceptual models. The original conceptual model of SWAT was applied to the non-karst areas to simulate allogenic recharge to karst aquifer while the modified conceptual model was applied to simulate autogenic recharge to karst aquifer. The modified conceptual model can explicitly represent different types of hydrological connectivity fast and slow recharge with fast and slow discharge. The SWAT-IGF was verified in a karst-dominated catchment located in Niedersachsen, Germany. Results show that the SWAT-IGF could be applied in both karst and non-karst areas. The recharge and discharge dynamics in karst areas could be well represented by the SWAT-IGF model.

## 5.2 Future Outlooks

### 5.2.1 General

The results from this study show that understanding hydrological connectivity, especially the subsurface hydrological connectivity, at a catchment scale are challenging tasks. This is mainly due to the lack of observed data. Data from experimental studies (e.g., tracer tests) and geological studies (aquifer properties) could provide useful information about the hydrological connection between different landscape units.

In most of the conceptual models, there is a lack of a general framework to represent subsurface hydrological connectivity. There have been different approaches for representing subsurface hydrological connectivity proposed, however, these approaches are restricted to certain cases. For example, there are two models were proposed to represent subsurface hydrological connectivity in the porous and karst areas in this study. This is due to the compromise between model complexity and model applicability. The model should be (1) complex enough to represent the targeted processes, and (2) simple enough to be applicable and verifiable with the existing available data.

The results from this study show that different types of subsurface hydrological connectivity could be represented in a the SWAT model. This was done by using another approaches for delineating the subsurface catchment while the surface catchment is delineated using the DEM model. This study, however, has not improved the representation of hydrological connectivity within a soil zone (surface run-on and run-off between different HRUs). This would require another approach to replace the HRU approach for delineating the surface into different landscape units.

The SWAT model and its modified version presented in this study is still a simplified representation of a real hydrological system. Therefore, they will be further modified to have a better representation of the real hydrological system. With the original SWAT and modified SWAT models presented in this study, the specific future outlooks for these models was presented in the following sections.

### 5.2.2 Original SWAT model

SWAT is an open source software and the SWAT source code has been undergoing various modifications. The study shows that SWAT source code is not error-free despite it has been widely used and tested. This study only reviewed and verified the hydrologic

routing subroutines of SWAT. Future studies are suggested to review and verify the other subroutines of SWAT separately. In order to do that, each subroutine of SWAT should be separated and tested independent of other subroutines.

The study have revealed that there are some errors related to the flood routing subroutines in several SWAT revisions. The magnitude of these errors could vary case to case. With large river and high evapotranspiration rate, the error could be significant when the uncorrected Muskingum subroutine is used. For flood forecast in long river with large retention, the error in the variable storage subroutine could be significant because it does not transform the flood wave. Therefore, revision is suggested with studies which used the affected flood routing subroutines.

The future version of SWAT, so-called SWAT+, is the total revision of the original SWAT code to facilitate object-oriented programming, code maintenance. However, the SWAT+ code reused many parts of the original SWAT code. Therefore, error in the original SWAT code could still exist in the SWAT+. The SWAT+ allows greater flexibility compared to the original SWAT in terms of defining the hydrological connectivity. Each HRU, aquifer, stream, etc., in SWAT+ was identified as a separate spatial object and users are allowed to define the hydrological connection between these objects. However, in large subbasins, there could be many spatial objects and high flexibility in defining the connection between these spatial objects. This could result in an overparameterization and an infinite loop (e.g., water could circulate between these objects without entering the discharge point). In addition, the hydrologic connection in SWAT+ is a one-way connection while in nature there could be a two-way connection (e.g., the flow direction between aquifers could be changed due to changes in the total hydraulic heads).

### 5.2.3 SWAT-MCA model

For improving the simulation of hydrological connectivity in porous aquifers, the SWAT-MCA was proposed. The SWAT-MCA model, however, is only applicable in regions where the groundwater aquifer is a single unconfined aquifer. In natural groundwater system, a multi-layer aquifer with both confined and unconfined aquifers could exist. Therefore, future study could extend the SWAT-MCA model for a multi-layer aquifer system. The hydraulic connection between stream and aquifer is simulated using a linear storage-discharge relationship. In this approach, return flow from the aquifer to stream is assumed to be linear with groundwater storage. The validity of this assumption should be checked with observed data or with physically-based distributed model.

The SWAT-MCA model uses the Thiessen polygon method for aquifer delineation. However, this delineation technique does not account for the hydrogeological characteristics of the aquifer (e.g., hydraulic conductivity and aquifer thickness). Future studies could use other delineation techniques to overcome this problem. In the SWAT-MCA model, flow occurs between cells which share the same border using the Darcy's law. However, there could be no flow between these cells, e.g., due to a layer of impermeable layer between them. Therefore, it is suggested that tracer tests should be done to check the groundwater flow path before aquifer delineation.

#### **5.2.4 SWAT-IGF model**

For improving the simulation of hydrological connectivity in karst-dominated regions, the SWAT-IGF model was demonstrated to be better than the original SWAT model. In this model, flow from the rock matrix to the conduit system and flow out of the conduit system were simulated by a linear-storage discharge relationship. Flow out of the conduit system, however, could be highly non-linear. Therefore, the non-linear storage discharge relationship could be used to represent this characteristic. The current version of the SWAT-IGF is only applicable for the case where the discharge of karst aquifer is located in a single subbasin. In reality, discharge from the karst system could be via several springs located at different subbasins. Therefore, further modification of the SWAT-MCA model is suggested. In addition, the SWAT-IGF only simulates flow quantity. Future studies could incorporate a solute transport subroutine into SWAT-IGF. Furthermore, the SWAT-IGF was only applied for a single area located in Germany. Testing of the model at other karst regions is necessary.

Herausgegeben im Selbstverlag  
des Institutes für Hydrologie und Wasserwirtschaft  
Gottfried Wilhelm Leibniz Universität Hannover

Appelstraße 9A, D-30167 Hannover

Tel.: 0511/762-2237

Fax: 0511/762-3731

E-Mail: [info@iww.uni-hannover.de](mailto:info@iww.uni-hannover.de)

2020

Alle Rechte beim Autor